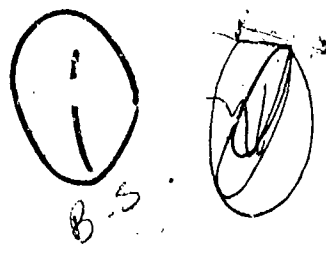


ADA 034523



AD

R-TR-75-035

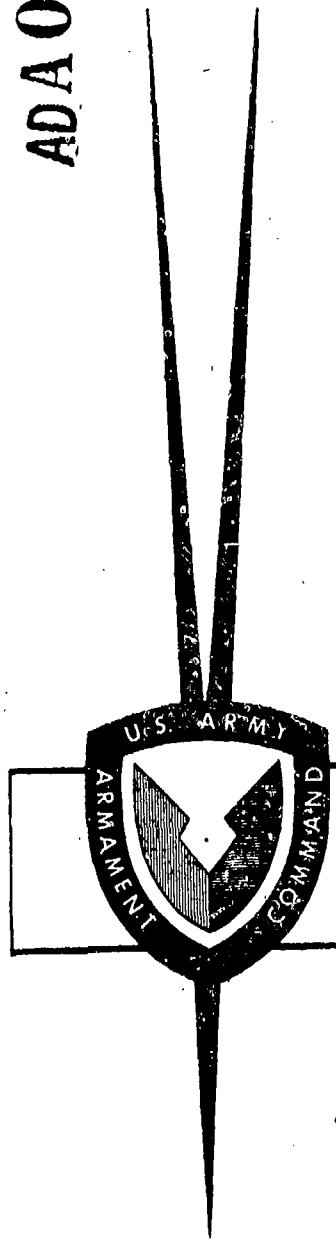
STUDY OF MAN-WEAPON REACTION
FORCES APPLICABLE TO THE FABRICATION
OF A STANDARD RIFLE FIRING FIXTURE

BY

THOMAS D. HUTCHINGS
ALBERT E. RAHE

1 OCTOBER 1975
FINAL REPORT

D D C
D D D
JAN 18 1977
C



RESEARCH DIRECTORATE

DISTRIBUTION STATEMENT

APPROVED FOR PUBLIC RELEASE; DISTRIBUTION UNLIMITED.

**GENERAL THOMAS J. RODMAN LABORATORY
ROCK ISLAND ARSENAL
ROCK ISLAND, ILLINOIS 61201**

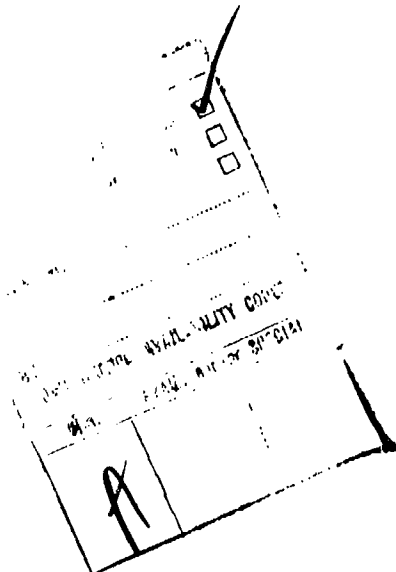
DISCLAIMER

The findings in this report are not to be construed as an official Department of the Army position, unless so designated by other authorized documents.

DISPOSITION INSTRUCTIONS

Destroy this report when it is no longer needed.

20 -> To demonstrate the feasibility of designing a universal mount fixture, a three degree of freedom mathematical model was developed that simulates the man and weapon as a coupled dynamical system. A sensitivity analysis was performed on both analog and digital computers to determine which of the system parameters are critical to the design of the mount and to obtain bounds on them. The mathematical simulation was supported by an extensive test firing program, involving shooters of various sizes firing the M16 rifle and the M79 and M203 grenade launchers. In these tests the shoulder reaction force and the dynamical motions of the man-weapon system were recorded. Information provided by the tests was used to estimate some of the critical parameters of the system and to provide a means for validating the model predictions. Result of this study indicate the feasibility of designing a universal small arms mount based on a two degree of freedom concept that would be capable of testing a variety of small arm weapons.



ACKNOWLEDGEMENTS

The authors wish to express their deep appreciation to Mr. Robert Coberly, Mr. Robert Radkiewicz, and to the test crew at Harry Diamond Laboratory for their contribution in the planning, execution and data reduction efforts, in each of the tests conducted in support of this study. We also wish to thank Mr. Joseph Wilson for his support in obtaining solutions on the analog computer. The authors also wish to acknowledge the help of typist Barbara Dengler and of Mr. Edward Karvelius, who prepared many of the figures contained in the report.

Special thanks is due to Mrs. Jolayne Yeager, of the Research Directorate, for her professional job of typing and assembly of this manuscript.

TABLE OF CONTENTS

	<u>PAGE</u>
1.0 INTRODUCTION	1-1
2.0 DERIVATION OF THE BIOMECHANICAL EQUATIONS OF MOTION FOR SHOULDER FIRED SMALL ARMS	2-1
2.1 Test Fixture Design Procedure	2-1
2.2 High Speed Photographic Test Results	2-1
2.3 Man-Weapon Model Assumptions	2-3
2.4 Historical Background on Human Biodynamical Research	2-5
2.5 System Kinetic Energy	2-6
2.6 System Potential Energy, Dissipative Mechanisms, and Generalized Forces	2-8
2.7 Dynamical Equations of Motion	2-9
2.8 Solution Techniques	2-12
3.0 MAN-WEAPON INTERACTION EXPERIMENTS	3-1
3.1 Description of Experimental Tests	3-1
3.2 M16A1 Test Results	3-3
3.3 M79 and M203 Grenade Launcher Tests	3-3
3.4 Measurement of the Shoulder Reaction Force	3-14
4.0 BIODYNAMICAL SENSITIVITY ANALYSIS	4-1
4.1 Introduction	4-1
4.2 Factors That Affect Weapon Translation	4-1
4.3 Factors That Affect Weapon Pitch Rotation	4-3
4.4 Recommended Design Configurations	4-19

TABLE OF CONTENTS (cont'd)

	<u>PAGE</u>
5.0 CONCLUSIONS AND RECOMMENDATIONS	5-1
5.1 Conclusions	5-1
5.2 Recommendations for Future Work	5-1
APPENDIX A - MODEL REPRESENTATIONS OF THE HUMAN BODY SEGMENTS	A-1
A.1 Head and Torso Representation	A-1
A.2 Right Arm, Left Arm and Weapon Configuration	A-4
A.3 Anthropometric Data and Calculated Results	A-9
APPENDIX B - DIGITAL COMPUTER PROGRAM LISTING	B-1
APPENDIX C - ANALOG COMPUTER SIMULATION	C-1
LITERATURE CITED	D-1

LIST OF ILLUSTRATIONS

<u>FIGURE</u>		<u>PAGE NO.</u>
1	Man-Weapon Interaction Model	2-3
2	M16 Breech Force vs. Time	2-5
3	Generalized Force Diagram	2-10
4	M16 High Speed Photographic Experiment	3-2
5	Experimental Data for the M16A1 Rifle	3-4
6	M79 and M203 Grenade Launcher Experiment	3-5
7	Film 8, Sequence 2 - Weapon Rotation	3-7
8	Film 8, Sequence 4 " " 	3-8
9	Film 8, Sequence 6 " " 	3-9
10	Film 9, Sequence 3 " " 	3-10
11	Film 9, Sequence 5 " " 	3-11
12	Film 9, Sequence 6 " " 	3-12
13	Film 9, Sequence 7 " " 	3-13
14	Measurement of Recoil Force and Weapon Pitch	3-15
15	Shoulder Force Measuring Device	3-16
16	Computation of Transmitted Recoil Force	3-17
17	Computation of Weapon Pitch Rotation θ	3-18
18	Shoulder Spring-Dashpot Model	4-2
19	Analog Computer Simulation-Small Man	4-4
20	Analog Computer Simulation-Medium Man	4-5
21	Analog Computer Simulation-Large Man	4-6
22	Sensitivity of Weapon Rotation to Torso Inertia	4-8
23	Weapon Pitch Rotation vs. Impulse	4-9

LIST OF ILLUSTRATIONS (cont'd)

<u>FIGURE</u>	<u>PAGE NO.</u>
24	Weapon Pitch Rotation vs. Firing Frequency 4-11
25	Weapon Pitch Rotation vs. Barrel Eccentricity 4-12
26	Weapon Pitch Rotation vs. $1/\sqrt{I_x}$ 4-13
27	Weapon Pitch Rotation vs. $\sqrt{K_\phi}$ 4-14
28	Man-Weapon Analysis Mount Force and Total Pitch Angle vs. Time 4-15
29	Man-Weapon Interaction-Weapon Translation 4-16
30	Man-Weapon Interaction-Theta Rotation 4-17
31	Man-Weapon Interaction-Phi Rotation 4-18
32	Three Degrees of Freedom Small Arms Mount Concept . . . 4-20
33	Two Degrees of Freedom Small Arms Mount Concept 4-20
A-1	Head and Torso Rigid Body A-2
A-2	Geometrical Arm and Hand Representations A-5
A-3	Weapon and Arm Rigid Body A-8
C-1	Simplified Analog Computer Diagram of Man-Weapon Interaction Equations C-2

LIST OF TABULAR DATA

<u>TABLE</u>	<u>PAGE NO.</u>
1 M203 GRENADE LAUNCHER TEST CONDITIONS	3-6
2 PARAMETERS THAT DO NOT AFFECT WEAPON ROTATION	4-7
3 SENSITIVITIES OF PARAMETERS THAT AFFECT WEAPON ROTATION	4-19
A-1 WEAPON PARAMETERS	A-7
A-2 WEIGHT AND ANTHROPOMETRIC DATA FOR THREE TEST SUBJECTS	A-10
A-3 CALCULATED BIOMECHANICAL PARAMETERS FOR THREE TEST SUBJECTS	A-10

1.0 INTRODUCTION

For many years the Army has encountered problems in hard stand test firings of shoulder supported weapons. There are two basic causes for these problems:

a. Test fixtures do not adequately represent actual firing situations, which results in an incongruity between data obtained in test firings and actual field use firings.

b. Test fixtures are not universal, so that a particular weapon might reveal one set of characteristics in one type of fixture and a different set in a second type of fixture. For the above reasons many weapon producers have, in the past, been forced to shut down production because their weapons failed to pass acceptance tests. It is estimated that over \$100,000 could have been saved on the M16 rifle program if only one of the many production shut downs due to weapon malfunctioning was eliminated.

The objectives of this report are to determine the feasibility of designing a small arms mount, that adequately simulates the mount reaction force for an actual shoulder supported firing configuration, and to propose a design concept of a mount fixture and arrive at the critical design parameters for the fixture.

To show the feasibility of designing a mounting fixture, a prototype mathematical model was developed that simulates the man and weapon as a coupled dynamical system. The derivation of the model equations is presented in Section 2.0.

Successfully modeling man as an integral part of a weapon system rests upon two important facts. First, the dynamical motions that occur in a typical shooting situation are characterized by small angle oscillatory motions of the human operator about an initial aiming position. Second, the applied breech pressure force consists of a periodic sequence of impulses. Man's neuro-muscular reaction time is slow compared with the weapon firing rate and his ability to think and actively respond to these force inputs does not influence the dynamics of the system until after a significant amount of time has elapsed. An initial passive response phase of motion is, therefore, a characteristic of the man-weapon interaction problem.

Before listing the specific modeling assumptions, a discussion of the exact nature of human dynamical response is presented. The human body is a nonhomogeneous composition of body segments with multiple degrees of freedom. In addition to being nonhomogeneous, each body segment is deformable because of blood flow and muscle action; furthermore, the human neuromuscular system behaves as a servo control mechanism to force inputs. Some peculiarities such as blood flow have little affect on the dynamical behavior of the human body. The dynamical representations of the body segments and the representation of the shooter's behavior as a servo control mechanism is treated by making certain mechanical assumptions.

Because of the overall complexity of the human body, mathematical models of mechanical systems involving human body interactions must pertain to rather specific configurations. Instead of modeling the man-weapon interaction problem for all types of firing positions, a more suitable analytical approach is to model one specific firing position. In this way the kinematical constraints become easier to prescribe and the resulting equations of motion become less complex. Usually two or three firing positions are standard for small arm weapons. The vertical standing position, with the rifle held up against the right shoulder, was chosen for this analysis primarily because the motions of the man and weapon in this position can be adequately represented with only three independent degrees of freedom.

For convenience the time history of motion of the man-weapon system is separated into a set of distinct phases. In particular, the human operator's neuromuscular response is separated into a passive phase followed by an active phase. Breach pressure forces for the M16 rifle consist of a series of impulses of approximately one millisecond duration, which repeat periodically approximately every 80 milliseconds. Because the human body is not capable of reacting actively to force inputs during the first 150-200 ms, this initial time interval is characterized by a passive response of the human operator. Afterwards, the neuromuscular system, which acts somewhat as a servo control mechanism, can significantly influence the weapon motion; however the physical effects of the man's active neuromuscular response generally are not noticeable until after 300 milliseconds have elapsed.

Much insight, in the problem of modeling man-weapon interactions, was provided by observations of high speed photographic films that were obtained from tests conducted at the Harry Diamond Laboratory. In these films, both the top view and the side view of a man firing the M16A1 rifle in automatic fire were recorded. A stationary grid was placed behind the test subjects to provide an inertial reference system. The rifle was held by the test subjects in each of three separate firing positions:

- a. off the hip
- b. on the right shoulder with the body in a vertical standing position
- c. on the right shoulder with the body in a slanted position

The vertical standing position was selected for the theoretical analysis.

Observations of the films helped to establish the predominant degrees of freedom of the system and the time history of motion in each coordinate. Additional high speed photographic data were obtained by Mr. Thomas Hutchings for the M79 and M203 grenade launchers. This data provided the time history motions for the higher impulse weapons (the M79 and M203 grenade launchers generate an impulse of about 2.5 lb-sec compared with 1.2 lb-sec for the M16 rifle). Additional data was obtained for the M16 rifle at the Keith L. Ware Simulation Laboratory, Rock Island Arsenal. A load cell device was used to measure the transmitted shoulder mount force and two displacement transducers were used to obtain the weapon rotation. These experiments are discussed more fully in Section 3.0. The data from these experiments provided considerable insight on how to construct the analytical model and also provided a means for estimating some of the unknown system parameters.

Section 4.0 contains the results of a sensitivity analysis that was performed with the man-weapon interaction model. As a result of this analysis, two prototype small arms mount designs are recommended. The conclusions and recommendations of this study are presented in Section 5.0.

2.0 DERIVATION OF THE BIOMECHANICAL EQUATIONS OF MOTION FOR SHOULDER FIRED SMALL ARMS

2.1 Test Fixture Design Procedure

The design specifications for the universal small arms mount fixture were obtained from analytical simulations of the biomechanical interaction problem. That is, the design configuration and design parameters of the mount are based on results of a dynamic analysis of the man-weapon interaction problem. The specific steps followed in this procedure are listed below:

- a. Determine, through observations of high speed film data, the minimum required number of independent degrees of freedom needed to represent the biomechanical interaction forces for shoulder supported small arm weapons.
- b. Develop a biodynamical model of the man-weapon system and determine the sensitivities, of mount force and of the pitching motion of the weapon, to variations in the various biomechanical system parameters.
- c. Obtain a preliminary design for a universal small arms test fixture based on the biomechanical analog and obtain bounds on the critical design parameters from results of the sensitivity analysis.

2.2 High Speed Photographic Test Results

In order to determine the number of independent degrees of freedom that are associated with the man-weapon interaction problem, several high speed photographic film tests were performed for shoulder supported firings of the M16A1 rifle and the M79 and M203 grenade launchers. These tests involved several shooters of various weights and heights so that the effects of variations in human mount characteristics would be observed. The data extracted from these tests include the transmitted recoil force and motions of the weapon and the shooter. The shoulder support firing configuration was selected for the tests, because the weapon mount forces are easier to measure and the biodynamical motions are less complex than for other standard firing configurations, such as the off-hip configuration.

Observations of the high speed photographic film data led to the development of a man-weapon biodynamics model. The films recorded the test subjects in both the top and side views. The top view was obtained by a 45° inclined mirror located directly above the test subject. During the tests, the shooters fired five rounds from the M16A1 rifle in single shot, semi-automatic, and burst modes, and fired single shots from the grenade launchers at various range settings. Observations of the film sequences for these tests indicated which rotational and translational motions of the weapon and shooter are predominant.

In addition to the translatory motion of the weapon toward the shoulder, two predominant motions of the man-weapon system were observed. These motions include:

a. A rotation in the vertical plane of the upper torso of the man, who initially (for approximately 0.3 second duration) pivoted about his hips. Afterwards the man appears to consciously react to the weapon recoil and his motion becomes more complex.

b. A rotation in the vertical plane of the weapon and the shooter's arms, pivoting about the shoulder. The top view revealed a negligible amount of yawing of either the shooter or the weapon compared with the vertical pitching rotations. Selected angles and position coordinates were measured for each film sequence using the Vanguard Motion Analyzer at the University of Iowa Hospital Biomechanics Laboratory in Iowa City, Iowa.

Results of the high speed photographic film tests reveal a period of relative inactivity in the pitching rotations for approximately the first 20-50 milliseconds after the commencement of each shot. This delay effect is probably caused by the compression of weapon padding and soft body tissue as the weapon translates toward the shoulder. After the weapon is fully compressed against the shoulder the remaining kinetic energy of the weapon induces the rotational pitching motions of both the man and the weapon. Yawing motion apparently was minimized by the stance of the man, as the weapon is held almost parallel with the breadth of his chest during firing. The net torque produced about the man's vertical yaw axis is therefore small.

2.3 Man-Weapon Model Assumptions

A mathematical model simulating the man-weapon biodynamical interactions from weapon recoil was then developed based on information supplied by the film data and on biomechanical data supplied by various sources. Figure 1 contains a schematic representation of the model. The X_1, X_2, X_3 coordinate system is a fixed system with the origin at the man's hip. Coordinate system Y_1, Y_2, Y_3 is attached to the right shoulder pivot and rotates with the weapon. The Y_2 axis is parallel to the gun barrel center-line. Variable x locates the center of mass of the weapon combined with the man's arms. Variable θ measures the absolute pitch of the man in the $X_2 - X_3$ plane and variable ϕ measures the pitch of the weapon relative to the man's trunk. The total pitch of the weapon is therefore the sum of angles θ and ϕ .

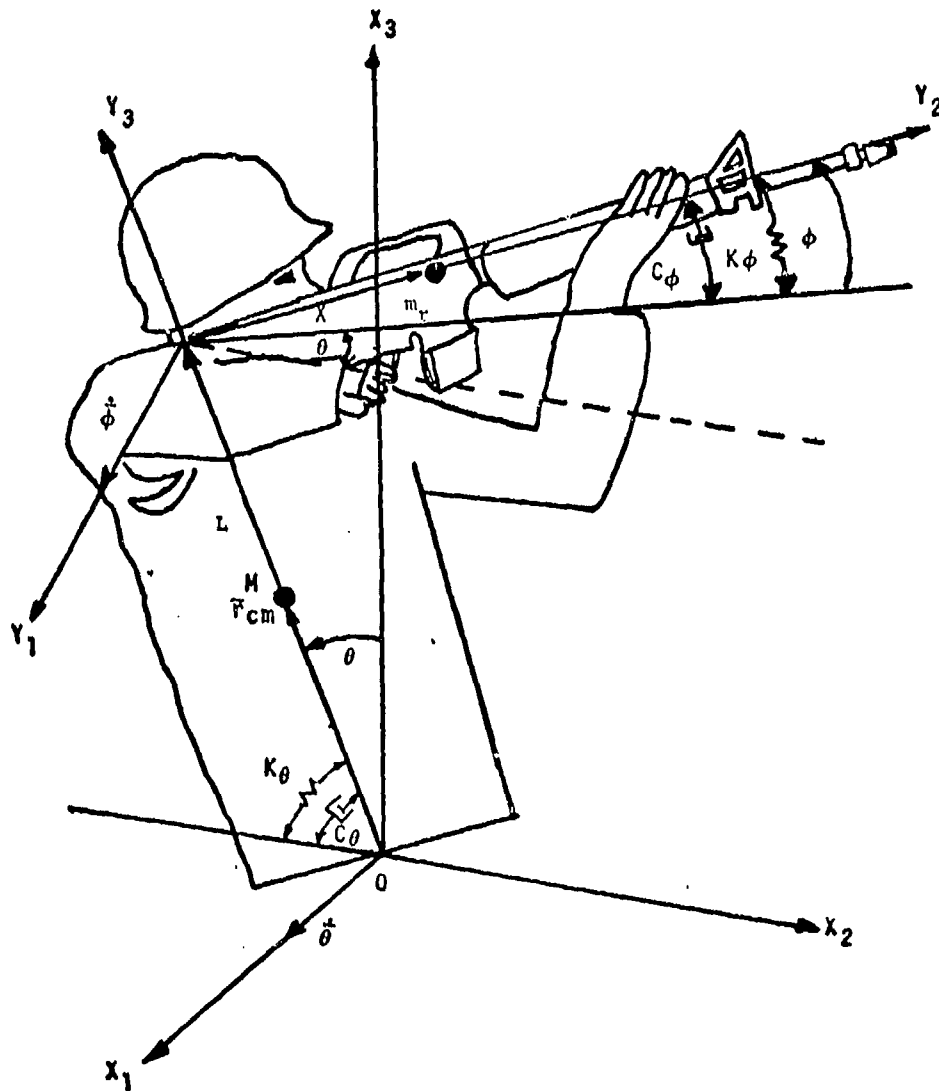


Figure 1 Man-Weapon Interaction Model

Because the development of the biodynamics model involves, in part, a mechanical description of the human body, several simplifying assumptions were required in order to arrive at a fairly simplified but realistic representation of the system. There is no simple or easy approach to modeling human body dynamics and very little useful data is available on biomechanical properties of the human body. The feasibility of successfully modeling man as an integral part of a weapon system rests upon several important considerations, which are discussed below:

(1) The breech pressure force for small arm weapons - rifles and grenade launchers - is impulsive. A typical breech pressure force curve for the M16A1 rifle is illustrated in Figure 2. Normally the M16A1 generates approximately 1.2 lb-sec impulses of about one millisecond duration that repeat periodically every 80 milliseconds.

(2) During the initial portion of a burst, the shooter responds passively to transmitted mount forces. Thus, even though he may anticipate the impulsive recoil force and prepares his muscles accordingly, there is an initial time interval during which the shooter is unable to respond actively to the pulse.

The duration of this passive phase depends primarily on the shooter's neuromuscular reaction characteristics. Moreover, the active response of the shooter intuitively should not have much influence on the time history of the transmitted recoil force. One might expect, however, that the active human control response, after approximately 0.3 seconds or so, might have a significant effect on the angular positioning of both the weapon and the man's upper torso.

c. Observations of the high speed photographic film data reveal that, during the passive response phase, the shooter's hips remain stationary; consequently only the upper torso and arm segments are represented in the biodynamics model.

d. High speed photographic films reveal that the maximum angular pitching motions of the man's upper torso and the weapon are generally less than 10° . A small angle approximation is, therefore, applicable in the formulation of the biodynamical equations of motion. Small angle approximations are particularly useful for generating problem solutions on the analog computer.

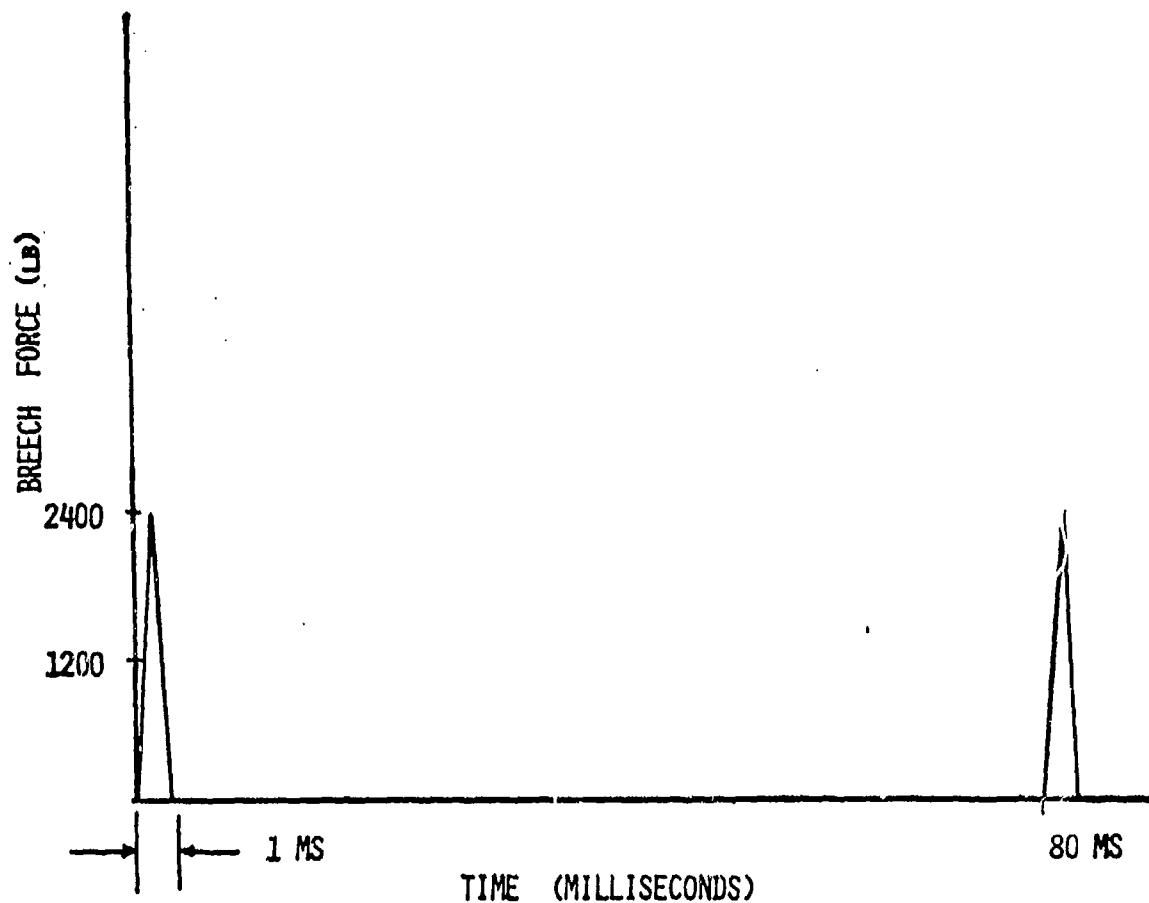


Figure 2 M16 Breech Force vs Time

e. The human body can be represented dynamically as a system of linked rigid bodies that are internally stable and homogeneous; furthermore, each rigid body can be represented by simple geometric forms (i.e. elliptical cylinder, frustrum of a cone, etc). These approximations of the human body have been used in the works published by the investigators listed in References 1, 2, 3.

2.4 Historical Background on Human Biodynamical Research

The lumped mass approach to modeling the dynamics of the human body requires the specification of segment masses, moments of inertia and centers of mass. Active interest in determining the segment characteristics of the

¹Whitsett, C.E., "Some Dynamic Response Characteristics of Weightless Man," Master of Science Thesis, Air Force Institute of Technology, Wright-Patterson Air Force Base, Ohio, AMPL-TR-63-18, AD 412541, 1962

²McCrank, J.M. and Seger, D.E., "Torque Free Rotational Dynamics of a Variable Configuration Body (Application to Weightless Man)," Master of Science Thesis, Air Force Institute of Technology, Wright-Patterson Air Force Base, Ohio, AD 610239, 1964

³McHenry, R.R. and Naab, K.N., "Computer Simulation of the Automobile Crash Victim in a Frontal Collision--A Validation Study," Cornell Aeronautical Laboratory, Inc., Buffalo, New York, CAL Report No. 4B-2126-V-1R, 1966

human body has been undertaken by numerous investigators. Braune and Fisher⁴ in 1889 performed experimental research on three cadavers and published a comprehensive study of weights, volumes, and centers of mass of the body and its segments. Later, in 1906, Fisher⁵ experimentally determined the moments of inertia of segments from a single cadaver. Since that time interest in this subject diminished until rather recently. Dempster⁶, in 1955, published a study on human biomechanics that contains experimental data taken from eight cadavers.

The specific data presented in this study includes segment weights, moments of inertia, densities, center of mass locations and volumes. Using data compiled by Dempster, Braune and Fisher, Barter⁷ in 1957 prepared a series of regression equations for predicting body segment weights from total body weight. These equations have been used extensively by biomechanical engineers and designers. In 1963 Santschi⁸ and his co-workers reported on moments of inertia and centers of mass of sixty-six live test subjects. Santschi attempted to answer the pertinent question of whether or not body segment parameters can be predicted, to a reasonable degree of accuracy, from anthropometric dimensions. He discovered a high correlation factor of segment centers of mass and moments of inertia with an individual's anthropometric dimensions.

2.5 System Kinetic Energy

The formulas that were used to predict the physical characteristics of the man's upper torso and arm segments are listed in Appendix A. Since the man-weapon interaction problem has been reduced to three independent degrees of freedom, the segment masses corresponding to the man's upper torso (i.e. the head and torso) are combined to form a single rigid body

⁴Braune, W. and Fischer, O., "The Center of Gravity of the Human Body as Related to the German Infantryman," Leipzig, ATI 138452, 1889

⁵Fischer, O., "Theoretical Fundamentals for a Mechanics of Living Bodies with Special Applications to Man as Well as to Some Processes of Motion of Machines," B.G. Teubner, Berlin, ATI 153668, 1906

⁶Dempster, W.T., "Space Requirements of the Seated Operator," Wright Air Development Center, TR-55-159, Wright-Patterson Air Force Base, Ohio, AD 87892, 1955

⁷Barter, J.T., "Estimation of the Mass of Body Segments," Wright Air Development Center, Wright-Patterson Air Force Base, Ohio, TR-57-260, AD 118222, 1957

⁸Santschi, W.R., DuBois, J., and Omoto, C., "Moments of Inertia and Centers of Gravity of the Living Human Body, Aerospace Medical Research Laboratories, Wright-Patterson Air Force Base, Ohio, AMRL-TDR-63-66, AD 410451, 1963

and the segment masses corresponding to the man's arm segments and hands and the weapon are combined to form a second rigid body. The rigid body comprising the trunk and the head is allowed to rotate in the vertical plane about the man's hip, while the rigid body comprising the man's arms and the weapon is allowed to translate in the direction of the recoil force and rotate vertically about the shoulder hinge. Any bending of the man's arms during a firing event is considered small and is neglected.

Referring to Figure 1, the kinetic energy of the system is given by

$$T = \frac{1}{2} \left[I_{cm} \dot{\theta}^2 + I_r (\dot{\theta} + \dot{\phi})^2 + M \dot{\bar{r}}_{cm} \cdot \dot{\bar{r}}_{cm} + m_r \dot{\bar{r}} \cdot \dot{\bar{r}} \right] \quad (2-1)$$

where

I_{cm} = Moment of inertia about the center of mass of the head-trunk rigid body.

I_r = Moment of inertia about the center of mass of the arm-weapon rigid body.

M = Mass of the head-trunk rigid body.

m_r = Mass of the arm-weapon rigid body.

$\dot{\bar{r}}_{cm}$ = Time derivative of the center of mass location of the head-trunk rigid body, and,

$\dot{\bar{r}}$ = Time derivative of the center of mass location of the arm-weapon rigid body.

In the X_1, X_2, X_3 frame, the components of vectors \bar{r}_{cm} and \bar{r} are

$$\bar{r}_{cm} = r_{cm} (-\sin \theta \hat{x}_2 + \cos \theta \hat{x}_3) \quad (2-2)$$

$$\begin{aligned} \bar{r} = & [x \cos (\theta + \phi) - L \sin \theta] \hat{x}_2 \\ & + [x \sin (\theta + \phi) + L \cos \theta] \hat{x}_3 \end{aligned} \quad (2-3)$$

Taking the time derivatives of expressions (2-2) and (2-3) and substituting into equation (2-1) leads finally to result

$$T = \left\{ \frac{1}{2} \left(I_{cm} + M r_{cm}^2 \right) \dot{\theta}^2 + I_r (\dot{\theta} + \dot{\phi})^2 + m_r \left[(\dot{x} - L \dot{\theta} \cos \phi)^2 + (x \dot{\phi} + (x + L \sin \phi) \dot{\theta})^2 \right] \right\} \quad (2-4)$$

2.6 System Potential Energy, Dissipative Mechanisms, And Generalized Forces

In order to obtain an expression for the system potential energy, the passive response of the man's muscles must be taken into account. Prior to firing, the shooter's muscles are in a state of preloading to support the weapon and to balance the forces of gravity on both the man and weapon. After the commencement of firing, the approximation is made that passive restoring forces, produced by the various muscles in the upper torso and arms, can be represented by a system of linear springs and dashpots. This approximation is justified based on the small orders of magnitude of the angular deformations resulting from weapon recoil torques. Torsional springs and dashpots are, therefore, included in the model to resist motions in each of the two rotational degrees of freedom. The rearward translatory motion of the weapon initially causes the fleshy padding on the shoulder to compress. Any further rearward displacement of the rifle results in the stretching of the muscles and ligaments that attach to the bone structure of the shoulder. Resistance offered by these muscles and ligaments is modeled by a relatively strong spring and dashpot, while the initial soft compression of the shoulder is modeled by a relatively weak spring. Having represented the elastic and viscous damping characteristics of the model, the system potential energy, V , then becomes

$$\begin{aligned}
 V = & \frac{1}{2} k_{\theta} (\theta - \theta_e)^2 + \frac{1}{2} k_{\phi} (\phi - \phi_e)^2 \\
 & + \begin{cases} \frac{1}{2} k_{x_w} (x - x_e)^2 & \text{for } x \geq x_s \\ \frac{1}{2} k_{x_s} (x - x_s)^2 + k_{x_w} (x_s - x_e) [x - \frac{1}{2} (x_s + x_e)] & \text{for } x < x_s \end{cases} \\
 & + M g r_{cm} (\cos \theta - \cos \theta_0) + m_r g [L(\cos \theta - \cos \theta_0) \\
 & + x \sin (\theta + \phi) - x_0 \sin (\theta_0 + \phi_0)] \quad (2-5)
 \end{aligned}$$

where

$k_{\theta}, k_{\phi}, k_{x_w}, k_{x_s}$ = system spring constants

θ_0, ϕ_0, x_0 = initial conditions for variables $\theta, \phi,$ and x respectively

θ_e, ϕ_e, x_e = static equilibrium spring positions

g = gravity constant

and

x_s = distance from the shoulder at which the shoulder spring stiffness changes value.

Because the only dissipative mechanisms in the model are viscous dampers, a dissipative force potential, P , can be defined and is given by

$$P = \frac{1}{2} c_x \dot{x}^2 + \frac{1}{2} c_\theta \dot{\theta}^2 + \frac{1}{2} c_\phi \dot{\phi}^2 \quad (2-6)$$

where c_x , c_θ , and c_ϕ are the damping constants for the variables x , θ , ϕ , respectively.

Referring to Figure 3, the generalized forces produced by the breech pressure force, $F(t)$, are

$$Q_x = -F(t) \quad (2-7a)$$

$$Q_\theta = (\bar{r}_{D/A} \times \bar{F}) \cdot \hat{x}_1$$

and

$$Q_\phi = (\bar{r}_{D/B} \times \bar{F}) \cdot \hat{y}_1$$

where

$$\begin{aligned} \bar{r}_{D/A} = & [-L \sin \theta + x \cos (\theta + \phi) - \delta \sin (\theta + \phi)] \hat{x}_2 \\ & + [L \cos \theta + x \sin (\theta + \phi) + \delta \cos (\theta + \phi)] \hat{x}_3 \end{aligned}$$

$$\bar{r}_{D/B} = x \hat{y}_2 + \delta \hat{y}_3$$

$$\begin{aligned} \bar{F} = & -F(t) \hat{y}_2 \\ = & -F(t) [\cos (\theta + \phi) \hat{x}_2 + \sin (\theta + \phi) \hat{x}_3] \end{aligned}$$

Expanding the above expressions for Q_θ and Q_ϕ yields finally the results

$$Q_\theta = (\delta + L \cos \phi) F(t) \quad (2-7b)$$

and

$$Q_\phi = \delta \cdot F(t) \quad (2-7c)$$

2.7 Dynamical Equations of Motion

The dynamical equations of motion of the man-weapon interaction problem were derived using the Lagrangian formulation,

$$\frac{d}{dt} \frac{\partial L}{\partial \dot{x}} - \frac{\partial L}{\partial x} + \frac{\partial P}{\partial \dot{x}} = Q_x \quad (2-8a)$$

$$\frac{d}{dt} \frac{\partial L}{\partial \dot{\theta}} - \frac{\partial L}{\partial \theta} + \frac{\partial P}{\partial \dot{\theta}} = Q_\theta \quad (2-8b)$$

$$\frac{d}{dt} \frac{\partial L}{\partial \dot{\phi}} - \frac{\partial L}{\partial \phi} + \frac{\partial P}{\partial \dot{\phi}} = Q_\phi \quad (2-8c)$$

where $L \stackrel{\Delta}{=} T - V$ is the Lagrangian potential function. Substituting equations (2-1) to (2-7) into equations (2-8) and rearranging terms leads finally to the following matrix equation:

$$\begin{bmatrix} a_{11} & -a_{21} & 0 \\ -a_{21} & a_{22} + a_{33} & a_{23} \\ 0 & a_{23} & a_{33} \end{bmatrix} \begin{Bmatrix} \ddot{x} \\ \ddot{\theta} \\ \ddot{\phi} \end{Bmatrix} = \begin{Bmatrix} f_x \\ f_\theta \\ f_\phi \end{Bmatrix} \quad (2-9)$$

where

$$a_{11} = m_r$$

$$a_{21} = m_r L \cos \phi$$

$$a_{22} = I_{cm} + M r_{cm}^2 + m_r L^2 + 2 m_r L x \sin \phi$$

$$a_{23} = a_{33} + m_r L x \sin \phi$$

$$a_{33} = I_r + m_r x^2$$

$$f_x = -F(t) + m_r x (\dot{\theta} + \dot{\phi})^2 + m_r \dot{\theta}^2 L \sin \phi - c_x \dot{x} - m_r g \sin (\theta + \phi)$$

$$- \begin{cases} k_{x_w} (x - x_e), & \text{for } x \geq x_s \\ k_{x_s} (x - x_s) + k_{x_w} (x_s - x_e), & \text{for } x < x_s \end{cases}$$

$$\begin{aligned}
f_g = & (\delta + L \cos \phi) F(t) - c_\theta \dot{\theta} \\
& - 2 m_r \dot{x} (\dot{\theta} + \dot{\phi}) (x + L \sin \phi) \\
& - m_r L x \dot{\phi} (2\dot{\theta} + \dot{\phi}) \cos \phi - k_\theta (\theta - \theta_e) \\
& + M g r_{cm} \sin \psi + m_r g [L \sin \theta - x \cos (\theta + \phi)]
\end{aligned}$$

$$\begin{aligned}
f_\phi = & \delta F(t) - 2 m_r x \dot{x} (\dot{\theta} + \dot{\phi}) + m_r L x \dot{\theta}^2 \cos \phi \\
& - c_\phi \dot{\phi} - k_\phi (\phi - \phi_e) - m_r g x \cos (\theta + \phi)
\end{aligned}$$

The static equilibrium spring positions x_e , θ_e , and ϕ_e are determined from the requirement that initially

$$f_x = f_\theta = f_\phi = 0$$

if $F(0) = 0$ and the initial velocity components are zero. These conditions imply

$$\begin{aligned}
f_x = & - F(t) + m_r x (\dot{\theta} + \dot{\phi})^2 + m_r \dot{\theta}^2 L \sin \phi \\
& - c_x \dot{x} - m_r g [\sin (\theta + \phi) - \sin (\theta_0 + \phi_0)] \\
& - \begin{cases} k_{x_w} (x - x_0), & \text{for } x \geq x_s \\ k_{x_s} (x - x_s) + k_{x_w} (x_s - x_0), & \text{for } x < x_s \end{cases} \\
f_\theta = & (\delta + L \cos \phi) F(t) - 2 m_r \dot{x} (\dot{\theta} + \dot{\phi}) (x + L \sin \phi) \\
& - m_r L x \dot{\phi} (2\dot{\theta} + \dot{\phi}) \cos \phi - c_\theta \dot{\theta} - k_\theta (\theta - \theta_0) \\
& + (M r_m + m_r L) g (\sin \theta - \sin \theta_0) - m_r g x [\cos (\theta + \phi) - \cos (\theta_0 + \phi_0)]
\end{aligned}$$

and

$$\begin{aligned}
f_\phi = & \delta F(t) - 2 m_r x \dot{x} (\dot{\theta} + \dot{\phi}) + m_r L x \dot{\theta}^2 \cos \phi \\
& - c_\phi \dot{\phi} - k_\phi (\phi - \phi_0) - m_r g x [\cos (\theta + \phi) - \cos (\theta_0 + \phi_0)].
\end{aligned}$$

2.8 Solution Techniques

Two methods were used to solve the matrix equation (2-9). In the first method, the system of equations were solved numerically on a digital

computer by the Runge-Kutta method. In order to apply the Runge-Kutta method, equation (2-9) is premultiplied by the inverse of the coefficient matrix and the resulting system of three second order differential equations is transformed into a system of six first order differential equations. This results in the set of matrix equations given below:

$$\frac{d}{dt} \begin{pmatrix} \dot{x} \\ \dot{\theta} \\ \dot{\phi} \end{pmatrix} = \frac{1}{\Delta} \begin{bmatrix} b_{11} & b_{12} & b_{13} \\ b_{12} & b_{22} & b_{23} \\ b_{13} & b_{23} & b_{33} \end{bmatrix} \begin{pmatrix} f_x \\ f_\theta \\ f_\phi \end{pmatrix} \quad (2-10a)$$

and

$$\frac{d}{dt} \begin{pmatrix} x \\ \theta \\ \phi \end{pmatrix} = \begin{pmatrix} \dot{x} \\ \dot{\theta} \\ \dot{\phi} \end{pmatrix} \quad (2-10b)$$

where

$$\begin{aligned} \Delta &= \det [a] \\ &= (a_{33}^2 - a_{23}^2 + a_{22} a_{33}) a_{11} - a_{21}^2 a_{33}, \\ &= (I_{cm} + M r_{cm}^2) m_r (I_r + m_r x^2) + I_r m_r^2 L^2 \sin^2 \phi, \\ b_{11} &= (I_{cm} + M r_{cm}^2 + m_r L^2) I_r + m_r x^2 (I_{cm} + M r_{cm}^2 + m_r L^2 \cos^2 \phi) \\ b_{12} &= (I_r + m_r x^2) m_r L \cos \phi \\ b_{13} &= - [I_r + m_r (x + L \sin \phi) x] m_r L \cos \phi, \\ b_{22} &= m_r (I_r + m_r x^2), \\ b_{23} &= - m_r [I_r + m_r x (x + L \sin \phi)], \end{aligned}$$

and

$$b_{33} = m_r [I_{cm} + M r_{cm}^2 + I_r + m_r (x + L \sin \phi)^2].$$

The solutions to equations (2-10) were obtained by separating the weapon cycle into two time intervals. For the one millisecond time interval, on

which the impulsive breech pressure force is applied, equations (2-10) are integrated with the assumption that the positional coordinates are constant. Thus let

$$I_F \triangleq \int_{t_k}^{t_k + 1} F(t) dt$$

where t_k = starting time for the shot and $t_k + 1 = t_k + 0.001$. The integration of equations (2-10) yields a set of initial conditions for the start of the second time interval,

$$\begin{Bmatrix} \dot{x}(t_k + 1) \\ \dot{\theta}(t_k + 1) \\ \dot{\phi}(t_k + 1) \end{Bmatrix} = \begin{Bmatrix} \dot{x}(t_k) \\ \dot{\theta}(t_k) \\ \dot{\phi}(t_k) \end{Bmatrix} + \frac{I_F}{\Delta(t_k)} \begin{bmatrix} b_{11} & b_{12} & b_{13} \\ b_{21} & b_{22} & b_{23} \\ b_{31} & b_{32} & b_{33} \end{bmatrix} \begin{Bmatrix} -1 \\ \delta + L \cos \phi \\ \delta \end{Bmatrix} \quad (2-11a)$$

$t=t_k$

and

$$\begin{Bmatrix} x(t_k + 1) \\ \theta(t_k + 1) \\ \phi(t_k + 1) \end{Bmatrix} = \begin{Bmatrix} x(t_k) \\ \theta(t_k) \\ \phi(t_k) \end{Bmatrix} \quad (2-11b)$$

For the remainder of the weapon cycle (i.e. until the commencement of the next shot), the equations (2-10) are solved by the Runge-Kutta method (with $F(t) = 0$) and equations (2-11) provide the initial conditions. This solution procedure is then repeated for each of the remaining shots in the burst. A listing of the computer program used to obtain the numerical solutions to the problem is provided in Appendix B.

The digital computer solutions to the biodynamics problem were obtained for a range of biomechanical parameters corresponding to a small, average and large shooter, and for a range of weapon parameters corresponding to the M16A1 rifle and the M79 and M203 grenade launchers. A sensitivity analysis was performed to obtain estimates of the unknown spring and dash-

pot parameters, for several of the weapon and shooter configurations. The results of this analysis are discussed in Section 4.0.

In the second solution method, the system of equations (2-9) were first simplified by small angle approximations, scaled and then programmed on an analog computer. Analog techniques are suitable for performing a parametric sensitivity analysis, because each system parameter can be conveniently changed by adjusting a pot setting and the solutions are displayed immediately on a recording device. Further details regarding the analog simulation are provided in Appendix C.

3.0 MAN-WEAPON INTERACTION EXPERIMENTS

3.1 Description of Experimental Tests

In order to gather the critical information needed to analytically describe the man-weapon interaction problem, three separate series of experiments were performed that involved test firings with several shooters of various sizes and various weapon types. Data gathered from these tests include:

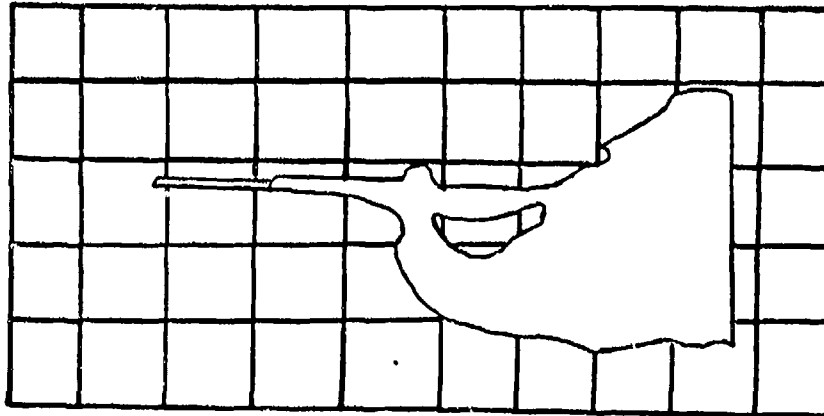
a. M16 data obtained from the Harry Diamond Laboratory using high speed photographic equipment to record time histories of rotations and displacements of body segments and of the weapon.

b. M79 and M203 grenade launcher data obtained at the Harry Diamond Laboratory test facility using high speed photographic equipment to record rotations and displacements of the weapon and the man.

c. M16 data from the Keith L. Ware Simulation Laboratory, obtained using a fixture between the shoulder and the weapon to measure force reactions at the shoulder and two displacement transducers located at the front and rear of the weapon to measure rotations of the weapon.

In both photographic data experiments at the Harry Diamond Laboratory, the shooters stood in front of a background of vertical and horizontal grid lines. These grid lines formed a fixed reference frame from which relative motions of the man and weapon were measured. Both top and side views were photographed. The top view was recorded by use of an inclined mirror placed directly above the test subject (see Figure 4). The film speed of 1100 frames/second was sufficiently fast to record the ejection of muzzle smoke after each shot from the M16 rifle. Thus the time of occurrence of each shot was measured for the five shot burst. Fixed reference points were selected at the intersections of stationary grid lines on the side and top views. For each frame, the positions of several selected points on the man and weapon were measured with respect to the selected reference points using a Vanguard Motion Analyzer. A computer program was then used to process and convert the raw data into values of angular displacements of the weapon and man.

OVERHEAD MIRROR VIEW



SIDE VIEW

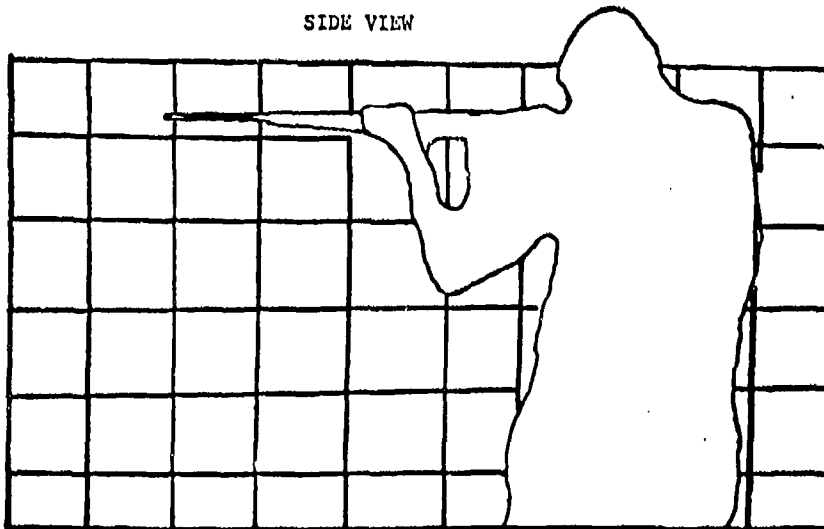


Figure 4 M16 High Speed Photographic Experiment

3.2 M16A1 Test Results

Some of the important observations and interpretations of the M16 data are discussed below. Two major angular motions of the weapon system were observed in addition to the translatory motion of the rifle towards the shoulder. They are:

- a. An angular deflection of the man's trunk that pivoted about his hip. This motion is referred to as pitch of the man.
- b. An angular pivoting of the arms and rifle about the man's shoulder. This motion is referred to as pitch of the rifle.

A plot of the two pitch coordinates versus time is shown in Figure 5. A period of relative inactivity is noticeable in the pitch of the man just after the first and second shots. During this period of inactivity, the weapon most likely is compressing against the soft muscular portion of the shoulder. A period of activity in the pitch coordinates follows the completion of the soft compressive phase. Yawing of the man and rifle was small compared with the pitching rotations. Yaw was minimized by the rigid stance of the man and his initial positioning of the rifle.

3.3 M79 and M203 Grenade Launcher Tests

The grenade launcher tests were performed on an experimental setup similar to the M16 experiment (see Figure 6). One difference was that fixed points on the man and the weapon were identified by circular pieces of reflective tape. The tape markings helped to simplify the data reduction on the Vanguard Motion Analyzer. Another modification in the grenade launcher tests was that the rotatory prism type camera was replaced with a shutter type camera, operating at a slower 500 frames/second, to improve the film resolution. The reduced film speed is sufficient to identify when the grenade exits the barrel and to obtain continuous time history data of all significant motions. Several film sequences were recorded with different size men who fired from both the shoulder and hip configurations. The data were reduced, on the Vanguard Motion Analyzer, by the Intertech Corporation in Iowa City, Iowa. In reduced form, the data provided pitch and yaw rotations of the weapon along with the pitch of the man and the weapon displacement.

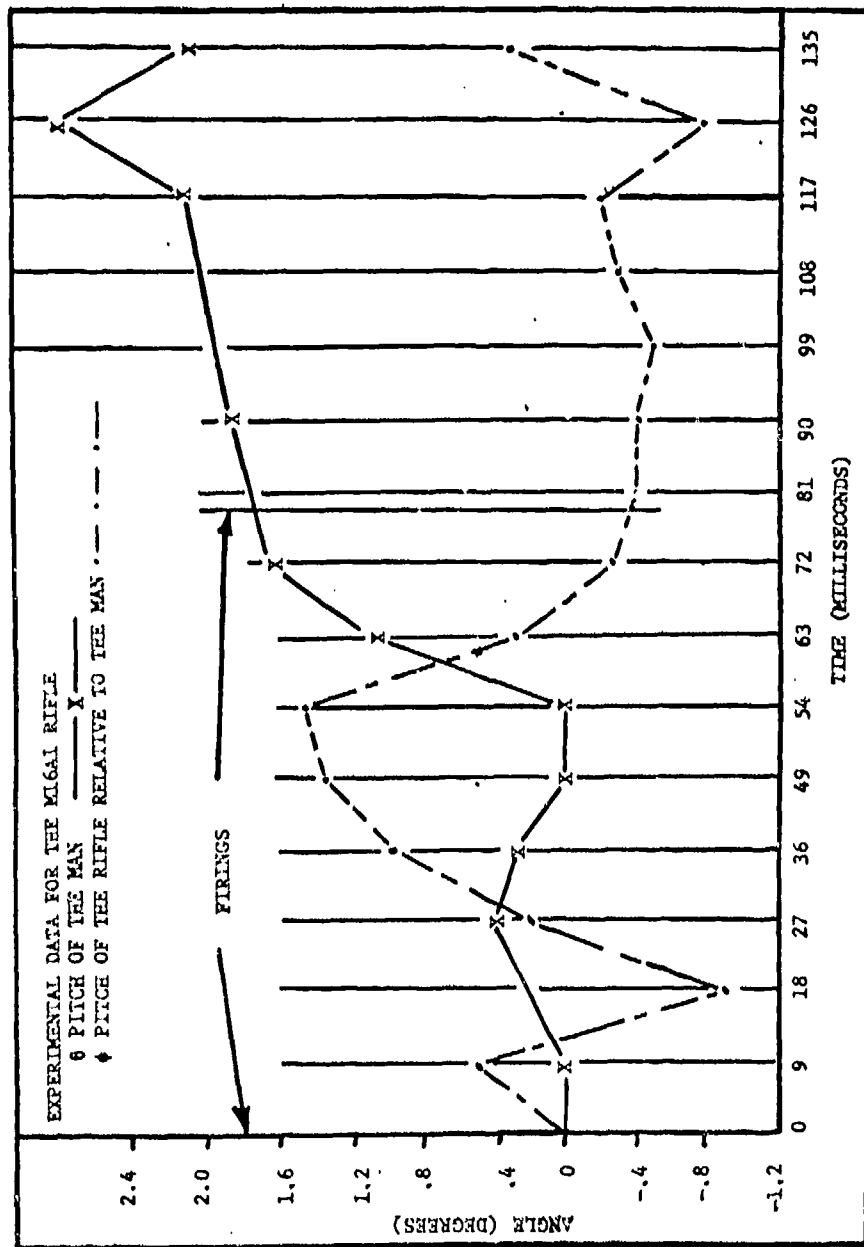
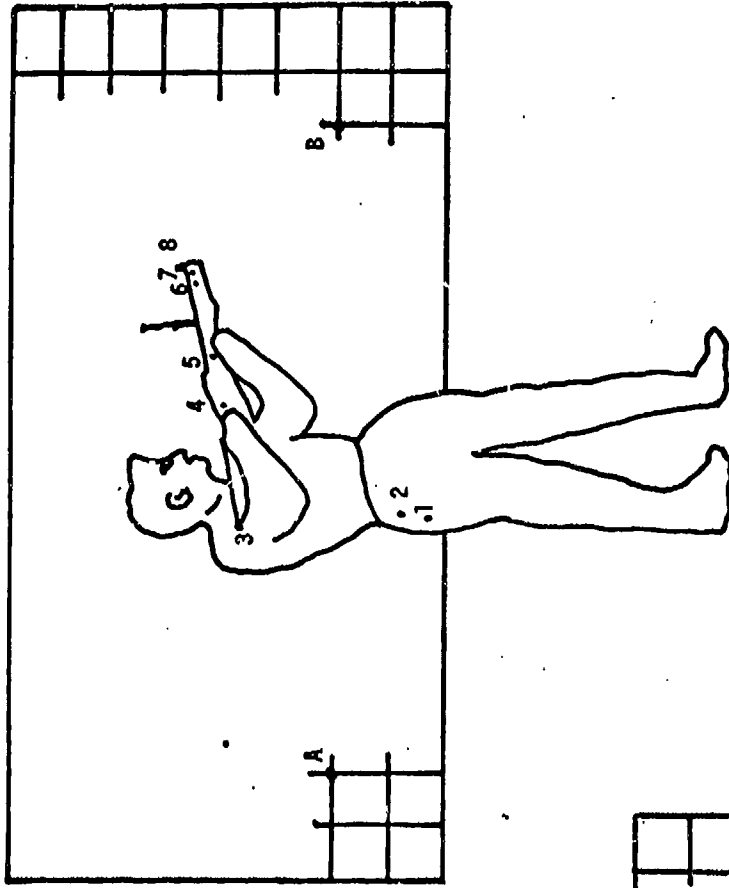


Figure 5 Experimental Data For The M16A1 Rifle



OVERHEAD MIRROR VIEW

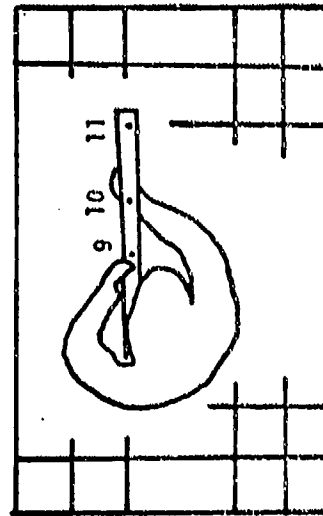


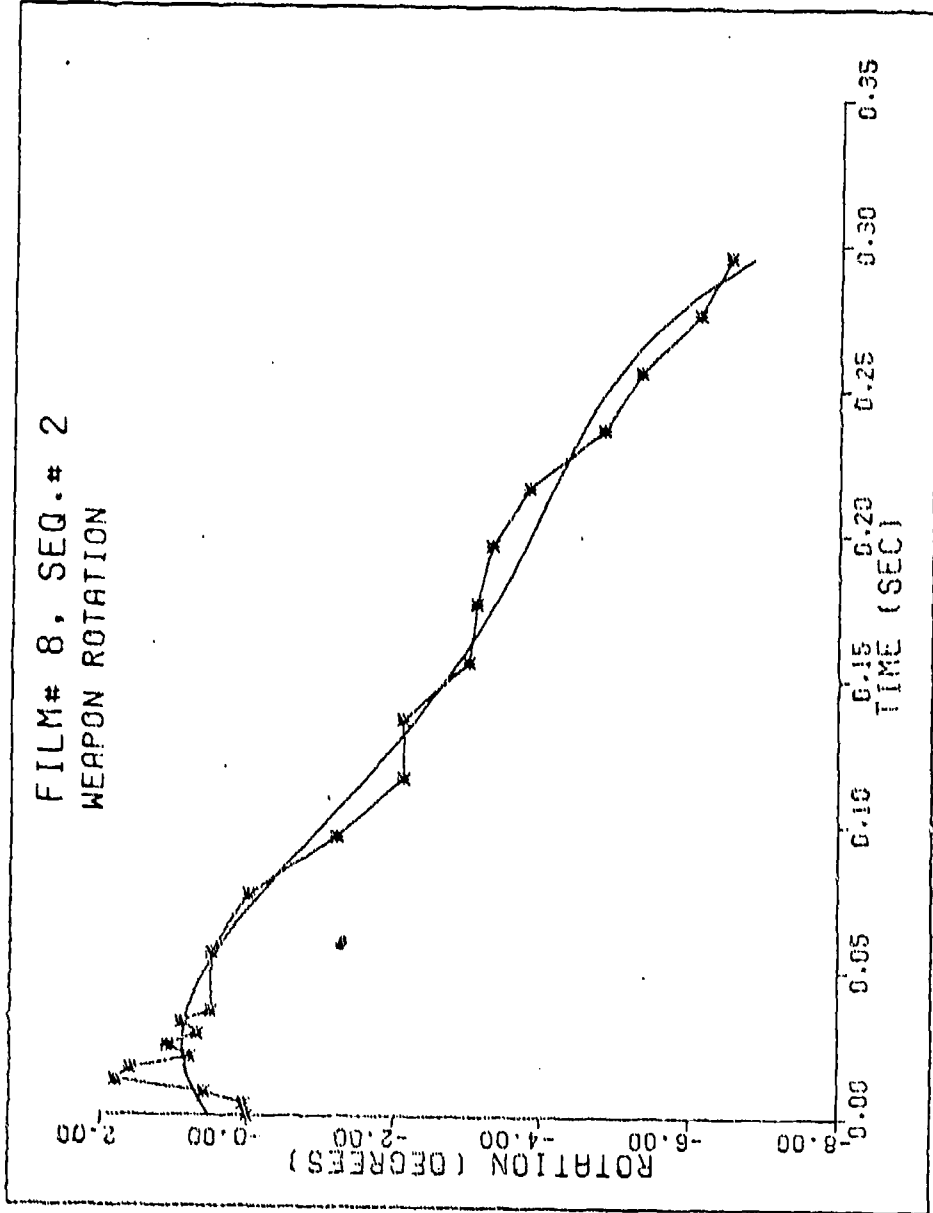
Figure 6 M79 and M203 Grenade Launcher Experiment

The M203 grenade launcher data were the most thoroughly studied data. The M203 grenade launcher is mounted below the barrel on the M16 rifle, thus causing this weapon to pitch downward rather than upward, as most other weapons do. Also the data for the shoulder support configuration reveal that the pitch rotation of the weapon varies somewhat with the size of the shooter. There is less pitch of the weapon for a heavier man than for a lighter man. This is expected because the heavier man has greater inertia. Firings from the hip produced less weapon pitch than firings from the shoulder. Again, this is expected since the constraints on the weapon in the hip firing position tend to limit the amount of weapon pitch rotation.

Plots of the total weapon rotation versus time have been generated for the test firings of the M79 and M203 grenade launchers. Several of the plots for the M203 grenade launcher tests appear in Figures 7 to 13. The test conditions for these film sequences are listed in Table 1. Each plot contains both the measured weapon pitch angle data points, connected by straight line segments, and a fourth order least square polynomial approximation to the data. The time interval begins at the commencement of firing and ends approximately when the man's active neuromuscular response starts to influence the motions of the system (i.e. at roughly 0.3 second). In each film sequence, the weapon pitches downward from the initial aim elevation angle to a maximum value of about seven degrees. The shapes of the plots vary somewhat both for different shooters and different aim elevations. The plots in Figures 11 and 12 reveal that different test results were obtained even for tests repeated under identical conditions. This may be due partly because of errors in data reduction and because the shooter does not prepare himself in exactly the same way for each shot.

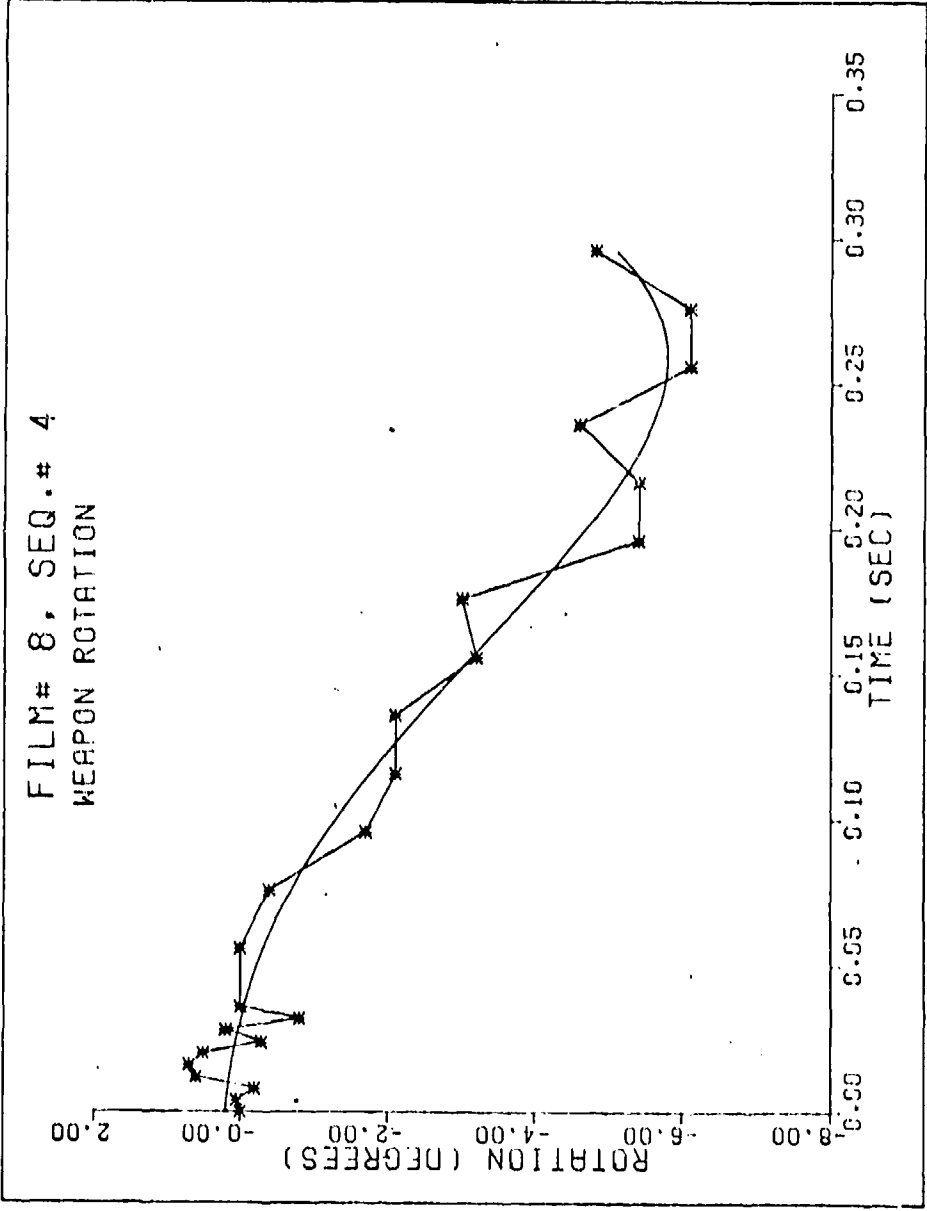
TABLE 1 M203 GRENADE LAUNCHER TEST CONDITIONS

FILM	SEQUENCE	SHOOTER WEIGHT (LB)	ELEVATION ANGLE (DEG)
8	2	140	5°
8	4	140	10°
8	6	140	20°
9	3	165	5°
9	5	165	10°
9	6	165	10°
9	7	165	20° - 25°



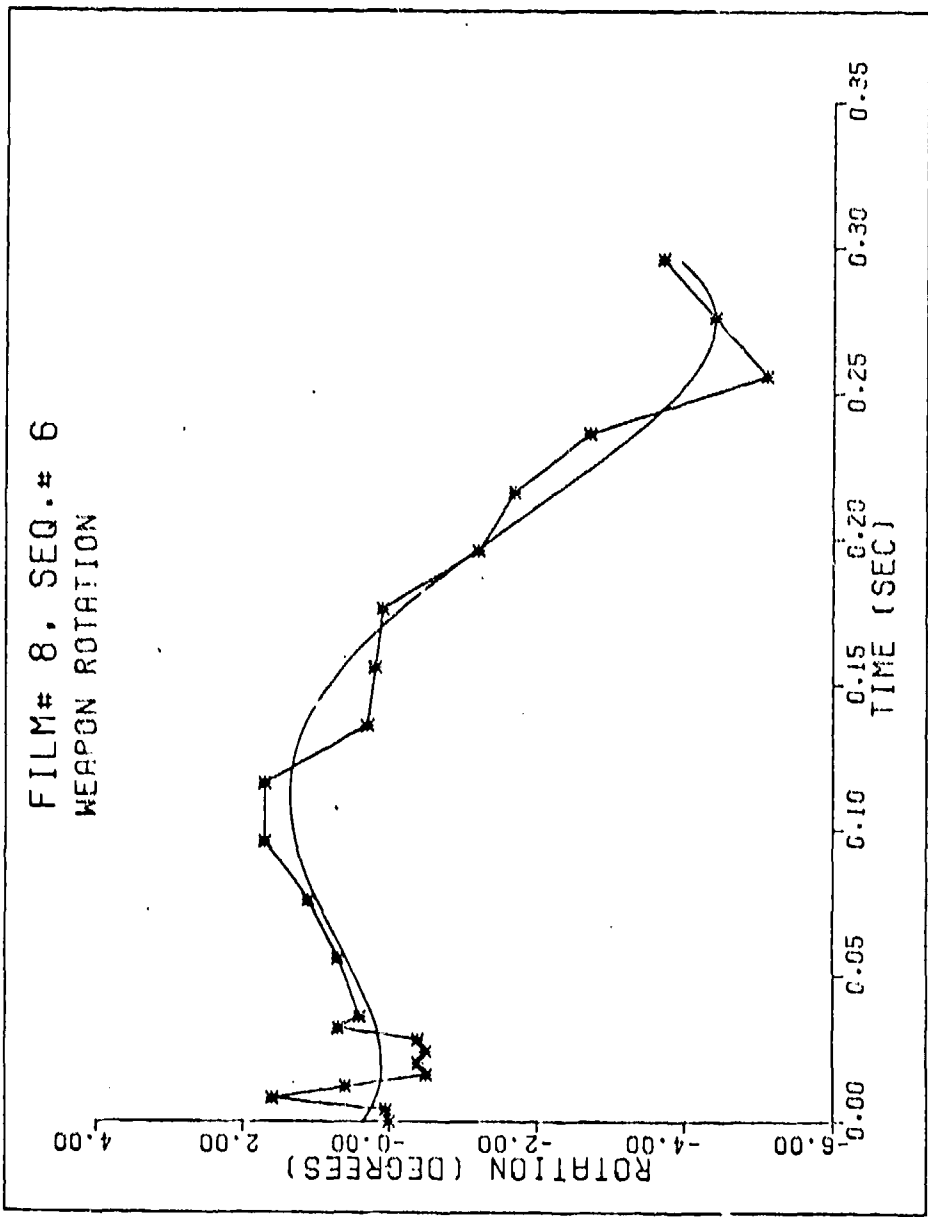
DATE= 6/23/75 TIME= 4:33 PM

Figure 7 Film# 8, Seq.# 2 - Weapon Rotation



DATE= 6/23/75 TIME= 4:33 PM

Figure 8 Film# 8, Seq.# 4 - Weapon Rotation



DATE= 6/23/75 TIME= 4:34 PM

Figure 9 Film# 8, Seq.# 6 - Weapon Rotation

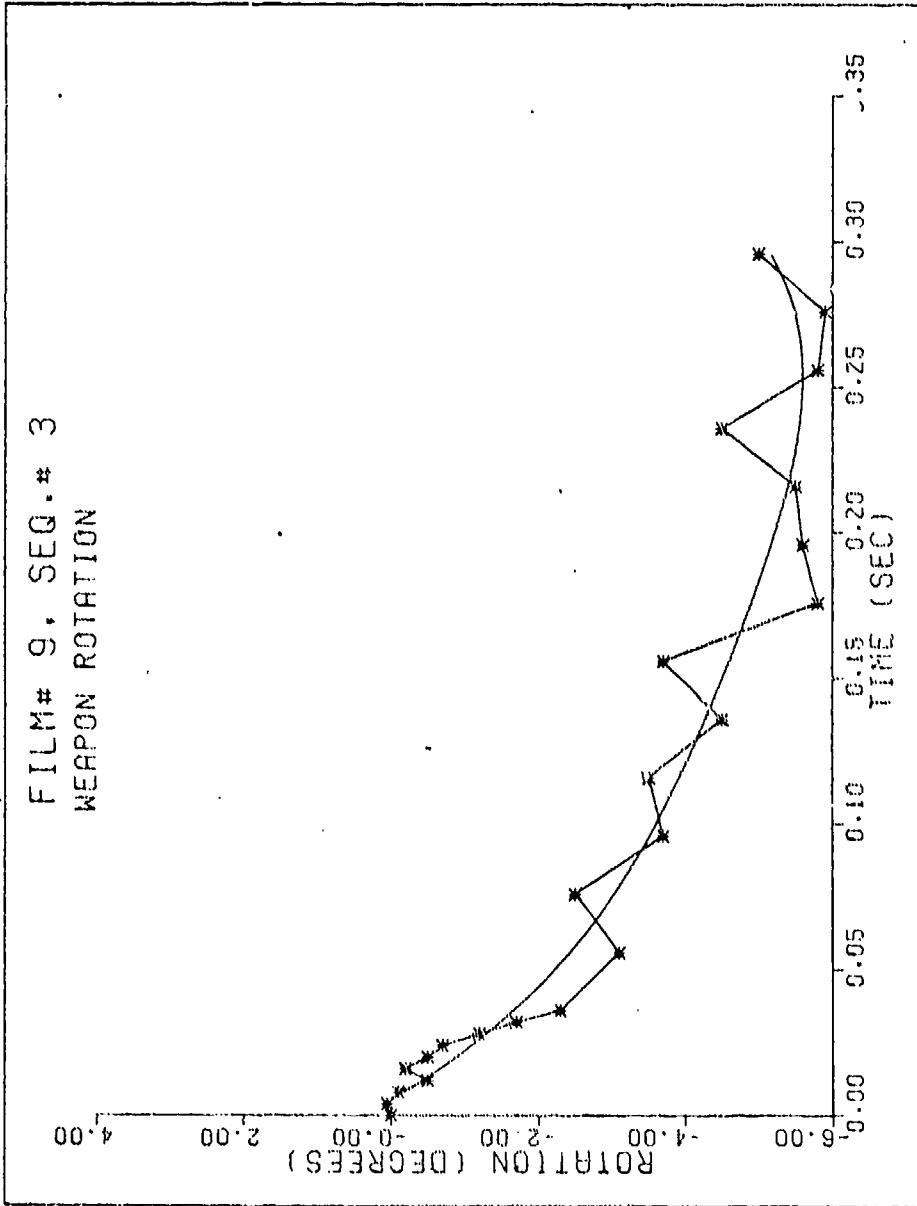
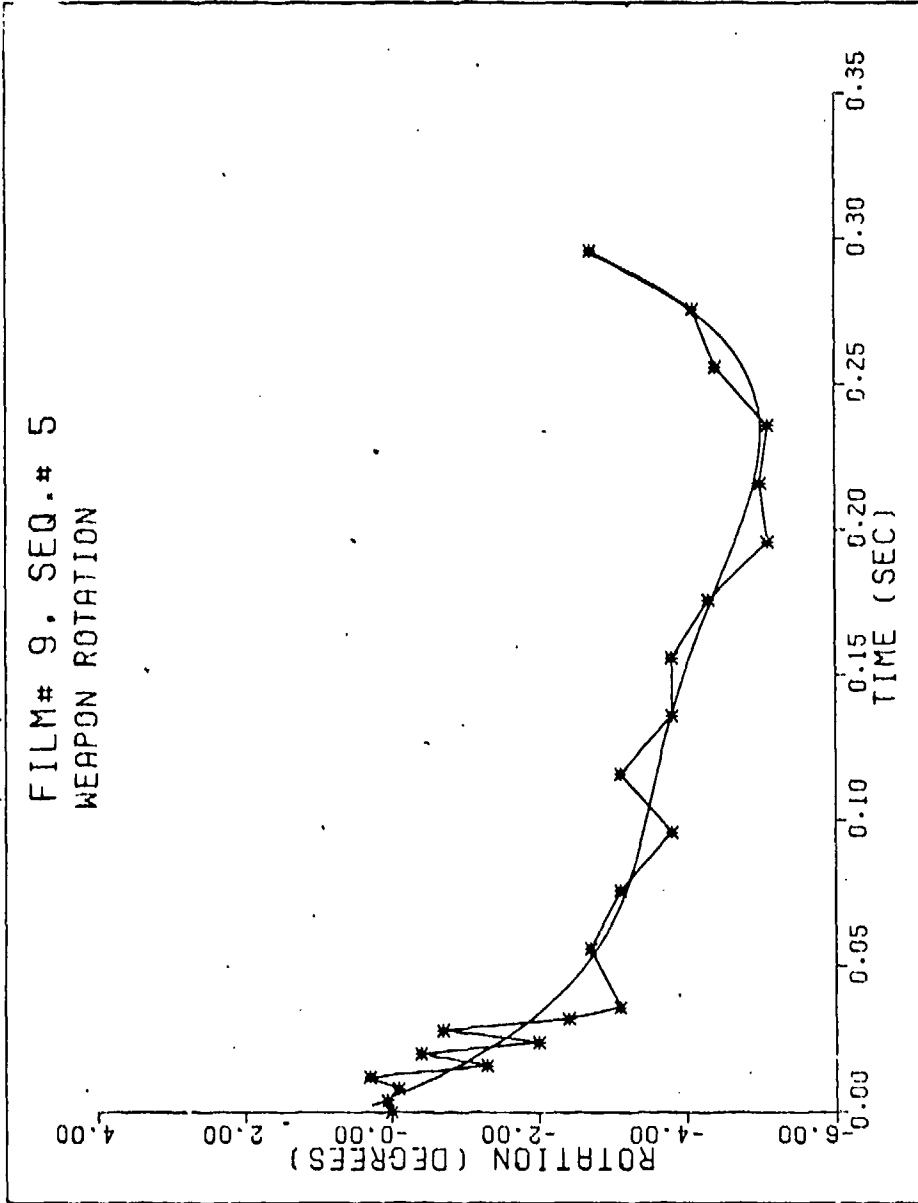


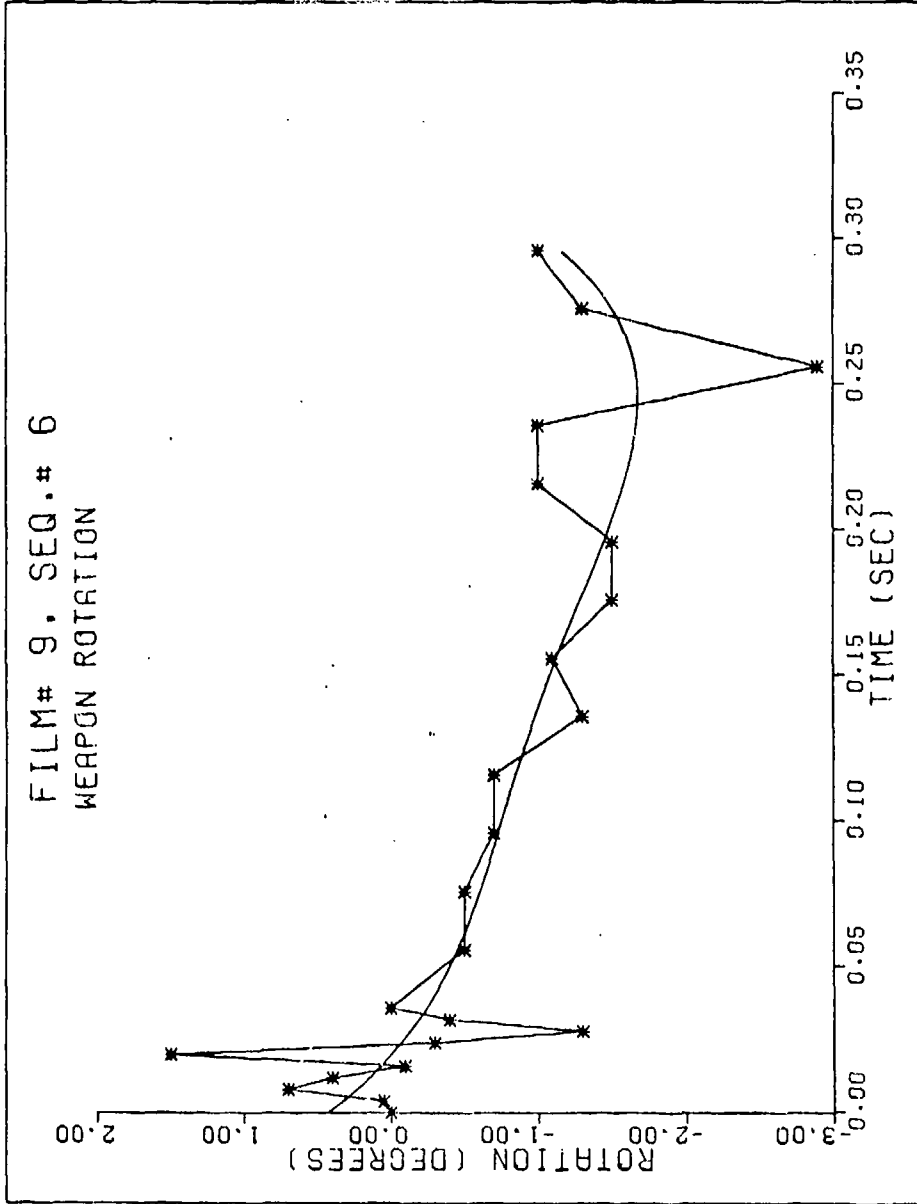
Figure 10 Film# 9, Seq.# 3 - Weapon Rotation

FILM# 9. SEQ.# 5
WEAPON ROTATION



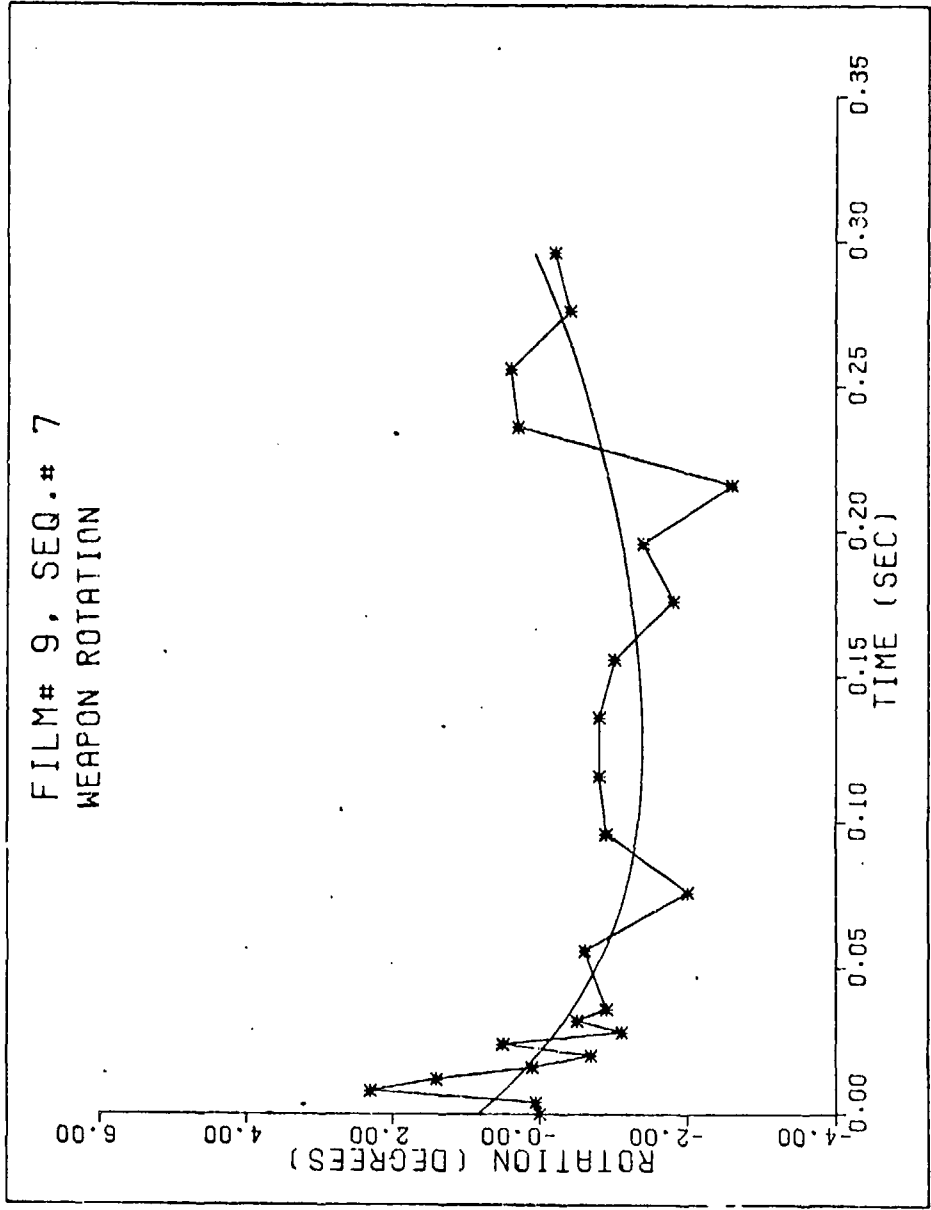
DATE= 6/23/75 TIME= 4:31 PM

Figure 11 Film# 9, Seq.# 5 - Weapon Rotation



DATE= 6/23/75 TIME= 4:31 PM

Figure 12 Film# 9, Seq.# 6 - Weapon Rotation



DATE= 6/23/75 TIME= 4:31 PM

Figure 13 Film# 9, Seq.# 7 - Weapon Rotation

3.4 Measurement of the Shoulder Reaction Force

Additional M16 data were obtained at the Keith L. Ware Simulation Laboratory. The experimental setup is shown in Figure 14. A shoulder fixture (see Figure 15) containing load cells and an accelerometer was used to measure the weapon recoil force transmitted to the man's shoulder. The force reaction at the shoulder is obtained by subtracting the inertial force of the fixture from the measured load cell force (see Figure 16). The linear potentiometers measured the vertical displacement of the weapon at two points on the rifle. Referring to Figure 17, the weapon pitch rotation, θ , is then calculated from the difference between the two vertical displacements.

The most significant conclusion that was drawn from the Ware Laboratory data is that the shoulder reaction force is of very short duration (i.e. impulsive) compared with the rifle firing cycle time. The maximum forces ranged from 20 to 180 pounds. Peak recoil forces tended to be greater for the larger riflemen than for the smaller riflemen. Also, the peak values tended to decrease significantly from round to round. The ratios of peak values for successive shots varied considerably among the tests. Ratios for successive peak recoil forces in the neighborhood of 0.85, however, were common.

The data gathered from these experiments provided insight for constructing the simulation model and provided a means for estimating some of the unknown parameters in the model (i.e. stiffness and damping constants). The time history data obtained by high speed photography is more reliable than the data measured by linear potentiometers, because the photographic technique does not have any direct influence on the experiment. On the other hand, the use of high speed photography to measure motions has the disadvantage of requiring a large amount of time and effort in data reduction.

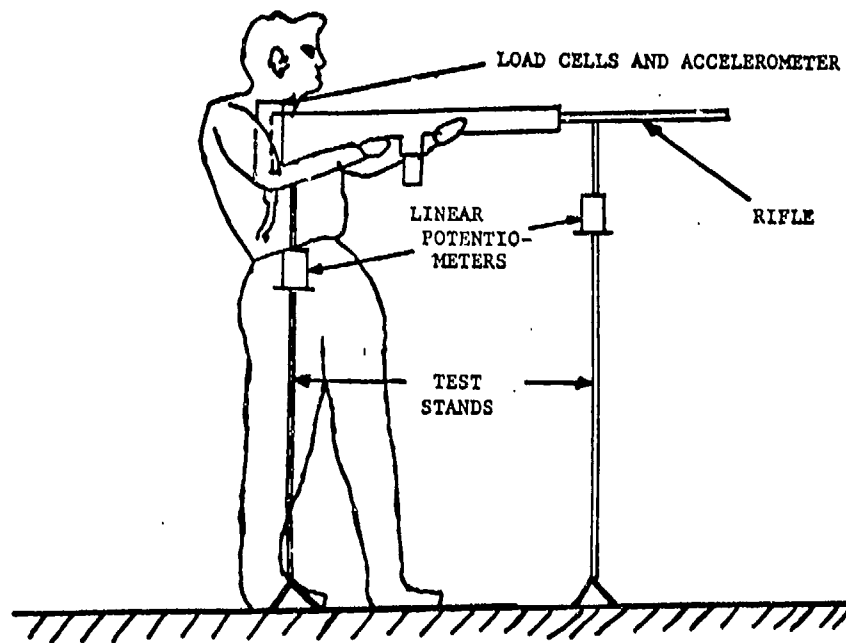


Figure 14 Measurement of Recoil Force and Weapon Pitch

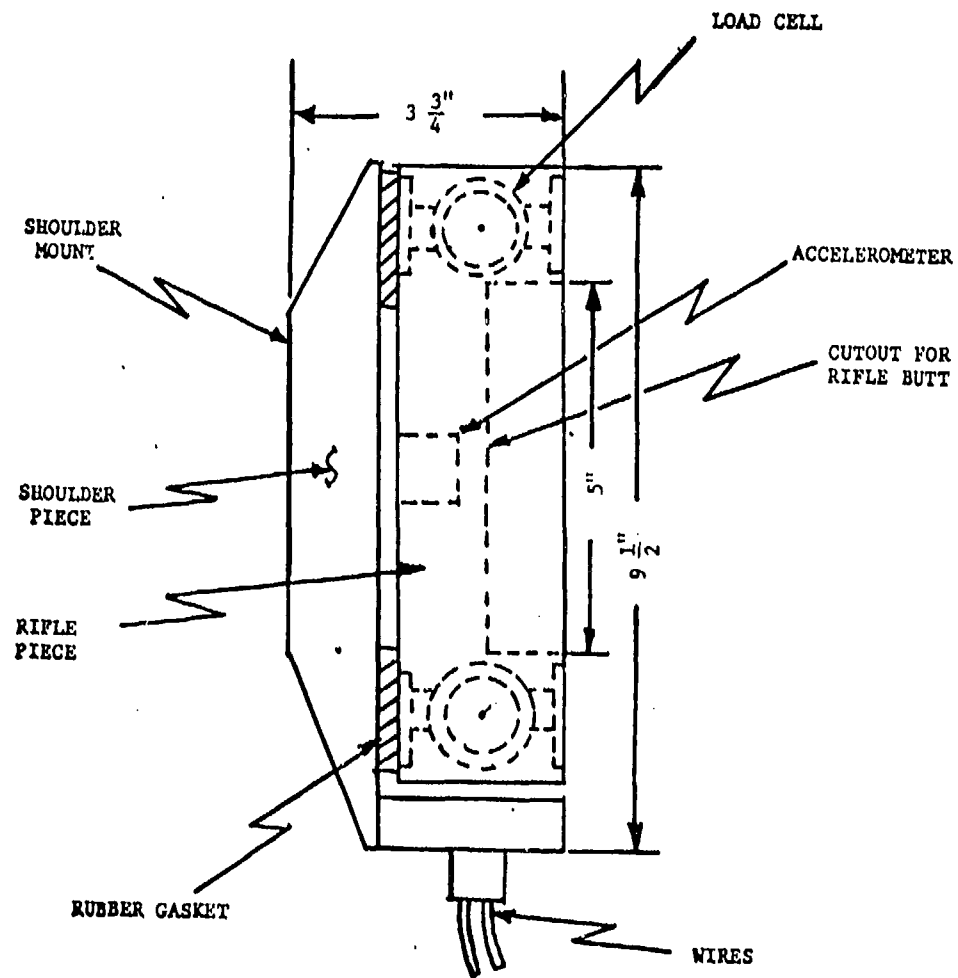
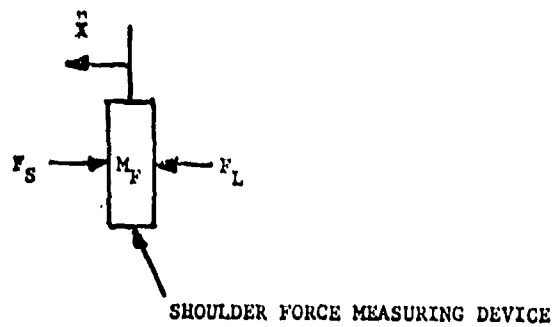


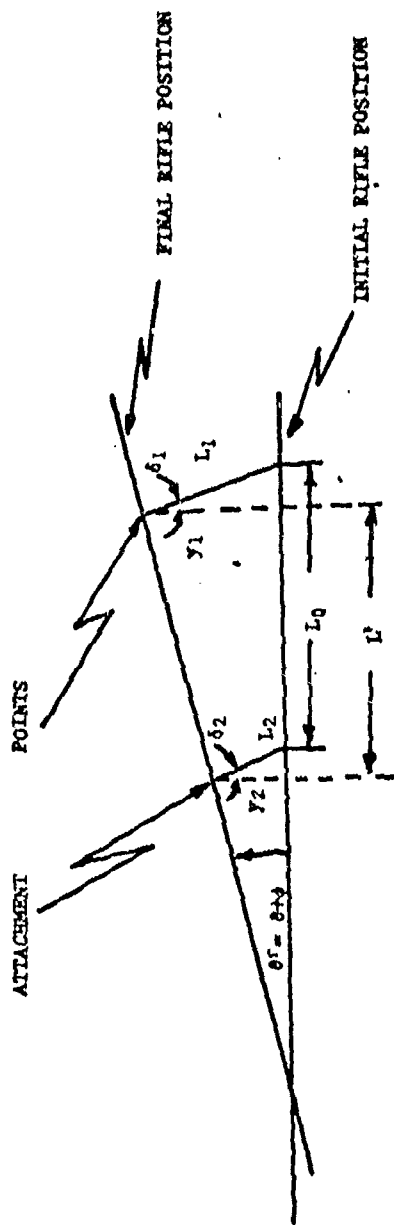
Figure 15 Shoulder Force Measuring Device



- M_F - MASS OF FIXTURE
 F_L - MEASURED FORCE (LOAD WITH CELLS)
 \ddot{x} - MEASURED ACCELERATION
 F_S - COMPUTED FORCE EXERTED ON THE SHOULDER

$$F_S = -F_L - M_F \ddot{x}$$

Figure 16 Computation of Transmitted Recoil Force



$\theta', \delta_1, \delta_2$ - SMALL ANGLES (Less than 10°)

$$L' = L_0 \cos \theta' \approx L_0$$

$$Y_1 = L_1 \cos \delta_1 \approx L_1$$

$$Y_2 = L_2 \cos \delta_2 \approx L_2$$

$$\tan \theta' \approx \frac{Y_1 + Y_2}{L'} \approx \frac{L_1 + L_2}{L_0}$$

Figure 17 Computation of Weapon Pitch Rotation 6

4.0 BIODYNAMICAL SENSITIVITY ANALYSIS

4.1 Introduction

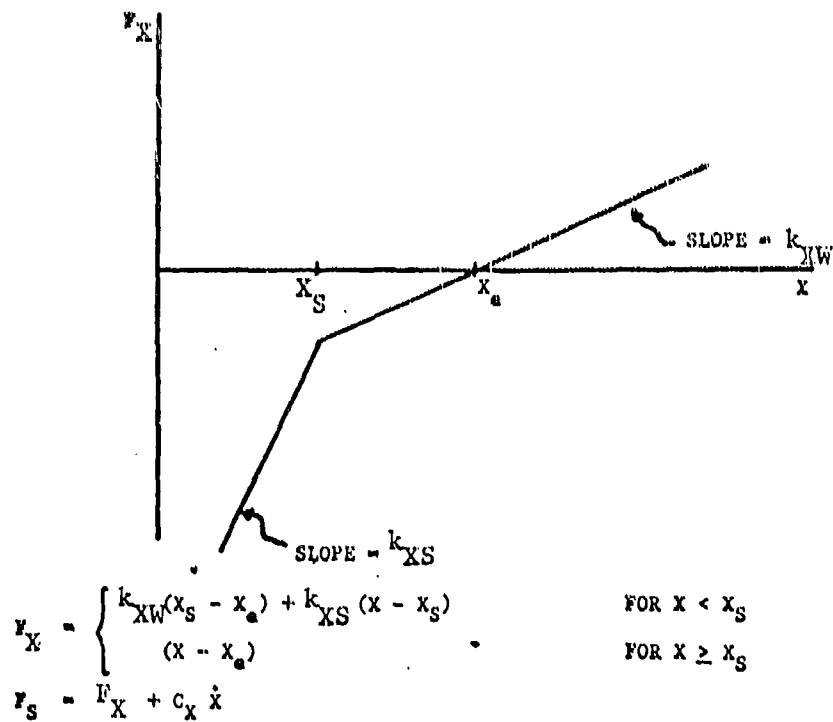
A sensitivity analysis was performed to determine which biomechanical parameters of the man-weapon system are critical to the design of a universal small arms mount. In this analysis, both the peak force at the shoulder and the absolute weapon pitch rotation after 0.3 seconds were taken as the primary output variables. The sensitivities of these output variables to systematic variations in each of the system parameters were obtained by numerical and analog computer solutions of the biodynamical equations of motion.

Both single and burst fire modes were analyzed. The driving force $F(t)$ in equations 2-7 represents what is commonly called the breech force. The important feature of this function is the short duration (about one millisecond) compared with the total cycle time (approximately 80 milliseconds). For the digital computer simulation, the function $F(t)$ is approximated by Dirac's delta function -- a symbolic function commonly used in mathematical physics that has finite area but is zero valued at all but one point on the time axis. Typical values for the impulse are 1.2 lb-sec for the M16 Rifle and 2.5 lb-sec for the M79 and M203 grenade launchers.

4.2 Factors That Affect Weapon Translation

The weapon shoulder support is represented in the model by a linear dashpot and a piecewise linear combination of spring elements, which results in variable shoulder stiffness. Thus the shoulder spring model (illustrated in Figure 18) represents the effects of both the soft compression of skin tissue and the stretching of the muscles and tendons that support the shoulder. The shoulder reaction force, F_s , is an explicit function of coordinate x , but since the man-weapon system is dynamically coupled, the shoulder reaction force also is influenced, to a lesser extent, by both the pitching coordinates θ and ϕ .

Because the shooter usually holds the weapon compressed firmly against his shoulder before firing and, in addition, because the impulsive breech force compresses the weapon against the shoulder, the shoulder support intuitively is expected to be in a state of strong compression (i.e. $x < x_s$) for most of the firing cycle. This hypothesis was substantiated by numerous computer simulations of the man-weapon interaction problem and also by observations of experimental load cell data of the shoulder reaction force.



WHERE

- x_e - DISTANCE AT WHICH THE WEAPON AND SHOULDER ARE IN STATIC EQUILIBRIUM
- x_s - DISTANCE AT WHICH THE SPRING STIFFNESS CHANGES
- k_{XW} - WEAK SHOULDER SPRING CONSTANT
- k_{XS} - STRONG SHOULDER SPRING CONSTANT
- c_X - SHOULDER DAMPING CONSTANT
- F_X - SHOULDER SPRING FORCE
- F_S - TRANSMITTED SHOULDER MOUNT FORCE

Figure 18 Shoulder Spring-Dashpot Model

A flexible shoulder model, consisting of a single linear shoulder spring and a dashpot, therefore provides an adequate representation of the shoulder impedance to weapon recoil loading.

Experimental results also indicate that the shoulder reaction force, like the breech force, is both impulsive and nearly periodic; and, in addition, the magnitude of the peak value of the shoulder force tends to decrease for successive shots in a burst. If the model damping coefficients are near critical, then the shoulder reaction force is spread over a longer portion of the firing cycle, and, furthermore, the peak values of the shoulder reaction force become sensitive predominantly to the damping term rather than the spring stiffness term. In order to duplicate the impulsive and the periodic character of the shoulder force, a damping factor between 10 and 30 percent of critical damping is required (i.e. $c_x = 2\zeta_x \sqrt{k_x m_r}$ where $0.1 \leq \zeta_x \leq 0.3$). A spring stiffness of 250 lb/in yields peak values for the reaction force of about 100 pounds. Using these values for the shoulder spring and dashpot parameters, the model generated shoulder force closely approximates the characteristics of the experimentally measured recoil force.

Results of the computer analysis reveal that only four parameters have any significant effect on the duration or the peak values of the recoil force, namely: the weapon impulse, I_r ; the combined mass of the weapon and the arms, m_r ; the spring stiffness, k_x ; and the damping constant, c_x . Analog computer simulations were made using inertial parameters associated with three different shooters (small, medium, and large) and these results are shown in Figures 19, 20, and 21 respectively. The shoulder damping constant, ranging from 10 to 30 percent of critical damping, was adjusted to give average peak recoil forces that correspond to measured results from experimental firings. As expected, the model results show a decrease in the weapon rotation as the size of the man increases. Only slight variations in the recoil force occur among the three cases.

4.3 Factors That Affect Weapon Pitch Rotation

Certain system parameters were found by computer analysis to have a significant effect on the absolute weapon pitch rotation, while other parameters were found to have very little effect on weapon rotation at all. Table 2 contains a list of those parameters that have very little effect on the rifle rotation. The torso mass, moment of inertia, and the torsional

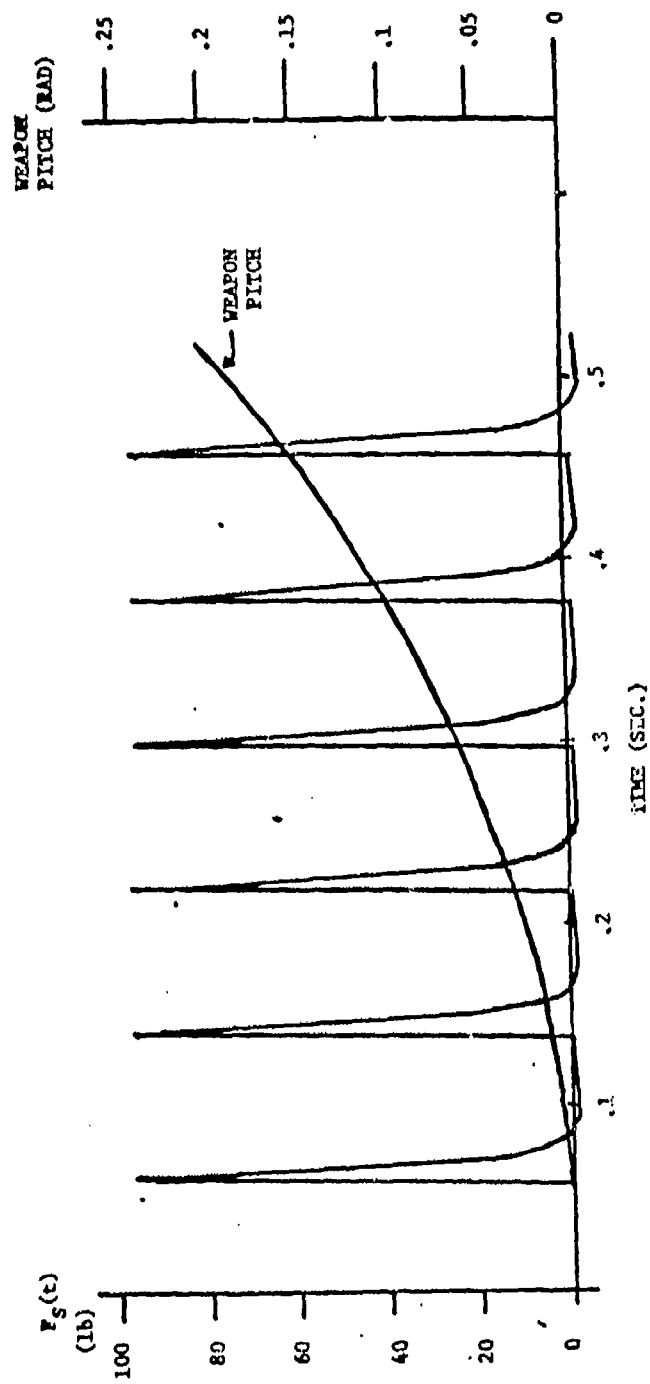


Figure 19 Analog Computer Simulation - Small Man
 Gunner: Bebling (145 lb, 5'6")

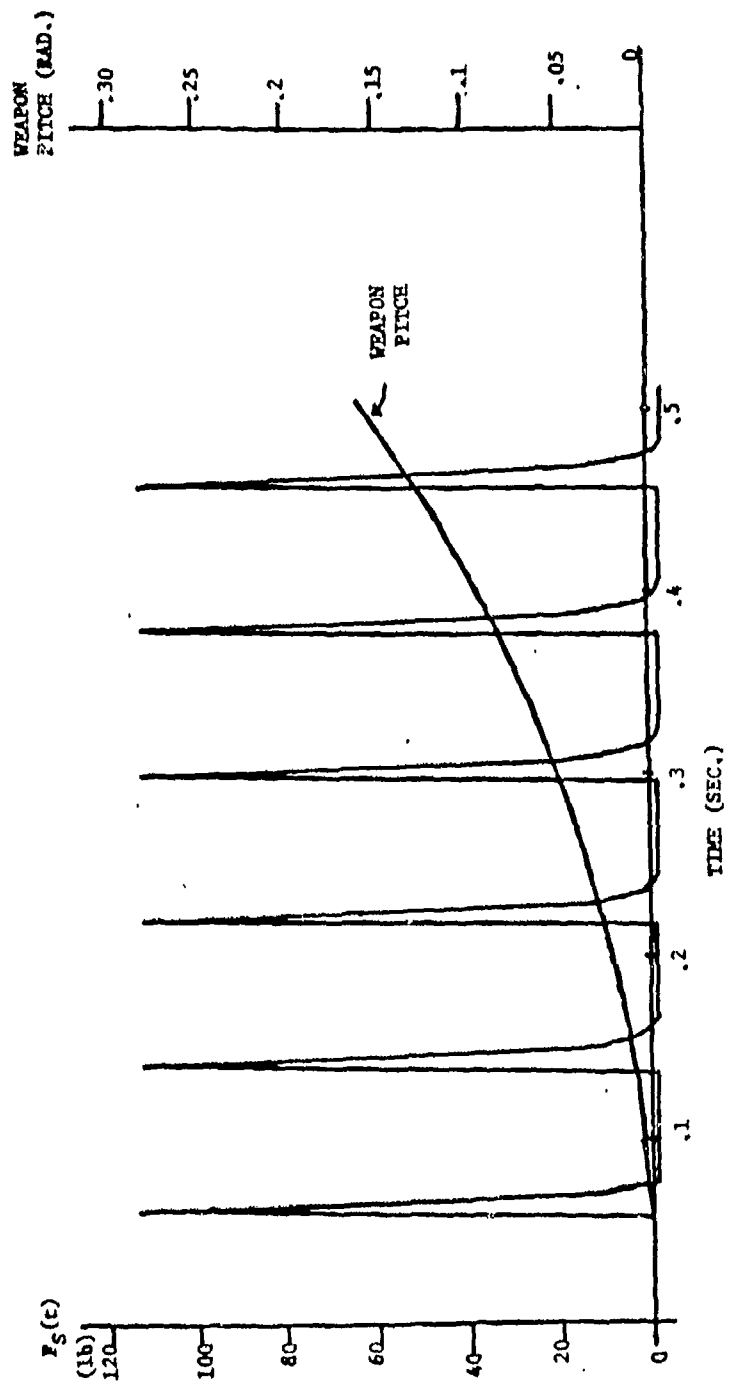


Figure 20 Analog Computer Simulation - Medium Man
 Gunner: Rekeeyer (165 lb, 6'1½")

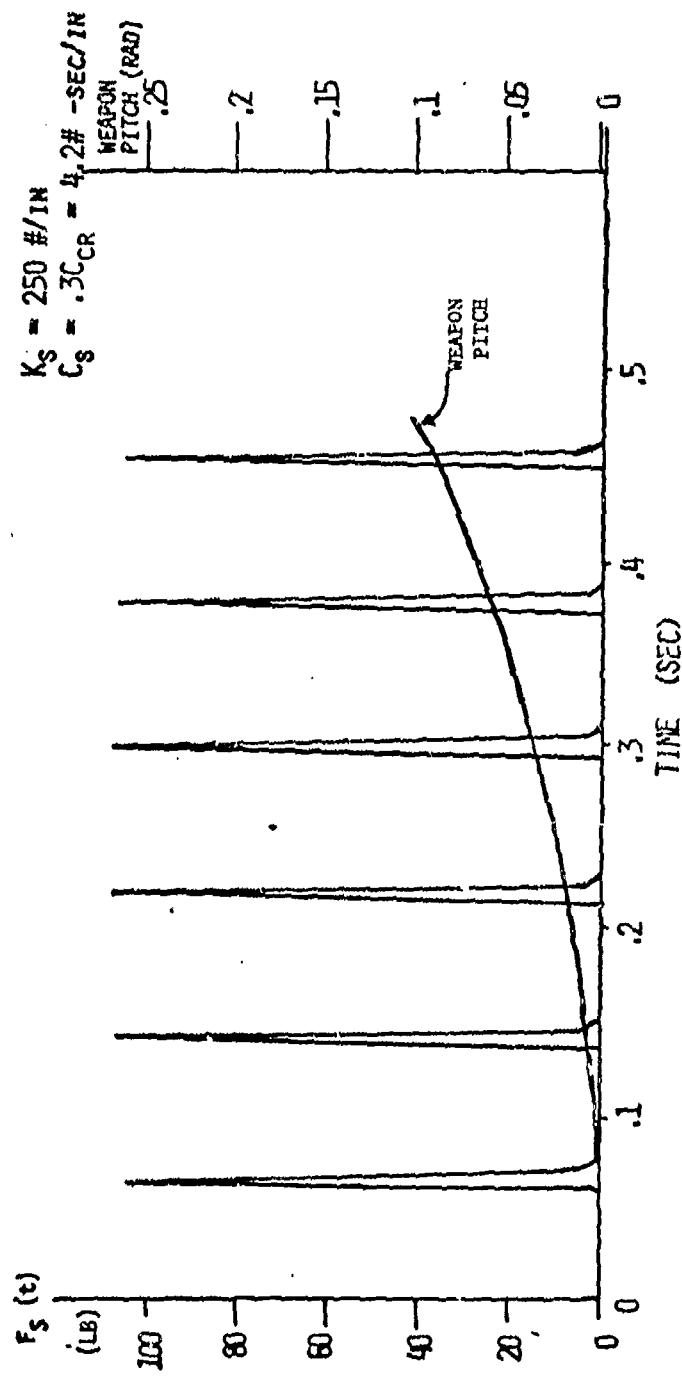


Figure 21 Analog Computer Simulation - Large Man
 Gunner: Boggs (228 lb, 5'11")

TABLE 2 PARAMETERS THAT DO NOT AFFECT WEAPON ROTATION

PARAMETER	DECREASED VALUE	RIFLE ROTATION	BEST APPROX.	RIFLE ROTATION	INCREASED VALUE	RIFLE ROTATION
k_0 (in-lb)	2.	3.84°	20.	3.84°	200.	3.83°
$\xi_\theta = \frac{c_\theta}{c_{\theta \text{ crit}}}$	0.	3.84°	0.5	3.84°	1.	3.83°
I_{cm} (lb-in-sec ²)	12.	3.87°	26.	3.84°	50.	3.83°
M (lb-sec ² /in)	0.15	3.77°	0.3	3.84°	0.45	3.84°
L (in)	10.	4.07°	21.	3.84°	30.	3.60°
r_{cm} (in)	5.	3.73	13.	3.84°	25.	3.90°

stiffness and damping coefficients for the θ coordinate do not affect the rifle rotation to any appreciable amount (a few hundredths of a degree at most). The weapon rotation is rather insensitive also to the length of the torso and the distance from the torso pivot point to the center of mass of the torso. These results provide some insight for designing a mount. They suggest that a representation of the torso is not really necessary for the design, in order to simulate the external dynamical motions of the weapon. In the model, the motion of the torso mass can be reduced to near zero by simply assigning a very large mass and moment of inertia. For example, by increasing the mass and moment of inertia by a factor of one thousand, the rotation of the weapon increases from a value of 3.84 degrees to a value of 4.06 degrees (see Figure 22). Although the torso rotation is reduced from 7.0 degrees in the nominal case to zero by increasing the mass and moment of inertia, the weapon rotation changes only by 0.2 degrees; consequently, the torso mass has very little effect on the total rotation of the weapon.

Figure 23 contains a plot of the weapon pitch versus the weapon impulse after 0.3 seconds have elapsed. Note the linear relationship between these two parameters and the significant effect the impulse has on the weapon rotation. The point marked "best approximation" on this and on other figures corresponds to the set of parameters that best represents the

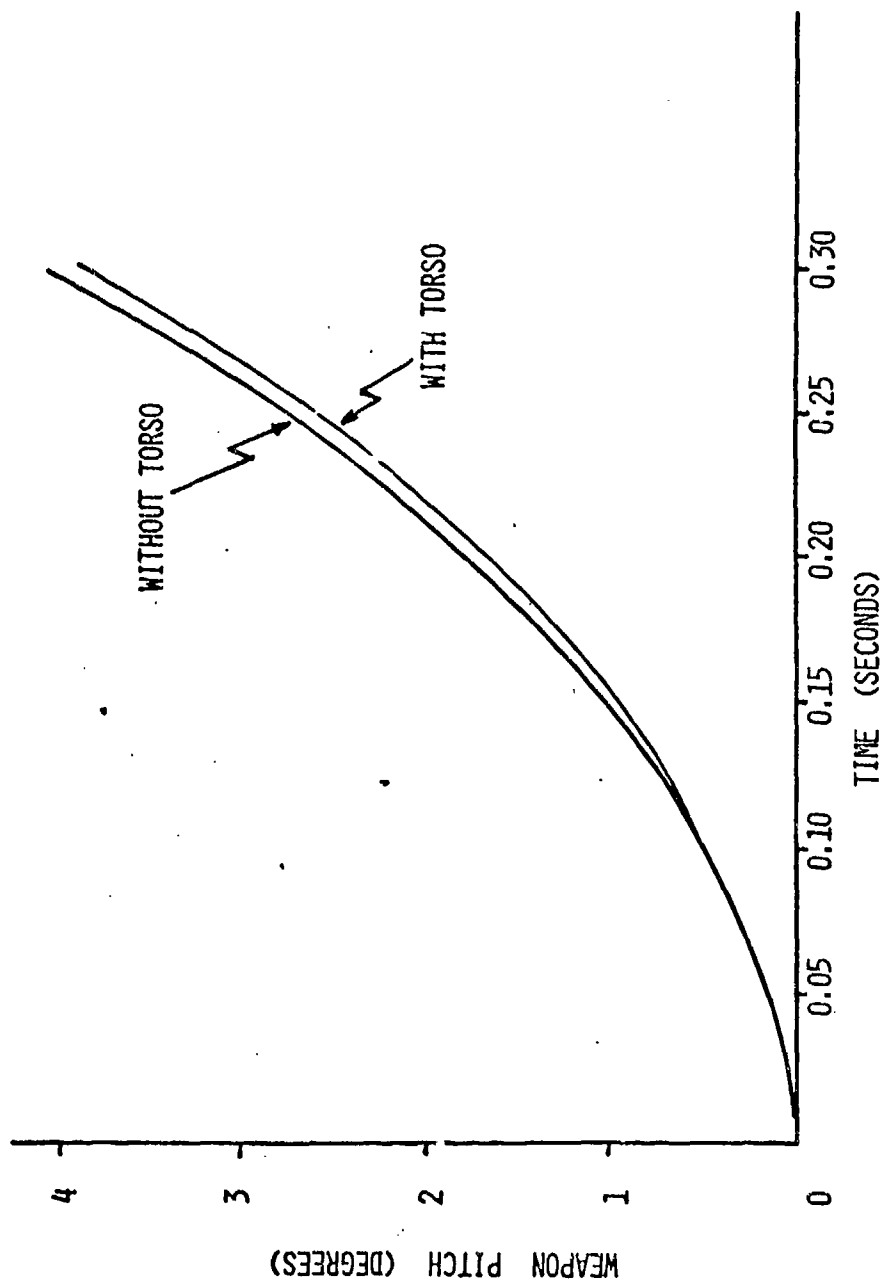


Figure 22 Sensitivity of Weapon Rotation to Torso Inertia

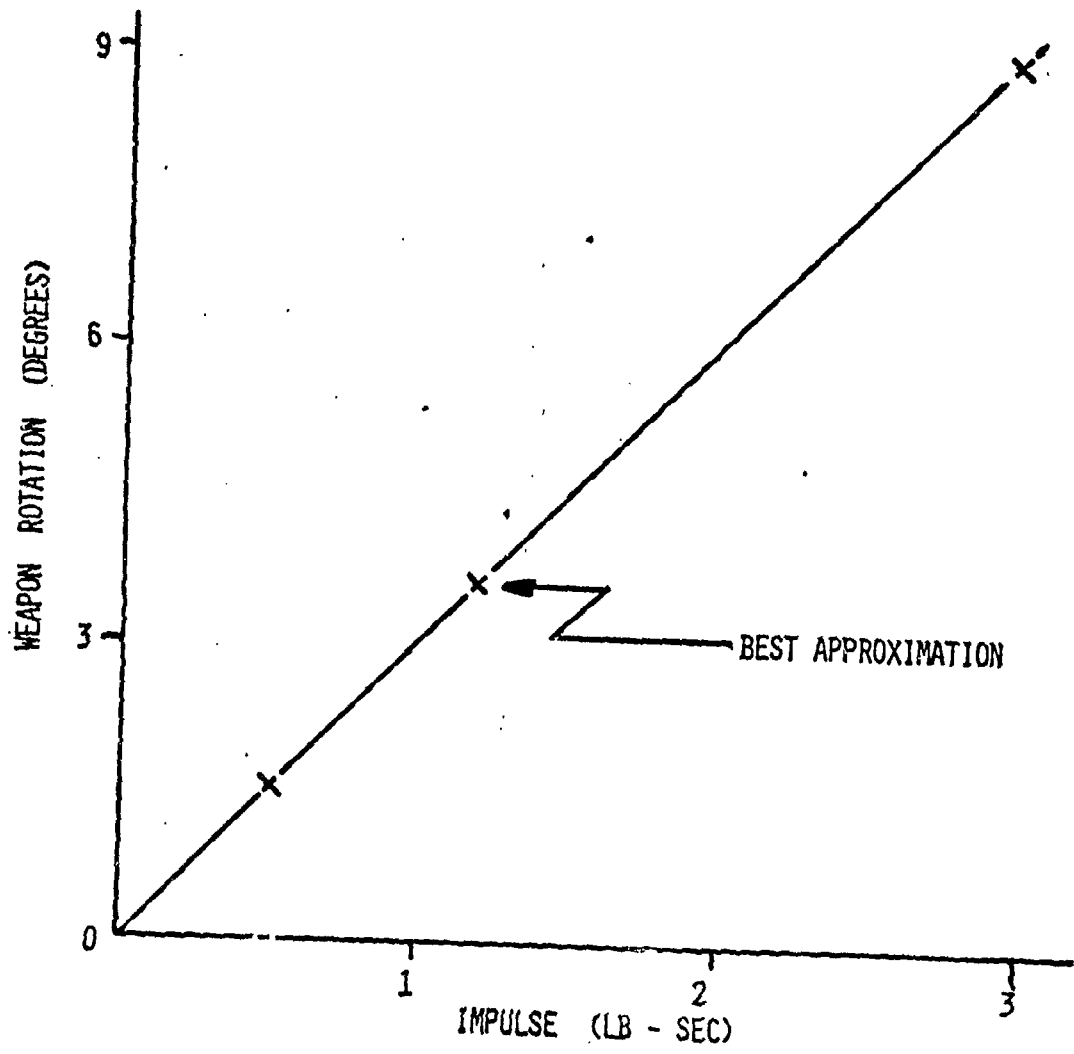


Figure 23 Weapon Pitch Rotation vs Impulse

dynamical characteristics of the 165 pound (medium sized) man. Figure 24 contains a plot of the weapon rotation at 0.3 seconds and at 0.15 seconds versus the firing frequency. Again there is a linear relationship between the weapon rotation and the firing frequency. Also the important conclusion can be made that, for a fixed number of rounds in a burst, increasing the firing frequency decreases the rifle rotation and hence lessens the weapon dispersion. Figure 25 shows the effect of the eccentricity of the breech force, δ , on the weapon rotation. This parameter represents the distance between the centerline of the barrel and the center of rotation of the weapon at the shoulder. The weapon pitch rotation varies linearly with δ . When δ is zero no torque is produced about the shoulder pivot point; nevertheless, 1.5 degrees of rotation occur after 0.3 seconds, which is due mainly to the rearward pitching of the torso. As the torso pitches rearward, the rifle pitch angle, ϕ , becomes negative, since the total system angular momentum is conserved after the application of the impulsive breech force. By appropriately positioning the stock with respect to the barrel centerline, the rotation of the weapon can be virtually reduced to zero.

Parameters that have a moderate influence on the rotation of the weapon are the inertial, stiffness and damping parameters associated with the man's arms and the weapon, namely, I_r , m_r , k_ϕ , c_ϕ , k_x , and c_x . In Figure 26 the rifle rotation is plotted as a function of $1/\sqrt{I_r}$. A straight line approximately fits the points. Similarly, a plot of the rifle rotation as a function of $\sqrt{k_\phi}$, (see Figure 27), results in a linear relationship. Thus the total rifle rotation varies linearly with both $1/\sqrt{I_r}$ and $\sqrt{k_\phi}$. In Table 3 the rifle rotation at 0.3 seconds is listed for a range of values of the parameters m_r , c_ϕ , c_x , and k_x .

Figures 28, 29, 30, and 31 contain the output of a digital computer simulation. The case represented is that of a 165 pound man firing the M16 rifle. The total rotation of the weapon, shown in Figure 28 is the sum of the torso rotation, θ , and the weapon rotation relative to the torso, ϕ . A characteristic feature of the simulation is the jump in acceleration in each of the coordinates after each shot, due to the impulsive breech force.

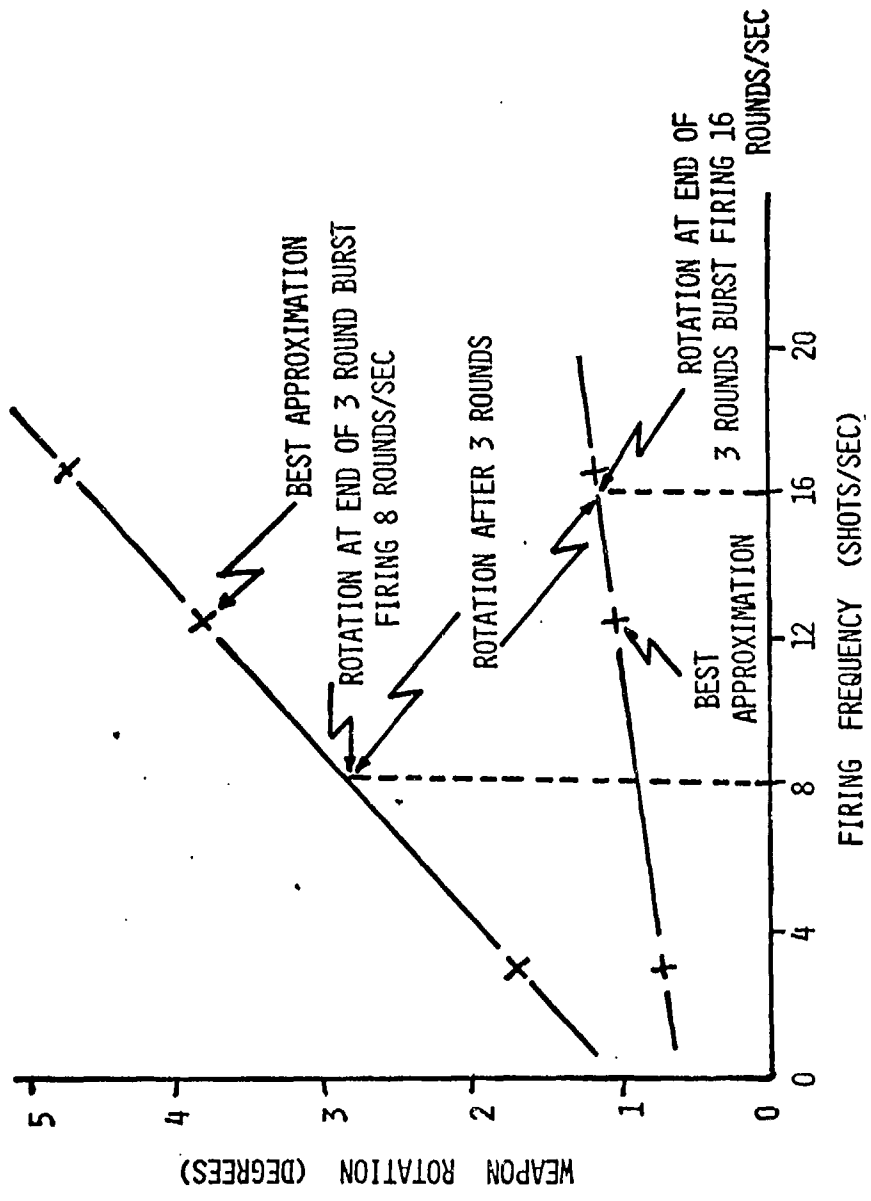


Figure 24 Weapon Pitch Rotation vs Firing Frequency

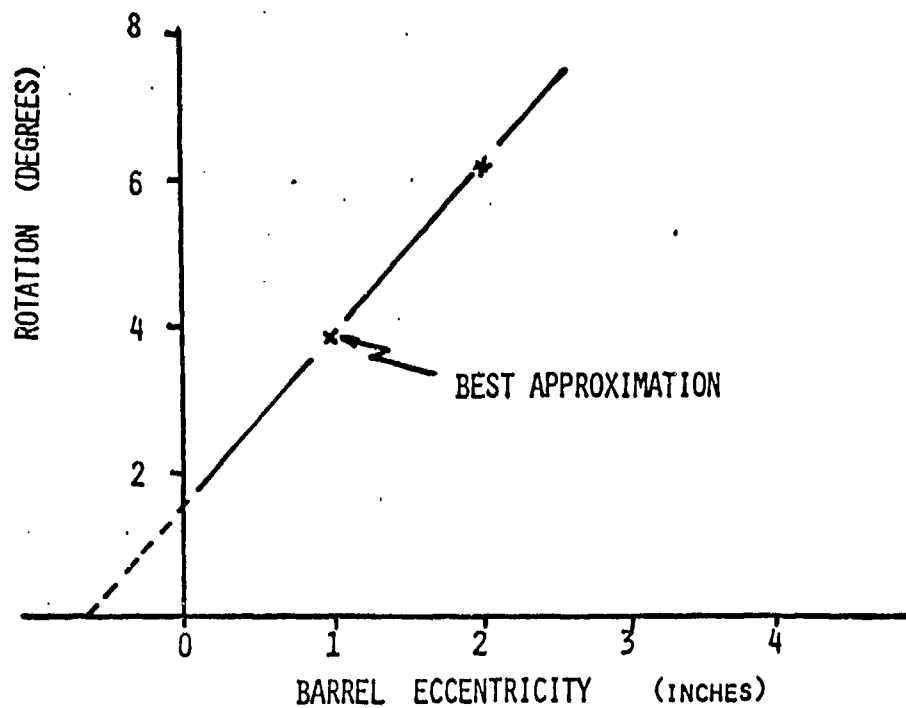


Figure 25 Weapon Pitch Rotation vs Barrel Eccentricity

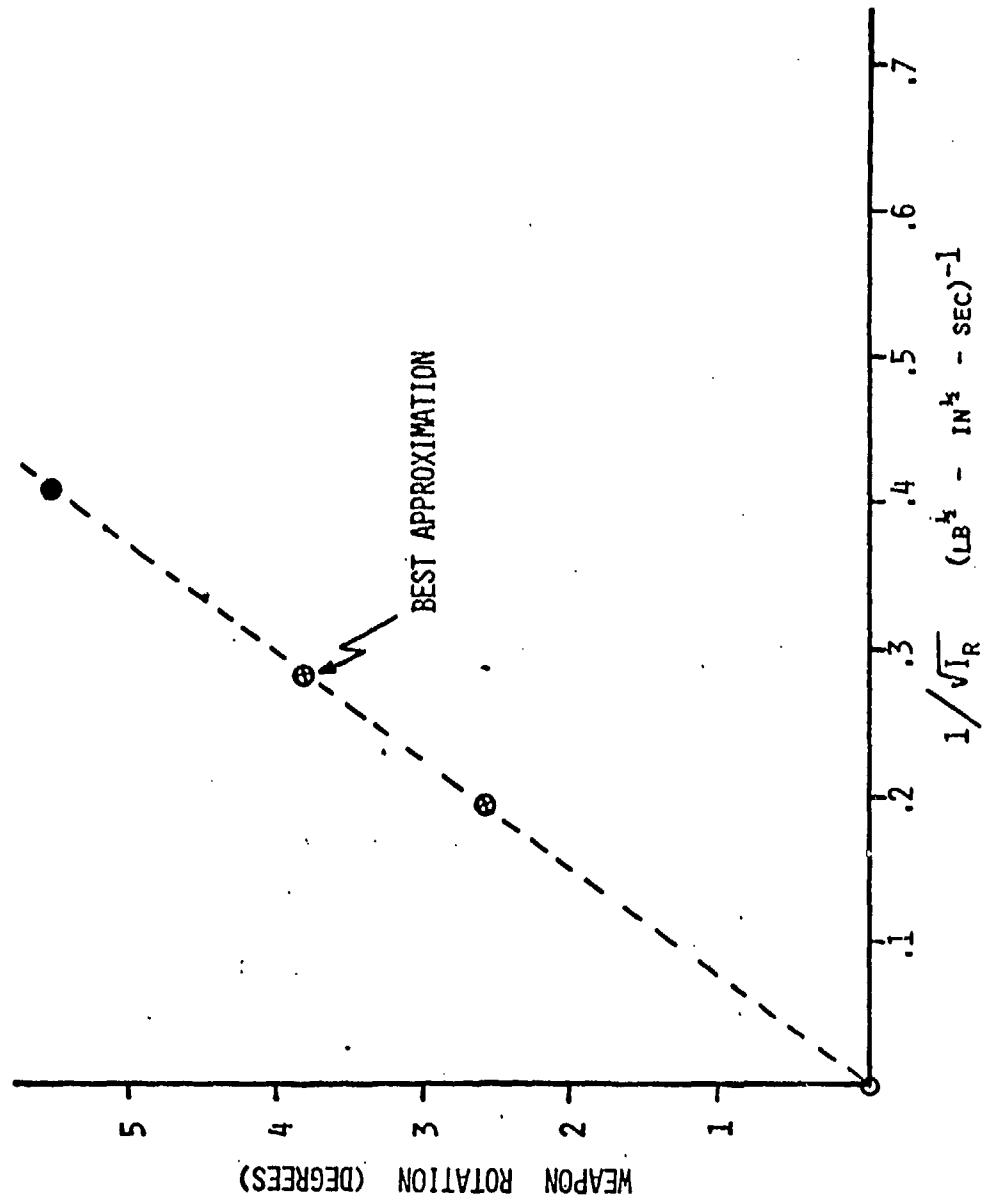


Figure 26 Weapon Pitch Rotation vs $1/\sqrt{I_R}$

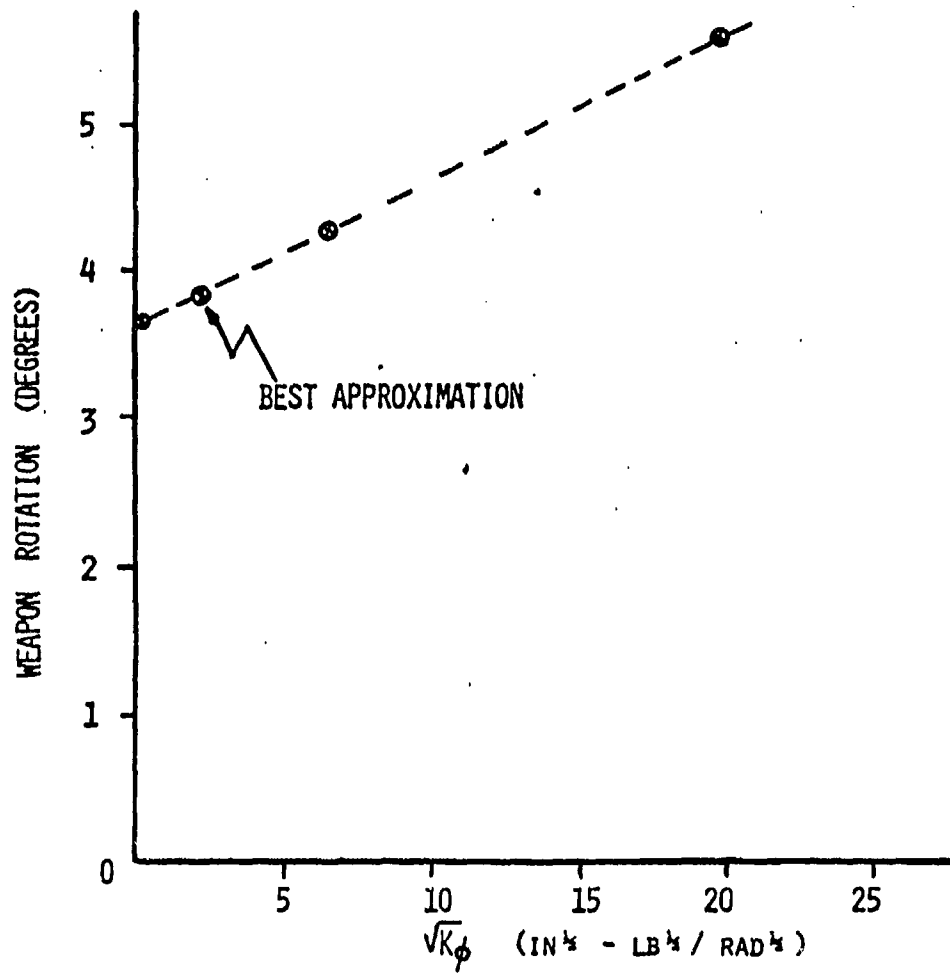


Figure 27 Weapon Pitch Rotation vs $\sqrt{K_\phi}$

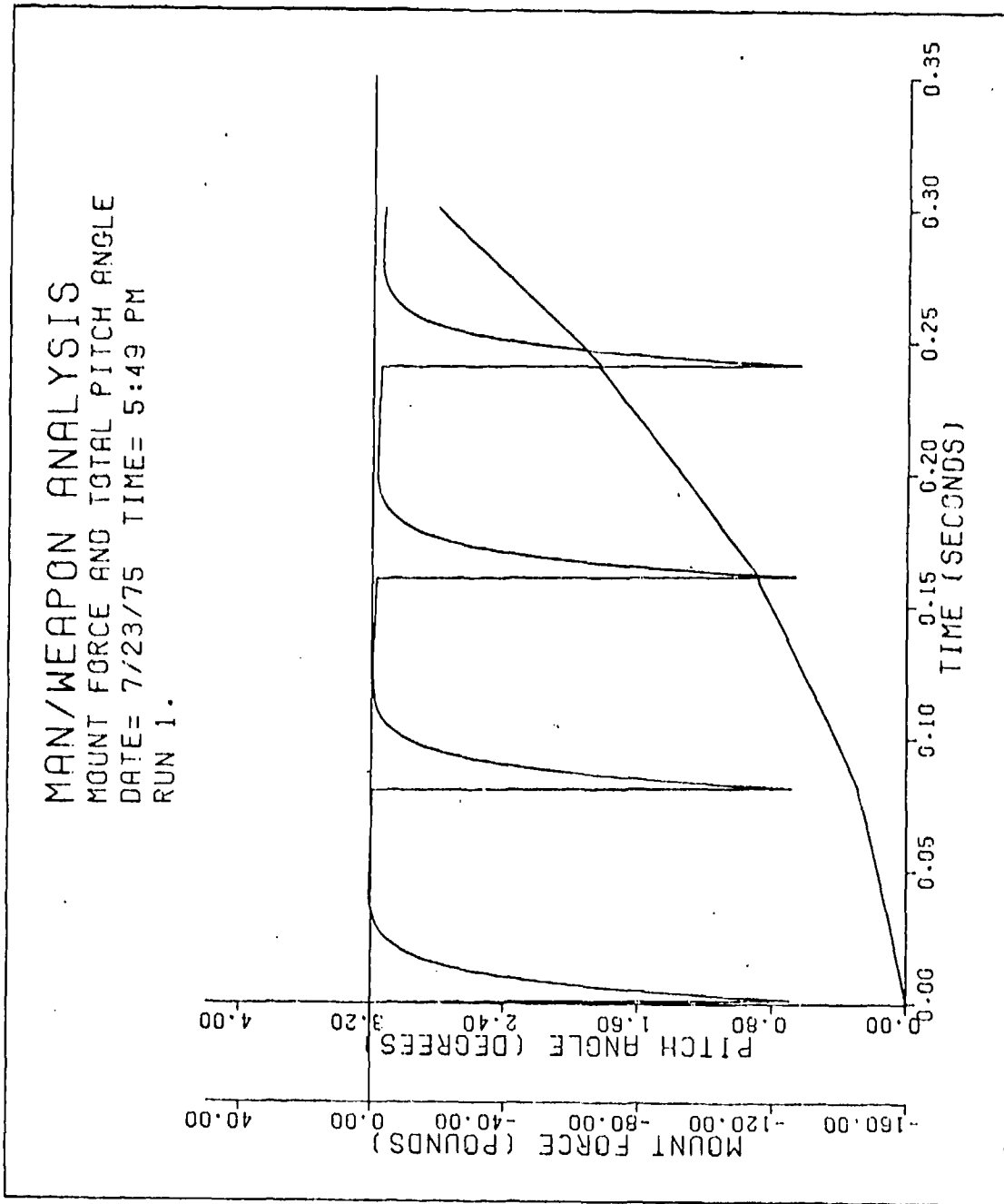
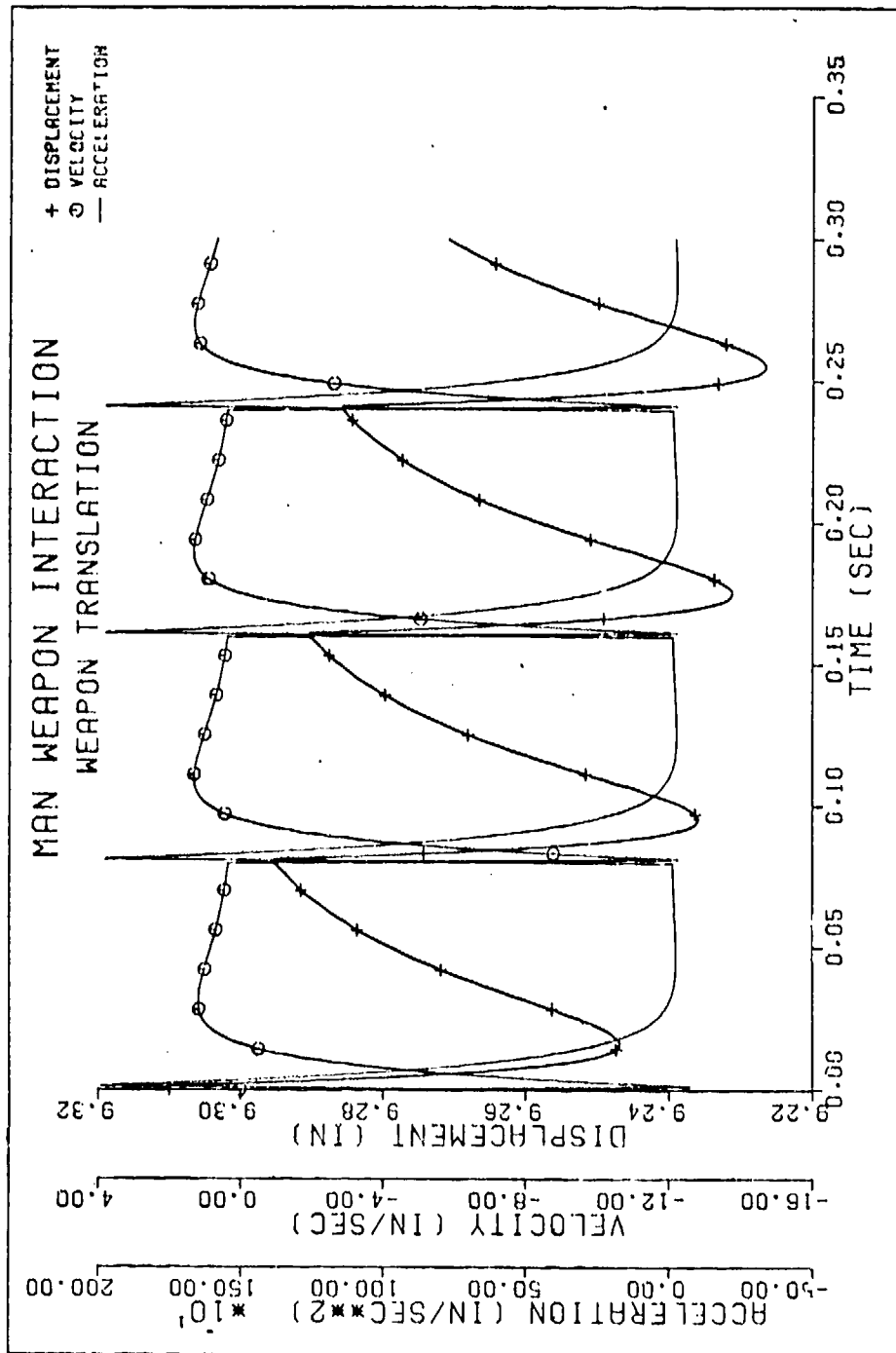
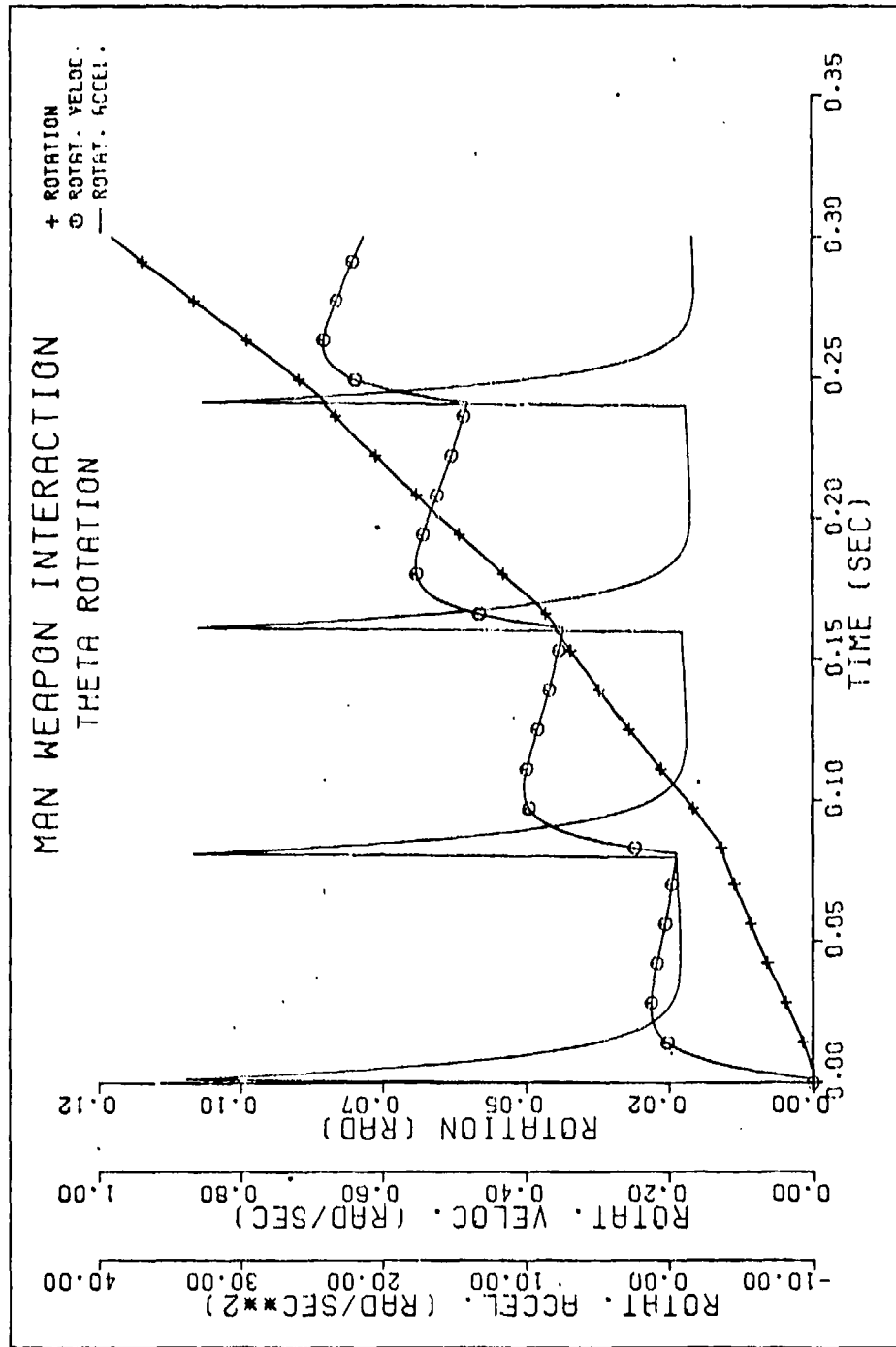


Figure 28 Man/Weapon Analysis- Mount Force and Total Pitch Angle



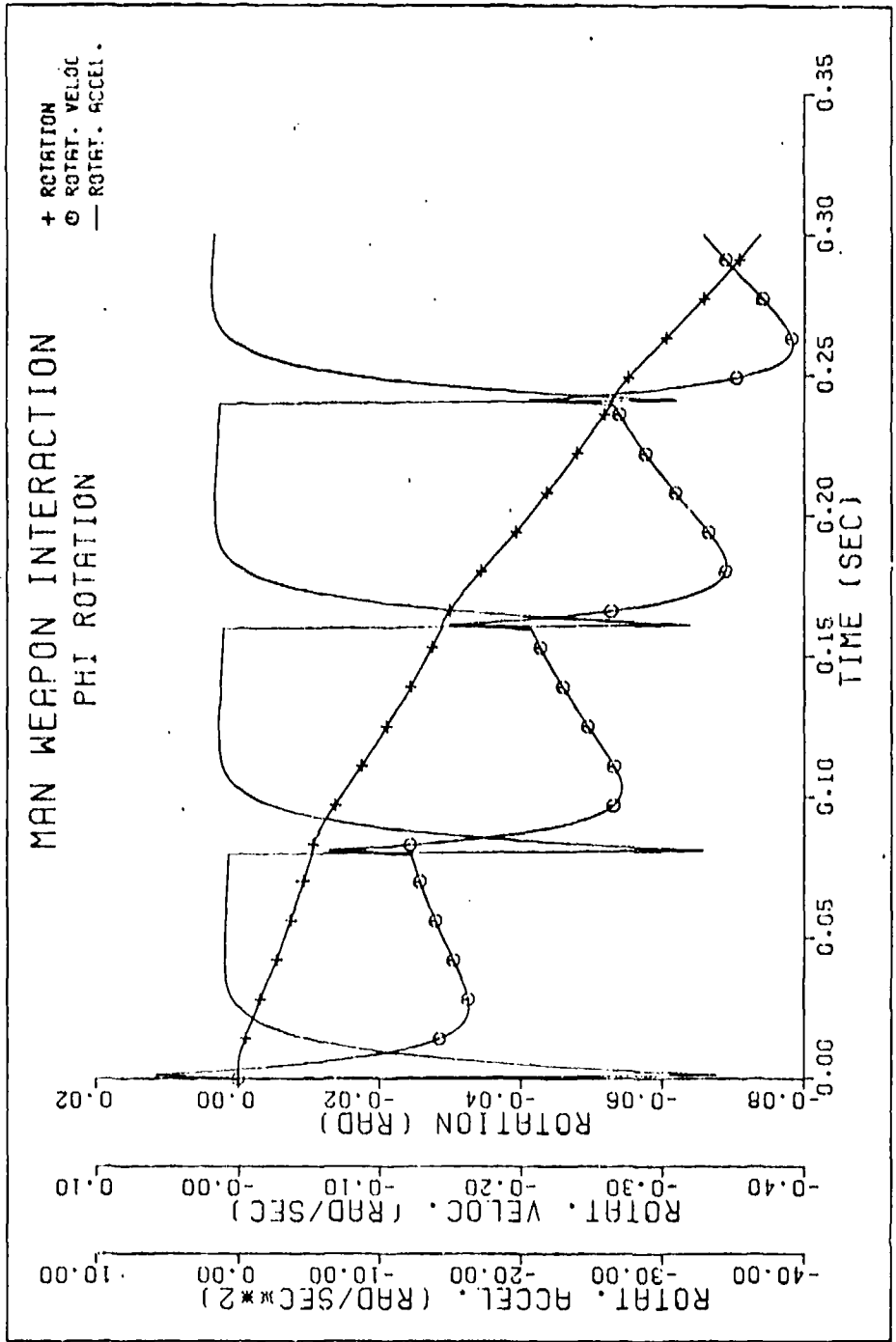
DATE= 7/23/75 TIME= 5:50 PM

Figure 29 Man Weapon Interaction- Weapon Translation



DATE= 7/23/75 TIME= 5:50 PM

Figure 30 Man Weapon Interaction- Theta Rotation



DATE= 7/23/75 TIME= 5:50 PM

Figure 31 Man Weapon Interaction - Phi Rotation

TABLE 3 SENSITIVITIES OF PARAMETERS THAT AFFECT WEAPON ROTATION

PARAMETER	INCREASED VALUE	RIFLE ROTATION	BEST APPROX.	RIFLE ROTATION	DECREASED VALUE	RIFLE ROTATION
m_r (lb-sec ² /in)	0.05	4.48°	0.099	3.84°	0.2	2.5
c_ϕ/c_ϕ crit	0.	3.69°	.5	3.84°	1.	4.02
k_s (lb/in)	5.	5.67°	25.	3.84°	250.	2.99
c_s/c_s crit	0.	5.29°	1.	3.84°	1.5	3.55

4.4 Recommended Design Configurations

Based on experimental findings and model predictions, two possible design configurations for a universal small arms mount are recommended and are illustrated in Figures 32 and 33. By appropriate choices for the masses, lengths, viscous damping constants, and spring stiffnesses, the mount can be designed such that its dynamical characteristics are analogous to the characteristics of the simulation model. The simplified version of the design in Figure 33 is based on the fact that the rotation of the torso mass does not significantly affect the weapon motion or the shoulder reaction force.

5.0 CONCLUSIONS AND RECOMMENDATIONS

5.1 Conclusions

a. Based on experimental results and model predictions, the force reaction at the shoulder can be approximated by a single linear spring and dashpot. By the proper adjustments of the spring and damper constants, both the impulsive and periodic behavior of the reaction force can be approximated as well as the magnitudes of the peak values.

b. The parameters that affect the peak forces at the shoulder are the shoulder spring stiffness, the shoulder damping coefficient, the impulse of the weapon, and the effective mass of the weapon, arms, and hands. Other model parameters have only a minor influence on the peak values of the shoulder reaction.

c. The weapon rotation after a specified time is not sensitive to the torso inertial or geometric parameters. By effectively removing this link in the model, the weapon rotation is not significantly changed. The parameters that affect the weapon rotation most are the weapon impulse, the eccentricity of the barrel centerline from the shoulder pivot point and the firing frequency. The weapon rotation was found to vary linearly with each of these parameters. Parameters that affect the weapon rotation but are of secondary significance are the effective inertial parameters for the weapon and arms, the torsional stiffness and damping of the weapon pitch, and the shoulder stiffness and damping constants.

d. The recommended configuration for a mount, based on experimental and analytical results, is presented in Figure 33. It allows for two degrees of freedom (pitch and translational) and contains a spring and damper to simulate the shoulder reaction force and an effective torsional spring and damper to simulate the man's torsional stiffness and damping characteristics.

5.2 Recommendations For Future Work

The recommendations for future work in developing a universal small arms mount design are presented below:

a. Additional tests should be performed to support the complete design of a universal small arms mount fixture or the modification of an existing design. The tests would be performed to refine the values obtained for the design parameters.

b. If further tests are conducted, a better method for measuring the shoulder reaction force would be to cut off the end section of weapon stock and insert one or two force washers and an accelerometer directly to the stock. This method would replace the need for the rather heavy and cumbersome shoulder force measuring device shown in Figure 15 and would therefore result in less errors in measurement.

c. Having additional experimental data, refine the mount parameters, using the biodynamics model to best approximate the actual shooter's response. Then incorporate the refined parameter values in the mount design.

d. Investigate existing mount designs to determine if modifications can be made on them to satisfy the design requirements of the recommended concept. If an existing mount is found that can be modified to meet these requirements, then the authors recommend that it be adapted to the design configuration in Figure 33 and tested.

e. Otherwise, if no existing design can be so modified, then a universal small arms mount should be designed from scratch based on the concept shown in Figure 33 and tested.

APPENDIX A

A.0 MODEL REPRESENTATION OF THE HUMAN BODY SEGMENTS

A.1 Head and Torso Representation

The formulas used to calculate the human body segment parameters and the methods for combining the body segments to represent the torso and arms are presented below. The head and trunk model representation is shown in Figure A-1. An ellipsoid of revolution represents the head, while elliptical cylinders represent the trunk. Each of the distances illustrated in Figure A-1 are defined by certain anthropometric dimensions. In particular,

$$a_{hd} = \frac{1}{2} (\text{stature} - \text{cervical height})$$

$$b_{hd} = (\text{head circumference}) / 2\pi,$$

$$a_t = \frac{1}{6} (\text{chest breadth} + \text{waist breadth} + \text{hip breadth})$$

$$b_t = \frac{1}{6} (\text{chest depth} + \text{waist depth} + \text{hip depth})$$

$$\ell_{ut} = \text{cervical height} - \text{substernal height},$$

and

$$\ell_{lt} = \text{substernal height} - \text{trochanteric height}.$$

The mass and moments of inertia for the head are given by the standard formulas for an ellipsoid of revolution,

$$m_{hd} = \frac{4}{3} \pi a_{hd} b_{hd}^2 \rho_{hd},$$

$$I_{aa_{hd}} = 4 m_{hd} b_{hd}^2,$$

and

$$I_{bb_{hd}} = I_{cc_{hd}} = m_{hd} (a_{hd}^2 + b_{hd}^2) / 5$$

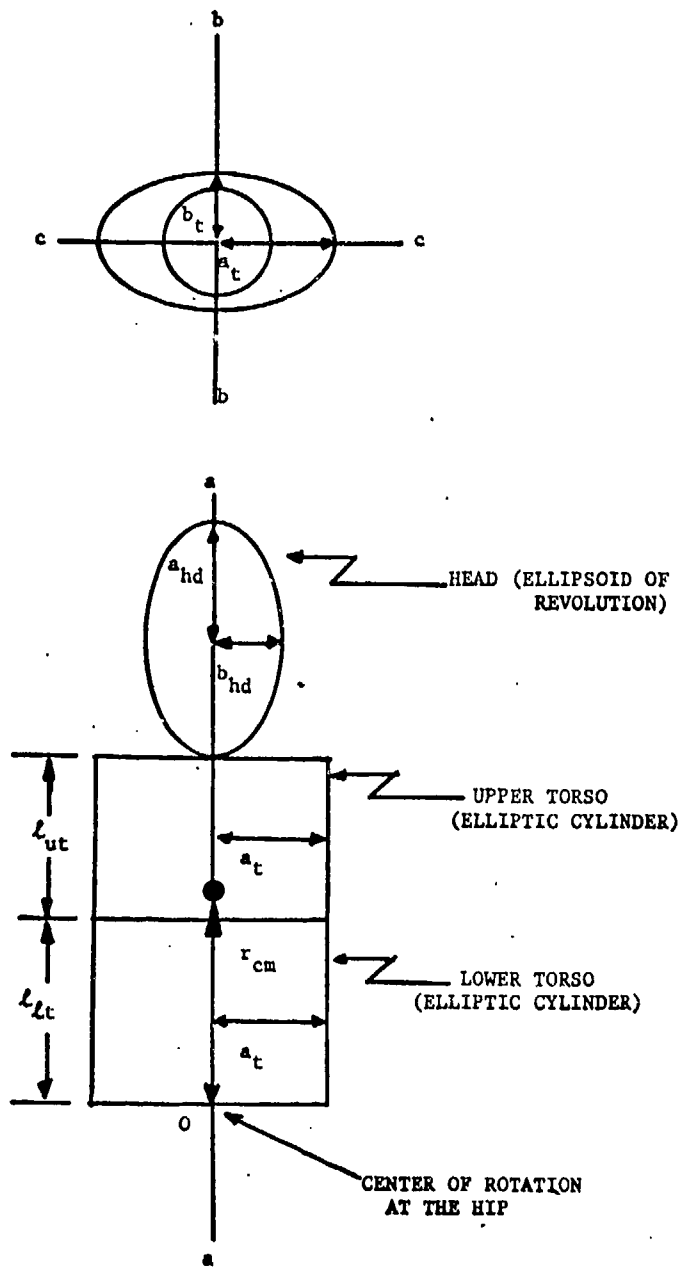


Figure A-1 Head and Torso Rigid Body

and the mass density

$$\rho_{hd} = 1.11 \times 10^3 \quad (\text{kg/m}^3)$$

was obtained from reference⁶. For the upper torso the mass and moments of inertia are given by

$$m_{ut} = \pi a_t b_t \ell_{ut} \rho_{ut}$$

$$I_{aa_{ut}} = m_{ut} (a_t^2 + b_t^2) / 4$$

$$I_{bb_{ut}} = m_{ut} (3 a_t^2 + \ell_{ut}^2) / 12$$

and

$$I_{cc_{ut}} = m_{ut} (3 b_t^2 + \ell_{ut}^2) / 12$$

Again the mass density

$$\rho_{ut} = 9.2 \times 10^2 \quad (\text{kg/m}^3)$$

was obtained from reference⁶, page 195. Likewise for the lower torso

$$m_{lt} = \pi a_t b_t \ell_{lt} \rho_{lt}$$

$$I_{aa_{lt}} = m_{lt} (a_t^2 + b_t^2) / 4$$

$$I_{bb_{lt}} = m_{lt} (3 a_t^2 + \ell_{lt}^2) / 12$$

$$I_{cc_{lt}} = m_{lt} (3 b_t^2 + \ell_{lt}^2) / 12$$

and

$$\rho_{lt} = 1.01 \times 10^3 \quad (\text{kg/m}^3)$$

In the model the head, upper torso and lower torso are combined into a single rigid body with mass M,

$$M = m_{hd} + m_{ut} + m_{lt}$$

⁶Dempster, W.T., "Space Requirements of the Seated Operator," Wright Air Development Center, TR-55-159, Wright-Patterson Air Force Base, Ohio, AD 78792, 1955

Furthermore, the center of mass location, r_{cm} , is given by

$$r_{cm} = [m_{hd} (\ell_{lt} + \ell_{ut} + a_{hd}) + m_{ut} (\ell_{lt} + 0.5 \ell_{ut}) + 0.5 m_{lt} \ell_{lt}] / M$$

and the moment of inertia, I_{cm} , about the center of mass of the head and trunk rigid body is given by,

$$I_{cm} = I_{bb_{hd}} + I_{bb_{ut}} + I_{bb_{lt}} + m_{hd} (r_{cm} - \ell_{ut} - \ell_{lt} - a_{hd})^2 + m_{ut} (r_{cm} - \ell_{lt} - 0.5 \ell_{ut})^2 + m_{lt} (r_{cm} - 0.5 \ell_{ut})^2$$

A.2 Right Arm, Left Arm and Weapon Configuration

The geometrical representations for the upper arm segments, forearm segments and hands are shown in Figure A-2. The hand is represented by a sphere with density

$$\rho_h = 1.148 \times 10^3 \quad (\text{kg/m}^3)$$

obtained from reference⁹ and mass,

$$m_h = 0.01 W + 0.1588 \quad (\text{kg})$$

where W = total body weight, obtained from reference⁷.

The radius and moment of inertia formulas for the spherical hand are

$$r_h = \frac{(3 m_h)^{1/3}}{\sqrt[3]{4 \pi \rho_h}}$$

and

$$J_{11h} = J_{22h} = J_{33h} = \frac{2}{5} m_h r_h^2$$

A frustum of a right circular cone is used to represent both the upper arm segment and the forearm segment. Lengths ℓ_u and ℓ_l are defined by anthropometric dimensions,

$$\ell_u = \text{acromial height} - \text{radiale height}$$

⁹Drillis, R. and Contini, R., "Body Segment Parameters," Office of Vocational Rehabilitation, Department of Health, Education & Welfare, N.Y. University, School of Engineering & Science, N.Y., Report 1166-03, 1966

⁷Barter, J.T., "Estimation of the Mass of Body Segments," Wright Air Development Center, Wright-Patterson Air Force Base, Ohio, TR-57-260, AD 118222, 1957

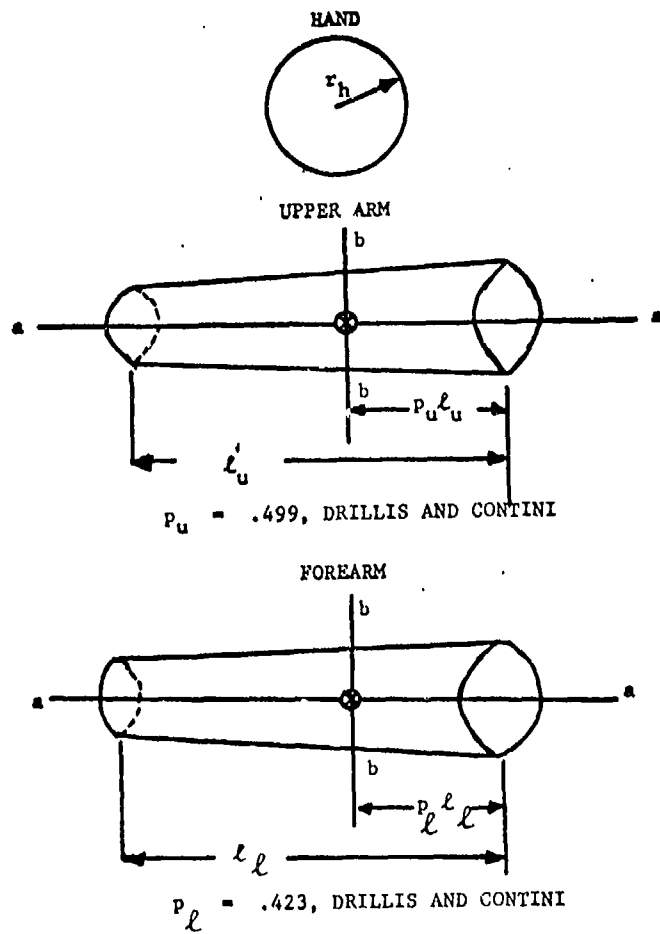


Figure A-2 Geometrical Arm and Hand Representations

and

$$\ell_{\ell} = \text{radiale height} - \text{stylion height}$$

coefficients p_u and p_f were obtained from reference⁹;

$$p_u = 0.449$$

$$p_{\ell} = 0.423$$

and the masses m_u and m_{ℓ} of the upper arm and forearm, respectively were obtained from reference⁷:

$$m_u = 0.04 W - 0.6577 \quad (\text{kg})$$

and

$$m_{\ell} = 0.02 W - 0.1134 \quad (\text{kg})$$

where W = total body weight (kg).

The moments of inertia of the upper arm are then given by the standard formulas for a frustrum of a cone,

$$J_{aa_u} = \frac{2 A_u m_u^2}{\rho_a \ell_u}$$

and

$$J_{bb_u} = J_{cc_u} = m_u [B_u \ell_u^2 + A_u m_u / (\rho_a \ell_u)]$$

where

$$A_u = \frac{\kappa_a + \mu_a^3 + \mu_a^4}{20 \pi \kappa_a^2}$$

$$B_u = \frac{3 [\kappa_a + 3\mu_a \kappa_a + (5 + \kappa_a) \mu_a^2]}{80 \kappa_a^2}$$

$$\mu_a = \frac{4 p_u - 1}{1 - 2 p_u + \sqrt{12 p_u (1 - p_u)}}^{-2}$$

and

$$\kappa_a = 1 + \mu_a + \mu_a^2$$

Moments of inertia formulas for the forearm are identical to those of the upper arm except that the coefficients l_u , p_u and m_u are replaced with l_ℓ , p_ℓ and m_ℓ respectively.

Figure A-3 contains an illustration of the two-dimensional geometrical configuration of the weapon and both arms. Point S locates the shoulder pivot point. For convenience the assumption is made that both arms are connected at point S. The right hand grasps the weapon at distance c_1 and the left hand grasps the weapon at distance c_2 and distance x_w locates the center mass of the weapon. Table A-1 contains the weapon mass, moment of inertia and center of gravity location of the M16 rifle and the M203 grenade launcher, as measured by Mr. T. Hutchings.

TABLE A-1 WEAPON PARAMETERS

PARAMETER	M-16	M203
m_w (lb)	8.6	9.4
I_w (lb-in-sec ²)	1.6	3.6
X_w (in)	17.	19.

Referring to Figure A-3, the total mass of the arm-weapon system and the center of mass location (x_o , y_o) are given by

$$m_r = 2 m_u + 2 m_\ell + 2 m_h + m_w$$

$$x_o = [m_u p_u l_u (\cos \alpha + \cos \beta) + m_\ell (l_u + p_\ell l_\ell) (\cos \alpha + \cos \beta) + m_h (c_1 + c_2) + m_w x] / m_r$$

and

$$y_o = [m_u p_u l_u + m_\ell (l_u + p_\ell l_\ell)] (\sin \alpha + \sin \beta) / m_r$$

where

$$\cos \beta = \frac{l_u^2 + c_1^2 - l_\ell^2}{2 l_u c_1}$$

$$\cos \alpha = \frac{l_u^2 + c_2^2 - l_\ell^2}{2 l_u c_2}$$

Finally the combined moment of inertia of the arm-weapon system about the center of mass becomes

$$\begin{aligned}
 J_{cm} = & 2 J_{11}_h + 2 J_{bb}_u + 2 J_{bb}_\ell + J_w \\
 & + m_h [(x_o - c_1)^2 + (x_o - c_2)^2 + y_o^2] \\
 & + m_u [(x_o - p_u \ell_u \cos \alpha)^2 + (x_o - p_u \ell_u \cos \beta)^2 \\
 & + (y_o - p_u \ell_u \sin \alpha)^2 + (y_o - p_u \ell_u \sin \beta)^2] \\
 & + m_\ell \{ [x_o - (\ell_u + p_\ell \ell_\ell) \cos \alpha]^2 + [x_o - (\ell_u + p_\ell \ell_\ell) \cos \beta]^2 \\
 & + [y_o - (\ell_u - p_\ell \ell_\ell) \sin \alpha]^2 + [y_o - (\ell_u - p_\ell \ell_\ell) \sin \beta]^2 \} \\
 & + m_w [(x_o - x_w)^2 + y_o^2]
 \end{aligned}$$

A.3 Anthropometric Data and Calculated Results

A list is provided, in Table A-2, of some typical weights and anthropometric dimensions for three men of various sizes (small, medium, large). This table contains a partial list of data that were measured by Santschi reference⁸. Table A-3 contains the calculated dimensions and inertial parameters based on the data in Table A-1 and A-2. The arm-weapon inertial parameter, I_{cm} , is somewhat larger than actual because the five pound shoulder force measuring device was included in the inertia and center of mass calculations. The results in Table A-3 show the orders of magnitude of the model parameters along with the expected variations for different size men.

⁸Santschi, W.R., DuBois, J., and Omoto, C., "Moments of Inertia and Centers of Gravity of the Living Human Body, Aerospace Medical Research Laboratories, Wright-Patterson Air Force Base, Ohio, AMRL-TDR-63-66, AD 410451, 1963

TABLE A-2 (SANTSCHI)
WEIGHT AND ANTHROPOMETRIC DATA FOR THREE TEST SUBJECTS

	SUBJECT 1	SUBJECT 2	SUBJECT 3
Weight	161.6 (lb)	172.2 (lb)	210.4 (lb)
Stature	66.9 (in)	73.0 (in)	72.3 (in)
Head Circ.	22.2	23.5	23.3
Chest Breadth	13.3	12.7	15.6
Waist Breadth	11.6	12.0	13.2
Hip Breadth	13.8	14.8	16.3
Chest Depth	9.3	10.3	10.4
Waist Depth	8.3	9.3	10.9
Hip Depth	10.5	10.6	10.5
Cervical ht.	56.3	62.7	62.4
Substernal ht.	47.8	50.8	50.7
Trochanteric ht.	33.5	39.2	38.5
Forearm Length	9.8	11.5	11.1
Upper Arm Length	12.8	13.7	14.0

TABLE A-3 CALCULATED BIOMECHANICAL PARAMETERS
FOR THREE TEST SUBJECTS

	SUBJECT #1	SUBJECT #2	SUBJECT #3
M (lb)	87.	97.	116.
I_{cm} (lb-in-sec ²)	18.	21.	26.
gm_r (lb)	32.	33.	38.
I_r (lb-in-sec ²)	9.7	11.	13.
L (in)	20.	21.	21.
r_{cm} (in)	13.	14.	13.
x_o (in)	9.6	9.5	9.3

APPENDIX B

B.0 DIGITAL COMPUTER PROGRAM LISTING

```

REAL M,MR,ICM,IR,L,KXW,KXS,KT,KP,MU,NU,K,IF
COMMON /$A/ M,MR,ICM,IR,L,D,XS,RCM,KXW,KXS,KT,KP,CDX,
* CDT,CDP,G,K,XO,TO,PO,STO,STPO,CTPO,TIM
COMMON /$PLOT/ NP,TIME(502),R(502),Z(502)
DIMENSION PRMT(5),RHS(6),Y(6),AUX(8,6),ERW(6)
EXTERNAL FCT,OUTP
CALL PLOTS(IBUF,IDUM,14)

C
C     ALL UNITS ARE IN THE POUND, INCH, SECOND SYSTEM
C

G = 386.4
NDIM = 6
NRUN = 0

C
C     READ INERTIA DATA
C
10 READ (5,1000,END=999) M,MR,ICM,IR
   NP = 0
   NRUN = NRUN + 1

C
C     READ DISTANCES
C
READ (5,1000) L,D,XS,RCM

C
C     READ SPRING CONSTANTS
C
READ (5,1000) KXW,KXS,KT,KP

C
C     READ DAMPING RATIOS
C
READ (5,1000) CRX,CRT,CRP

C
C     CALCULATE DAMPING COEFFICIENTS
C
CDX = CRX*2.*SQRT(KXS*MR)
CDT = CRT*2.*SQRT(KT*ICM)
CDP = CRP*2.*SQRT(KP*IR)

C
C     READ INTEGRATION PARAMETERS: START TIME, STOP TIME,
C     TIME INTERVAL, UPPER ERROR BOUND, AND PRINT PARAMETER
C
READ (5,1000) (PRMT(I),I=1,4)

C
C     READ INITIAL CONDITIONS: XDOT(1-3), X(1-3)
C

```



```

X0 = Y(4)
TO = Y(5)
PO = Y(6)
STO = SIN(TO)
CTO = COS(TO)
SPO = SIN(PO)
CPO = COS(PO)
STFO = SIN(TO + PO)
CTPO = COS(TO + PO)
MU = MR*L*CPO
DL = L*CPO + D
CALL OUTP(T,Y,RHS,IHLF,NDIM,PRMT)
20 PRMT(1) = TIM + TDUR
   PRMT(2) = TIM + TINT
   IF(PRMT(1).GE.TEND) GO TO 50
   IF(PRMT(2).GT.TEND) PRMT(2) = TEND
   DO 25 I=1,3
25  RHS(I) = ERW(I)
   ETA = Y(4) + L*SPO
   NU = IR + MR*Y(4)**2
   B11 = K*NU + MR*IR*L**2 + (MU*Y(4))**2
   B12 = NU*MU
   B13 = -(IR + MR*Y(4)*ETA)*MU
   B22 = MR*NU
   B23 = -MR*(IR + MR*Y(4)*ETA)
   B33 = MR*(K + IR + MR*ETA**2)
   DELTA = K*MR*NU + IR*(MR*L*SPJ)**2
   Y(1) = Y(1) + IF*(-B11 + B12*DL + B13*D)/DELTA
   Y(2) = Y(2) + IF*(-B12 + B22*DL + B23*D)/DELTA
   Y(3) = Y(3) + IF*(-B13 + B23*DL + B33*D)/DELTA
C
C      INTEGRATE THE MAN/WEAPON EQUATIONS
C
CALL RKGS(PRMT,Y,RHS,NDIM,IHLF,FCT,OUTP,AUX)
WRITE(6,2500) IHLF
GO TO 20
50 WRITE(6,3500)
   DO 60 I=1,NP
   WRITE(6,4500) I,TIME(I),R(I),Z(I)
60 CONTINUE
C
C      PLOT RESULTS
C
CALL CALPLT(NRUN)
GO TO 10

```

```

999 CALL PLOT(12.0,0.0,999)
1000 FORMAT(8F10.0)
1500 FORMAT('1',T4,'TIME',T17,'XDOT',T37,'TDOT',T57,'PDOT',T77,'X',
* T97,'T',T117,'P')
2000 FORMAT('1THREE DEGREE OF FREEDOM MAN/WEAPON MODEL INPUT',5X,'RUN '
* .I3/
* 'OINERTIA DATA:'/T3,'M',T28,'MR',T53,'ICM',T78,'IR')
2500 FORMAT('OIHLE =',I3//)
3000 FORMAT(1X,4(E15.8,10X))
3500 FORMAT('1 NP',T10,'TIME',T30,'RECOIL',T50,'PITCH')
4000 FORMAT('ODISTANCES:'/T3,'L',T28,'D',T53,'XS',T78,'RCM')
4500 FORMAT(' ',I3,T10,F8.5,T30,E15.8,T50,E15.8)
5000 FORMAT('OSPRING CONSTANTS:'/T3,'KXW',T28,'KXS',T53,'KT',T78,'KP')
5500 FORMAT('OVELOCITY ERROR WEIGHTS:'/T3,'XDOT',T28,'TDOT',T53,'PDOT')
6000 FORMAT('OCRITICAL DAMPING RATIOS:'/T3,'CRX',T28,'CRT',T53,'CRP')
6500 FORMAT('OPOSITION ERROR WEIGHTS:'/T3,'X',T28,'T',T53,'P')
7000 FORMAT('ORKGS PARAMETERS:'/T3,'START TIME',T28,'STOP TIME',
* T53,'TIME INCR',T78,'ERROR BOUND')
7500 FORMAT('OTIME PARAMETERS:'/T3,'TOUR',T28,'TINT',T53,'IF')
8000 FORMAT('OINITIAL VELOCITIES:'/T3,'XDOT',T28,'TDOT',T53,'PDOT')
9000 FORMAT('OINITIAL POSITIONS:'/T3,'X',T28,'T',T53,'P')
STOP
END

```

```
SUBROUTINE CALPLT(NRUN)
COMMON /*PLOT/ NP,TIME(502),R(502),Z(502)
DIMENSION T(4),DAT(7)
T(1) = TIME(1)
T(2) = TIME(NP)
FRN = NRUN
```

C
C
C

```
PREPARE FOR THE FIRST PLOT
```

```
CALL NEWPEN(1)
CALL PLOT(0.0,-15.0,-3)
CALL DASHP(0.0,16.0,0.3)
CALL PLOT(1.0,-15.0,-3)
CALL PLOT(0.0,3.0,-3)
CALL RECT(0.0,0.0,7.5,9.0,0.0,2)
CALL PLOT(1.5,0.75,-3)
CALL SCALE(T,7.0,2,1)
CALL SCALE(R,5.25,NP,1)
CALL SCALE(Z,5.25,NP,1)
TIME(NP+1) = T(3)
TIME(NP+2) = T(4)
```

C
C
C

```
DRAW AXES AND GRAPHS
```

```
CALL AXIS(0.0,0.0,'TIME (SECONDS)',-14.7,0.0,0.0,T(3),T(4):
CALL AXIS(0.0,0.0,'PITCH ANGLE (DEGREES)',21.5,25.90,0.0,Z(NP+1),
* Z(NP+2))
ZEROP = ABS(Z(NP+1)/Z(NP+2))
CALL PLOT(0.0,ZEROP,3)
CALL PLOT(7.0,ZEROP,2)
CALL LINE(TIME,Z,NP,1,0,1)
CALL NEWPEN(2)
CALL AXIS(-0.75,0.0,'MOUNT FORCE (POUNDS)',20.5,25.90,0.0,
* R(NP+1),R(NP+2))
ZEROP = ABS(R(NP+1)/R(NP+2))
CALL PLOT(-0.75,ZEROP,3)
CALL PLOT(7.00,ZEROP,2)
CALL LINE(TIME,R,NP,1,0,1)
```

C
C
C

```
WRITE TITLE HEADINGS
```

```
CALL NEWPEN(1)
CALL SYMBOL(1.5,6.25,0.21,'MAN/WEAPON ANALYSIS',0.0,19)
CALL SYMBOL(1.5,6.0,0.14,'MOUNT FORCE AND TOTAL PITCH ANGLE',
* 0.0,33)
```

```
CALL OBOATE(DAT)
CALL SYMBOL(1.5,5.75,0.14,DAT,0.0,28)
CALL SYMBOL(1.5,5.50,0.14,'RUN ',0.0,4)
CALL NUMBER(999.,999.,0.14,FRN,0.0,0)
```

C
C
C

PREPARE FOR THE NEXT PLOT

```
CALL PLOT(8.5,-15.0,-3)
CALL DASHP(0.0,16.0,0.3)
RETURN
END
```

```

SUBROUTINE FCT(T,Y,RHS)
REAL M,MR,ICM,IR,L,KXW,KXS,KT,KP,MU,NU,K
COMMON /$A/ M,MR,ICM,IR,L,D,XS,RCM,KXW,KXS,KT,KP,CDX,
* CDT,CDP,G,K,XO,TO,PO,STO,STPO,CTPO,TIM
DIMENSION Y(6),X(3),XD(3),RHS(6)
DO 10 I=1,3
J=I+3
X(I) = Y(J)
10 XD(I) = Y(I)
STP = SIN(X(2) + X(3))
CTP = COS(X(2) + X(3))
ST = SIN(X(2))
CT = COS(X(2))
SP = SIN(X(3))
CP = COS(X(3))
MU = MR*L*CP
ETA = X(1) + L*SP
NU = IR + MR*X(1)**2
B11 = K*NU + MR*IR*L**2 + (MU*X(1))**2
B12 = NU*MU
B13 = -(IR + MR*X(1)*ETA)*MU
B22 = MR*NU
B23 = -MR*(IR + MR*X(1)*ETA)
B33 = MR*(K + IR + MR*ETA**2)
DELTA = K*MR*NU + IR*(MR*L*SP)**2
FX = MR*X(1)*(XD(2) + XD(3))**2 + MR*L*SP*XD(2)**2 + MR*D*(STPO
* -STP)
FKX = KXW*(X(1) - XO) + CDX *XD(1)
IF(X(1).LT.XS) FKX = KXS*(X(1)-XS)+KXW*(XS-XO)+CDX *XD(1)
FX = FX - FKX
FT = -2.*MR*ETA*XD(1)*(XD(2)+XD(3))-X(1)*MU*XD(3)*(2.*XD(2)+XD(3))
* -CDT*XD(2)-KT*(X(2)-TO) + (M*RCM+MR*L)*D*(ST-STO)
* -MR*D*(X(1)*CTP-XO*CTPO)
FP = -2.*MR*X(1)*XD(1)*(XD(2)+XD(3))+MU*XD(1)*XD(2)**2-CDP*XD(3)
* -KP*(X(3)-PO)-MR*D*X(1)*CTP +MR*D*XO*CTPO
RHS(1) = (FX*B11 + FT*B12 + FP*B13)/DELTA
RHS(2) = (FX*B12 + FT*B22 + FP*B23)/DELTA
RHS(3) = (FX*B13 + FT*B23 + FP*B33)/DELTA
RHS(4) = XD(1)
RHS(5) = XD(2)
RHS(6) = XD(3)
RETURN
END

```

```

SUBROUTINE GUTP(T,Y,RHS,IHLF,NDIM,PRMT)
REAL M,MR,ICM,IR,L,KXW,KXS,KT,KP,MU,NU,K
COMMON /$A/ M,MR,ICM,IR,L,D,XS,RCM,KXW,KXS,KT,KP,CDX,
* CDT,COP,G,K,XO,TO,PO,STO,STPO,CTPO,TIM
COMMON /$PLOT/ NP,TIME(502),R(502),Z(502)
DIMENSION Y(6),RHS(6),PRMT(5)
TIM = T
CPI = 180./3.1415927
NP = NP + 1
IF(NP.GT.500) GO TO 50
R(NP) = KXW*(Y(4) - XO) + CDX *Y(1)
IF(Y(4).LT.XS) R(NP) = KXS*(Y(4) - XS) + KXW*(XS - XO) + CDX *Y(1)
Z(NP) = (Y(5) + Y(6))*CPI
TIME(NP) = T
50 CONTINUE
C ***** ADDITION FOR OTHER PLOTS *****
WRITE(3)T,Y,RHS
WRITE(6,1000) T,Y
1000 FORMAT(!X,F8.5,T10.6(5X,E15.8))
RETURN
END

```

C		RKGS	10
C	RKGS	20
C		RKGS	30
C	SUBROUTINE RKGS	RKGS	40
C		RKGS	50
C	PURPOSE	RKGS	80
C	TO SOLVE A SYSTEM OF FIRST ORDER ORDINARY DIFFERENTIAL	RKGS	70
C	EQUATIONS WITH GIVEN INITIAL VALUES.	RKGS	80
C		RKGS	90
C	USAGE	RKGS	100
C	CALL RKGS (PRMT,Y,DERY,NDIM,IHLF,FCT,OUTP,AUX)	RKGS	110
C	PARAMETERS FCT AND OUTP REQUIRE AN EXTERNAL STATEMENT.	RKGS	120
C		RKGS	130
C	DESCRIPTION OF PARAMETERS	RKGS	140
C	PRMT - AN INPUT AND OUTPUT VECTOR WITH DIMENSION GREATER	RKGS	150
C	OR EQUAL TO 5, WHICH SPECIFIES THE PARAMETERS OF	RKGS	160
C	THE INTERVAL AND OF ACCURACY AND WHICH SERVES FOR	RKGS	170
C	COMMUNICATION BETWEEN OUTPUT SUBROUTINE (FURNISHED	RKGS	180
C	BY THE USER) AND SUBROUTINE RKGS. EXCEPT PRMT(5)	RKGS	190
C	THE COMPONENTS ARE NOT DESTROYED BY SUBROUTINE	RKGS	200
C	RKGS AND THEY ARE	RKGS	210
C	PRMT(1)- LOWER BOUND OF THE INTERVAL (INPUT),	RKGS	220
C	PRMT(2)- UPPER BOUND OF THE INTERVAL (INPUT),	RKGS	230
C	PRMT(3)- INITIAL INCREMENT OF THE INDEPENDENT VARIABLE	RKGS	240
C	(INPUT),	RKGS	250
C	PRMT(4)- UPPER ERROR BOUND (INPUT). IF ABSOLUTE ERROR IS	RKGS	260
C	GREATER THAN PRMT(4), INCREMENT GETS HALVED.	RKGS	270
C	IF INCREMENT IS LESS THAN PRMT(3) AND ABSOLUTE	RKGS	280
C	ERROR LESS THAN PRMT(4)/50, INCREMENT GETS DOUBLED.	RKGS	290
C	THE USER MAY CHANGE PRMT(4) BY MEANS OF HIS	RKGS	300
C	OUTPUT SUBROUTINE.	RKGS	310
C	PRMT(5)- NO INPUT PARAMETER. SUBROUTINE RKGS INITIALIZES	RKGS	320
C	PRMT(5)=0. IF THE USER WANTS TO TERMINATE	RKGS	330
C	SUBROUTINE RKGS AT ANY OUTPUT POINT, HE HAS TO	RKGS	340
C	CHANGE PRMT(5) TO NON-ZERO BY MEANS OF SUBROUTINE	RKGS	350
C	OUTP. FURTHER COMPONENTS OF VECTOR PRMT ARE	RKGS	360
C	FEASIBLE IF ITS DIMENSION IS DEFINED GREATER	RKGS	370
C	THAN 5. HOWEVER SUBROUTINE RKGS DOES NOT REQUIRE	RKGS	380
C	AND CHANGE THEM. NEVERTHELESS THEY MAY BE USEFUL	RKGS	390
C	FOR HANDING RESULT VALUES TO THE MAIN PROGRAM	RKGS	400
C	(CALLING RKGS) WHICH ARE OBTAINED BY SPECIAL	RKGS	410
C	MANIPULATIONS WITH OUTPUT DATA IN SUBROUTINE OUTP.	RKGS	420
C	Y - INPUT VECTOR OF INITIAL VALUES. (DESTROYED)	RKGS	430
C	LATERON Y IS THE RESULTING VECTOR OF DEPENDENT	RKGS	440
C	VARIABLES COMPUTED AT INTERMEDIATE POINTS X.	RKGS	450

C	DERY	- INPUT VECTOR OF ERROR WEIGHTS. (DESTROYED)	RKGS 460
C		THE SUM OF ITS COMPONENTS MUST BE EQUAL TO 1.	RKGS 470
C		LATERON DERY IS THE VECTOR OF DERIVATIVES, WHICH	RKGS 480
C		BELONG TO FUNCTION VALUES Y AT A POINT X.	RKGS 490
C	NDIM	- AN INPUT VALUE, WHICH SPECIFIES THE NUMBER OF	RKGS 500
C		EQUATIONS IN THE SYSTEM.	RKGS 510
C	IHLF	- AN OUTPUT VALUE, WHICH SPECIFIES THE NUMBER OF	RKGS 520
C		BISECTIONS OF THE INITIAL INCREMENT. IF IHLF GETS	RKGS 530
C		GREATER THAN 10, SUBROUTINE RKGS RETURNS WITH	RKGS 540
C		ERROR MESSAGE IHLF=11 INTO MAIN PROGRAM. ERROR	RKGS 550
C		MESSAGE IHLF=12 OR IHLF=13 APPEARS IN CASE	RKGS 560
C		PRMT(3)=0 OR IN CASE SIGN(PRMT(3)).NE.SIGN(PRMT(2)-	RKGS 570
C		PRMT(1)) RESPECTIVELY.	RKGS 580
C	FCT	- THE NAME OF AN EXTERNAL SUBROUTINE USED. THIS	RKGS 590
C		SUBROUTINE COMPUTES THE RIGHT HAND SIDES DERY OF	RKGS 600
C		THE SYSTEM TO GIVEN VALUES X AND Y. ITS PARAMETER	RKGS 610
C		LIST MUST BE X,Y,DERY. SUBROUTINE FCT SHOULD	RKGS 620
C		NOT DESTROY X AND Y.	RKGS 630
C	OUTP	- THE NAME OF AN EXTERNAL OUTPUT SUBROUTINE USED.	RKGS 640
C		ITS PARAMETER LIST MUST BE X,Y,DERY,IHLF,NDIM,PRMT.	RKGS 650
C		NONE OF THESE PARAMETERS (EXCEPT, IF NECESSARY,	RKGS 660
C		PRMT(4),PRMT(5),...) SHOULD BE CHANGED BY	RKGS 670
C		SUBROUTINE OUTP. IF PRMT(5) IS CHANGED TO NON-ZERO,	RKGS 680
C		SUBROUTINE RKGS IS TERMINATED.	RKGS 690
C	AUX	- AN AUXILIARY STORAGE ARRAY WITH 8 ROWS AND NDIM	RKGS 700
C		COLUMNS.	RKGS 10
C			RKGS 720
C			RKGS 730
C	REMARKS		
C		THE PROCEDURE TERMINATES AND RETURNS TO CALLING PROGRAM, IF	RKGS 740
C		(1) MORE THAN 10 BISECTIONS OF THE INITIAL INCREMENT ARE	RKGS 750
C		NECESSARY TO GET SATISFACTORY ACCURACY (ERROR MESSAGE	RKGS 760
C		IHLF=11).	RKGS 770
C		(2) INITIAL INCREMENT IS EQUAL TO OR HAS WRONG SIGN	RKGS 780
C		(ERROR MESSAGES IHLF=12 OR IHLF=13).	RKGS 9Z
C		(3) THE WHOLE INTEGRATION INTERVAL IS WORKED THROUGH.	RKGS 800
C		(4) SUBROUTINE OUTP HAS CHANGED PRMT(5) TO NON-ZERO.	RKGS 810
C			RKGS 820
C	SUBROUTINES AND FUNCTION SUBPROGRAMS REQUIRED		RKGS 830
C		THE EXTERNAL SUBROUTINES FCT(X,Y,DERY) AND	RKGS 840
C		OUTP(X,Y,DERY,IHLF,NDIM,PRMT) MUST BE FURNISHED BY THE USER.	RKGS 850
C			RKGS 860
C	METHOD		RKGS 870
C		EVALUATION IS DONE BY MEANS OF FOURTH ORDER RUNGE-KUTTA	RKGS 880
C		FORMULAE IN THE MODIFICATION DUE TO GILL. ACCURACY IS	RKGS 890
C		TESTED COMPARING THE RESULTS OF THE PROCEDURE WITH SINGLE	RKGS 900

C	AND DOUBLE INCREMENT.	RKGS 910
C	SUBROUTINE RKGS AUTOMATICALLY ADJUSTS THE INCREMENT DURING	RKGS 920
C	THE WHOLE COMPUTATION BY HALVING OR DOUBLING. IF MORE THAN	RKGS 930
C	10 BISECTIONS OF THE INCREMENT ARE NECESSARY TO GET	RKGS 940
C	SATISFACTORY ACCURACY, THE SUBROUTINE RETURNS WITH	RKGS 950
C	ERROR MESSAGE IHLF=11 INTO MAIN PROGRAM.	RKGS 960
C	TO GET FULL FLEXIBILITY IN OUTPUT, AN OUTPUT SUBROUTINE	RKGS 970
C	MUST BE FURNISHED BY THE USER.	RKGS 980
C	FOR REFERENCE. SEE	RKGS 990
C	RALSTON/WILF, MATHEMATICAL METHODS FOR DIGITAL COMPUTERS,	RKGS1000
C	WILEY, NEW YORK/LONDON, 1960, PP.110-120.	RKGS1010
C		RKGS1020
C	RKGS1030
C		RKGS1040
C	SUBROUTINE RKGS(PRMT,Y,DERY,NDIM,IHLF,FCT,OUTP,AUX)	RKGS1050
C		RKGS1060
C		RKGS1070
	DIMENSION Y(1),DERY(1),AUX(8,1),A(4),B(4),C(4),PRMT(1)	
	DO 1 I=1,NDIM	RKGS1090
1	AUX(8,I)=.06666667*DERY(I)	RKGS1100
	X=PRMT(1)	RKGS1110
	XEND=PRMT(2)	RKGS1120
	H=PRMT(3)	RKGS1130
	PRMT(5)=0.	RKGS1140
	CALL FCT(X,Y,DERY)	RKGS1150
C		RKGS1160
C	ERROR TEST	RKGS1170
	IF(H*(XEND-X))38,37,2	RKGS1180
C		RKGS1190
C	PREPARATIONS FOR RUNGE-KUTTA METHOD	RKGS1200
2	A(1)=.5	RKGS1210
	A(2)=.2928932	RKGS1220
	A(3)=1.707107	RKGS1230
	A(4)=.1666667	RKGS1240
	B(1)=2.	RKGS1250
	B(2)=1.	RKGS1260
	B(3)=1.	RKGS1270
	B(4)=2.	RKGS1280
	C(1)=.5	RKGS1290
	C(2)=.2928932	RKGS1300
	C(3)=1.707107	RKGS1310
	C(4)=.5	RKGS1320
C		RKGS1330
C	PREPARATIONS OF FIRST RUNGE-KUTTA STEP	RKGS1340
	DO 3 I=1,NDIM	RKGS1350

	AUX(1,I)=Y(I)	RKQS1360
	AUX(2,I)=DERY(I)	RKQS13 0
	AUX(3,I)=0.	RKQS1380
3	AUX(6,I)=0.	RKQS1390
	IREC=0	RKQS1400
	H=H+H	RKQS1410
	IHLF=-1	RKQS1420
	ISTEP=0	RKQS1430
	IEND=0	RKQS1440
C		RKQS1450
C		RKQS1460
C	START OF A RUNGE-KUTTA STEP	RKQS1470
	4 IF((X+H-XEND)*H)7.6.5	RKQS1480
	5 H=XEND-X	RKQS1490
	6 IEND=1	RKQS1500
C		RKQS1510
C	RECORDING OF INITIAL VALUES OF THIS STEP	RKQS1520
	7 CALL OUTP(X,Y,DERY,IREC,NDIM,PRMT)	RKQS1530
	IF(PRMT(5))40.8.40	RKQS1540
	8 ITEST=0	RKQS1550
	9 ISTEP=ISTEP+1	RKQS1560
C		RKQS1570
C		RKQS1580
C	START OF INNERMOST RUNGE-KUTTA LOOP	RKQS1590
	J=1	RKQS1600
10	AJ=A(J)	RKQS1610
	BJ=B(J)	RKQS1620
	CJ=C(J)	RKQS1630
	DO 11 I=1,NDIM	RKQS1640
	R1=H*DERY(I)	RKQS1650
	R2=AJ*(R1-BJ*AUX(6,I))	RKQS1660
	Y(I)=Y(I)+R2	RKQS1670
	R2=R2+R2+R2	RKQS1680
11	AUX(6,I)=AUX(6,I)+R2*CJ*R1	RKQS1690
	IF(J-4)12,15,15	RKQS1700
12	J=J+1	RKQS1 10
	IF(J-3)13,14,13	RKQS1720
13	X=X+.5*H	RKQS1730
14	CALL FCT(X,Y,DERY)	RKQS1740
	GO TO 10	RKQS1750
C	END OF INNERMOST RUNGE-KUTTA LOOP	RKQS1760
C		RKQS1770
C		RKQS1780
C	TEST OF ACCURACY	RKQS1790
15	IF(ITEST)16,16,20	RKQS1800

C		RKGS1810
C	IN CASE ITEST=0 THERE IS NO POSSIBILITY FOR TESTING OF ACCURACY	RKGS1820
	16 DO 17 I=1,NDIM	RKGS1830
	17 AUX(4,I)=Y(I)	RKGS1840
	ITEST=1	RKGS1850
	ISTEP=ISTEP+ISTEP-2	RKGS1860
	18 IHLF=IHLF+1	RKGS1870
	X=X-H	RKGS1880
	H=.5*H	RKGS1890
	DO 19 I=1,NDIM	RKGS1900
	Y(I)=AUX(1,I)	RKGS1910
	DERY(I)=AUX(2,I)	RKGS1920
	19 AUX(6,I)=AUX(3,I)	RKGS1930
	GOTO 9	RKGS1940
C		RKGS1950
C	IN CASE ITEST=1 TESTING OF ACCURACY IS POSSIBLE	RKGS1960
	20 IMOD=ISTEP/2	RKGS1970
	IF(ISTEP-IMOD-IMOD)21,23,21	RKGS1980
	21 CALL FCT(X,Y,DERY)	RKGS1990
	DO 22 I=1,NDIM	RKGS2000
	AUX(5,I)=Y(I)	RKGS2010
	22 AUX(7,I)=DERY(I)	RKGS2020
	GOTO 9	RKGS2030
C		RKGS2040
C	COMPUTATION OF TEST VALUE DELT	RKGS2050
	23 DELT=0.	RKGS2060
	DO 24 I=1,NDIM	RKGS2070
	24 DELT=DELT+AUX(8,I)*ABS(AUX(4,I)-Y(I))	RKGS2080
	IF(DELT-PRMT(4))28,28,25	RKGS2090
C		RKGS2100
C	ERROR IS TOO GREAT	RKGS2110
	25 IF(IHLF-10)26,36,36	RKGS2120
	26 DO 27 I=1,NDIM	RKGS2130
	27 AUX(4,I)=AUX(5,I)	RKGS2140
	ISTEP=ISTEP+ISTEP-4	RKGS2150
	X=X-H	RKGS2160
	IEND=0	RKGS2170
	GOTO 18	RKGS2180
C		RKGS2190
C	RESULT VALUES ARE GOOD	RKGS2200
	28 CALL FCT(X,Y,DERY)	RKGS2210
	DO 29 I=1,NDIM	RKGS2220
	AUX(1,I)=Y(I)	RKGS2230
	AUX(2,I)=DERY(I)	RKGS2240
	AUX(3,I)=AUX(6,I)	RKGS2250

	Y(I)=AUX(6,I)	RK0S2260
29	DERY(I)=AUX(7,I)	RK0S2270
	CALL OUTP(X-H.Y.DERY,IHLF,NDIM,PRMT)	RK0S2280
	IF(PRMT(6))40,30,40	RK0S2290
30	DO 31 I=1,NDIM	RK0S2300
	Y(I)=AUX(1,I)	RK0S2310
31	DERY(I)=AUX(2,I)	RK0S2320
	IREC=IHLF	RK0S2330
	IF(IEND)32,32,39	RK0S2340
C		RK0S2350
C	INCREMENT GETS DOUBLED	RK0S2360
32	IHLF=IHLF-1	RK0S2370
	ISTEP=ISTEP/2	RK0S2380
	H=H+H	RK0S2390
	IF(IHLF)4,33,33	RK0S2400
33	IMOD=ISTEP/2	RK0S2410
	IF(ISTEP-IMOD-IMOD)4,34,4	RK0S2420
34	IF(DELT-.02*PRMT(4))35,35,4	RK0S2430
35	IHLF=IHLF-1	RK0S2440
	ISTEP=ISTEP/2	RK0S2450
	H=H+H	RK0S2460
	GOTO 4	RK0S2470
C		RK0S2480
C		RK0S2490
C	RETURNS TO CALLING PROGRAM	RK0S2500
36	IHLF=11	RK0S2510
	CALL FCT(X,Y,DERY)	RK0S2520
	GOTO 39	RK0S2530
37	IHLF=12	RK0S2540
	GOTO 39	RK0S2550
38	IHLF=13	RK0S2560
39	CALL OUTP(X,Y,DERY,IHLF,NDIM,PRMT)	RK0S2570
40	RETURN	RK0S2580
	END	RK0S2590

APPENDIX C

C.0 ANALOG COMPUTER SIMULATION

The analog computer program required to solve the three degree-of-freedom model is shown in Figure C-1. The diagram shown is simplified over that actually used, in that it does not contain scaling or gain factor information, nor does it show certain inverter amplifiers required by the non-linear equipment. Standard analog techniques are used throughout the program, except perhaps where multiplier feedback was used around the $\ddot{\theta}$ and $\ddot{\phi}$ summers in preference to resorting to the use of less accurate division circuitry. The generation and control of the firing pulse $F(t)$ was achieved by use of an internal timer, a logic gate (G), and a delay flop (P) to activate two integrators separately from the rest of the computer equipment. The timer controlled the firing frequency and the delay-flop controlled the duration of the $F(t)$ function. Equations 2-9 required linearization before they could be implemented on the analog computer. Small angle approximations were made and certain higher-order terms were removed. The final set of differential equations solved was as follows:

$$m_r \ddot{x} = m_r L \ddot{\theta} + m_r x \dot{\theta}^2 + m_r x \dot{\phi}^2 - (c_x \dot{x} + k_x \{x - x_0\}) - F(t)$$

$$[I_{cm} + I_r + M r_{cm}^2 + m_r (x^2 + L^2)] \ddot{\theta} = m_r L \ddot{x} - (I_r + m_r x^2) \ddot{\phi}$$

$$- m_r L x \dot{\phi}^2 - c_\theta \dot{\theta} - k_\theta \theta - m_r g (x - x_0) + L F(t)$$

$$(I_r + m_r x^2) \ddot{\phi} = - (I_r + m_r x^2) \ddot{\theta} + m_r L x \dot{\theta}^2 - c_\phi \dot{\phi} - k_\phi \phi - m_r g (x - x_0) + \delta F(t)$$

The main variables of interest (those monitored in actual tests) are output from the computer solution as F_{RECOIL} , the force felt on the gunners shoulder, and the total pitch angle $(\theta + \phi)$.

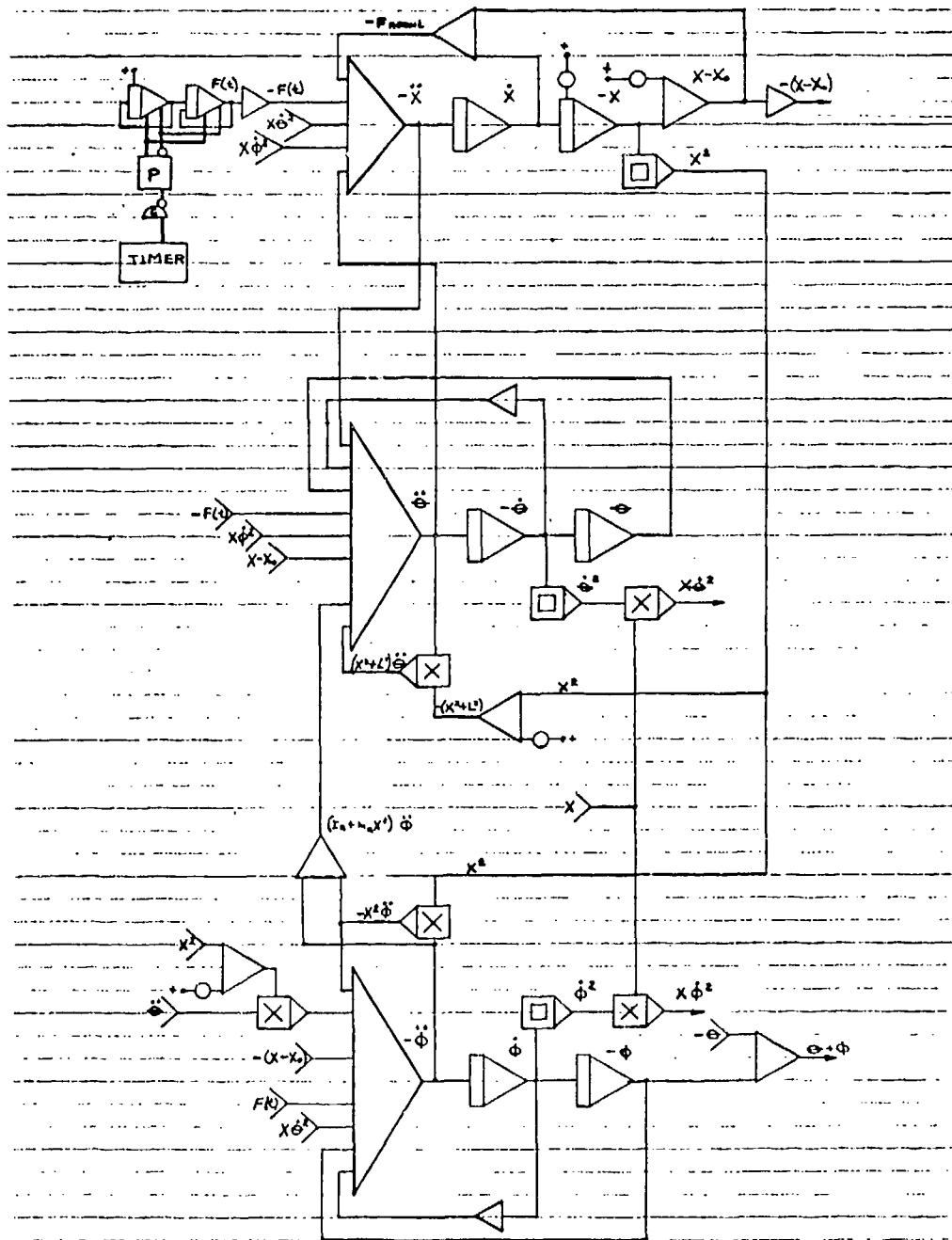


Figure C-1 Simplified Analog Computer Diagram of
Man-Weapon Interaction Equations

LITERATURE CITED

1. Whitsett, C.E., "Some Dynamic Response Characteristics of Weightless Man," Master of Science Thesis, Air Force Institute of Technology, Wright-Patterson Air Force Base, Ohio, AMRL-TR-63-18, AD 412541, 1962
2. McCrank, J.M. and Seger, D.R., "Torque Free Rotational Dynamics of a Variable Configuration Body (Application to Weightless Man)," Master of Science Thesis, Air Force Institute of Technology, Wright-Patterson Air Force Base, Ohio, AD 610239, 1964
3. McHenry, R.R. and Naab, K.N., "Computer Simulation of the Automobile Crash Victim in a Frontal Collision--A Validation Study," Cornell Aeronautical Laboratory, Inc., Buffalo, New York, CAL Report No. 4B-2126-V-1R, 1966
4. Braune, W. and Fischer, O., "The Center of Gravity of the Human Body As Related to the German Infantryman," Leipzig, ATI 138452, 1889
5. Fischer, O., "Theoretical Fundamentals for a Mechanics of Living Bodies with Special Applications to Man as Well as to Some Processes of Motion of Machines," B.G. Tubner, Berlin, ATI 153668, 1906
6. Dempster, W.T., "Space Requirements of the Seated Operator," Wright Air Development Center, TR-55-159, Wright-Patterson Air Force Base, Ohio, AD 87892, 1955
7. Barter, J.T., "Estimation of the Mass of Body Segments," Wright Air Development Center, Wright-Patterson Air Force Base, Ohio, TR-57-260, AD 118222, 1957
8. Santschi, W.R., DuBois, J. and Omoto, C., "Moments of Inertia and Centers of Gravity of the Living Human Body, Aerospace Medical Research Laboratories, Wright-Patterson Air Force Base, Ohio, AMRL-TDR-63-66, AD 410451, 1963
9. Drillis, R. and Contin, R., "Body Segment Parameters," Office of Vocational Rehabilitation, Department of Health, Education and Welfare, N.Y. University, School of Engineering and Science, New York, Report 1166-03, 1966

DISTRIBUTION LIST

Office of the Director of Defense
Research & Engineering
Room 3D-1085, The Pentagon
Washington, DC 20301 (1)

Defense Documentation Center
ATTN: TIPDR (12)
Cameron Station
Alexandria, VA 22314

HQDA (SAUS-OR)
ATTN: Dr. Daniel Willard (1)
Washington, DC 20310

Commander
CDEC
ATTN: Tech Library, Box 22 (1)
Fort Ord, CA 93941

Commander
US Army Harry Diamond Laboratories
ATTN: DRXDO-SA (1)
Washington, DC 20438

US Army Infantry School Library
Infantry Hall (1)
Fort Benning, GA 31905

Commander
Infantry School (2)
Fort Benning, GA 31905

Commander
US Army Training & Doctrine Command
ATTN: Tech Library (1)
ATTN: MS-1 (1)
Ft. Monroe, VA 23351

Dept of Operations Analysis
Naval Postgraduate School
ATTN: Prof. James K. Arima (1)
Monterey, CA 93940

Commander
Yuma Proving Ground
ATTN: Tech Library (1)
Yuma, AZ 85364

Director
US Army Aviation HRU
ATTN: Librarian (1)
P.O. Box 428
Ft. Rucker, AL 36362

HQDA (DAMA-WS) (1)
Washington, DC 20310

HQDA (DAMA-RA) (1)
Washington, DC 20310

Commander
US Army Materiel Development &
Readiness Command
ATTN: DRCRD (2)
ATTN: DRCRD-W (1)
ATTN: DRCRD-T (1)
5001 Eisenhower Ave.
Alexandria, VA 22333

Commander
US Army Armament Command
ATTN: DRSAR-RD, Mr. Brinkman (2)
ATTN: DRSAR-RDT (1)
ATTN: DRSAR-RDG, Mr. Craighead (1)
Rock Island, IL 61201

Commander
TRADOC Systems Analysis Agency
White Sands Missile Range (1)
New Mexico 88002

Commander
US Army Forces Command
ATTN: AFCGRDC (1)
Ft. McPherson, GA 30330

DISTRIBUTION LIST (Cont'd)

Commander
Rock Island Arsenal
ATTN: SARRI-LR (20)
ATTN: SARRI-LPL (2)
ATTN: SARRI-L (1)
ATTN: SARRI-LS, Dr. Gyorog (1)
ATTN: SARRI-LS-I, Mr. Ackley (1)

Commander
USA Combined Arms Combat
Developments Activity
ATTN: ATCACC (1)
Fort Leavenworth, KS 66027

Superintendent
US Military Academy
ATTN: Dept of Ordnance (1)
West Point, NY 10996

Director
US Army Ballistic Research
Laboratory
ATTN: DRXDR-IBL, Mr. Lentz (1)
Aberdeen, MD 21005

Commander
Frankford Arsenal
ATTN: SARFA-N6000 (1)
ATTN: SARFA-C2500 (1)
ATTN: SARFA-J7500 (1)
Philadelphia, PA 19137

Institute for Defense Analysis
ATTN: Dr. J. Orlansky (1)
400 Army-Navy Drive
Arlington, VA 22202

Superintendent
US Air Force Academy (1)
Colorado Springs, CO 80914

Office of Naval Research
Code 455
Washington, DC 20360 (1)

Commander
US Army Materiel Command
ATTN: SARPA-SA (1)
Picatinny Arsenal
Dover, NJ 07801

Commander
Aberdeen Proving Ground
ATTN: DRSTE-MT-M (1)
Aberdeen Proving Ground, MD 21005

Commander
US Army Test & Evaluation Command
ATTN: DRSTE-BA (1)
ATTN: DRSTE-TS (1)
Aberdeen Proving Ground, MD 21005

Commandant
US Army Field Artillery School
ATTN: Tech Library (1)
Fort Sill, OK 73503

Director
US Army Human Engineering
Laboratory (1)
Aberdeen, MD 21005

Director
US Army Materiel System Analysis
Agency
ATTN: DRXSY-G (1)
ATTN: DRXSY-GI (2)
ATTN: DRXSY-C (1)
ATTN: DRXSY-ADE (1)
Aberdeen Proving Grd, MD 21005

AFAL/DLY
Eglin AFB, FL 32542 (1)

Naval Weapons Center
ATTN: Technical Library (Code 753)
China Lake, CA 93555 (1)

DISTRIBUTION LIST UPDATE

- - - FOR YOUR CONVENIENCE - - -

Government regulations require the maintenance of up-to-date distribution lists for technical reports. This form is provided for your convenience to indicate necessary changes or corrections.

If a change in our mailing lists should be made, please check the appropriate boxes below. For changes or corrections, show old address *exactly* as it appeared on the mailing label. Fold on dotted lines, tape or staple the lower edge together, and mail.

Remove Name From List

Change or Correct Address

Old Address:

Corrected or New Address:

COMMENTS

Date: _____ Signature: _____

Technical Report #

FOLD HERE

Return Address:

POSTAGE AND FEES PAID
DEPARTMENT OF THE ARMY
DOD 314



OFFICIAL BUSINESS
Penalty for Private Use \$300

Commander
Rock Island Arsenal
Attn: SARRI-LR
Rock Island, Illinois 61201

FOLD HERE

AD ACCESSION NO.
Research Directorate, General Thomas J. Rodman Laboratory
Rock Island Arsenal, Rock Island, Illinois 61201
Study of Man-Weapon Reaction Forces Applicable to the
Fabrication of a Standard Rifle Firing Fixture
Final Report

UNCLASSIFIED

1. M16 Rifle
2. M79 Grenade Launcher
3. M203 Grenade Launcher
4. Biodynamics
5. Mathematical Model
6. Simulation
7. Man-Weapon
8. Small Arms Mount
9. Recoil

I. Thomas D. Hutchings and Albert E. Rahe
II. Research Directorate
III. General Thomas J. Rodman Laboratory
Rock Island Arsenal

86 Pages, Incl Figures

A study was conducted of the man-weapon interaction force relationship to define the parameters to be incorporated in the design of a universal small arms test fixture, that simulates man as a flexible mount. This report contains the results of Phase I of the program, which is to provide the engineering data and preliminary drawings required for the fabrication of a prototype test fixture. Phase II will provide for the manufacture and evaluation of the test fixture. To demonstrate the feasibility of designing a

DISTRIBUTION

Approved for public release, distribution unlimited

AD ACCESSION NO.
Research Directorate, General Thomas J. Rodman Laboratory
Rock Island Arsenal, Rock Island, Illinois 61201
Study of Man-Weapon Reaction Forces Applicable to the
Fabrication of a Standard Rifle Firing Fixture
Final Report

UNCLASSIFIED

1. M16 Rifle
2. M79 Grenade Launcher
3. M203 Grenade Launcher
4. Biodynamics
5. Mathematical Model
6. Simulation
7. Man-Weapon
8. Small Arms Mount
9. Recoil

I. Thomas D. Hutchings and Albert E. Rahe
II. Research Directorate
III. General Thomas J. Rodman Laboratory
Rock Island Arsenal

86 Pages, Incl Figures

A study was conducted of the man-weapon interaction force relationship to define the parameters to be incorporated in the design of a universal small arms test fixture, that simulates man as a flexible mount. This report contains the results of Phase I of the program, which is to provide the engineering data and preliminary drawings required for the fabrication of a prototype test fixture. Phase II will provide for the manufacture and evaluation of the test fixture. To demonstrate the feasibility of designing a

DISTRIBUTION

Approved for public release, distribution unlimited

AD ACCESSION NO.
Research Directorate, General Thomas J. Rodman Laboratory
Rock Island Arsenal, Rock Island, Illinois 61201
Study of Man-Weapon Reaction Forces Applicable to the
Fabrication of a Standard Rifle Firing Fixture
Final Report

UNCLASSIFIED

1. M16 Rifle
2. M79 Grenade Launcher
3. M203 Grenade Launcher
4. Biodynamics
5. Mathematical Model
6. Simulation
7. Man-Weapon
8. Small Arms Mount
9. Recoil

I. Thomas D. Hutchings and Albert E. Rahe
II. Research Directorate
III. General Thomas J. Rodman Laboratory
Rock Island Arsenal

86 Pages, Incl Figures

A study was conducted of the man-weapon interaction force relationship to define the parameters to be incorporated in the design of a universal small arms test fixture, that simulates man as a flexible mount. This report contains the results of Phase I of the program, which is to provide the engineering data and preliminary drawings required for the fabrication of a prototype test fixture. Phase II will provide for the manufacture and evaluation of the test fixture. To demonstrate the feasibility of designing a

DISTRIBUTION

Approved for public release, distribution unlimited

AD ACCESSION NO.
Research Directorate, General Thomas J. Rodman Laboratory
Rock Island Arsenal, Rock Island, Illinois 61201
Study of Man-Weapon Reaction Forces Applicable to the
Fabrication of a Standard Rifle Firing Fixture
Final Report

UNCLASSIFIED

1. M16 Rifle
2. M79 Grenade Launcher
3. M203 Grenade Launcher
4. Biodynamics
5. Mathematical Model
6. Simulation
7. Man-Weapon
8. Small Arms Mount
9. Recoil

I. Thomas D. Hutchings and Albert E. Rahe
II. Research Directorate
III. General Thomas J. Rodman Laboratory
Rock Island Arsenal

86 Pages, Incl Figures

A study was conducted of the man-weapon interaction force relationship to define the parameters to be incorporated in the design of a universal small arms test fixture, that simulates man as a flexible mount. This report contains the results of Phase I of the program, which is to provide the engineering data and preliminary drawings required for the fabrication of a prototype test fixture. Phase II will provide for the manufacture and evaluation of the test fixture. To demonstrate the feasibility of designing a

DISTRIBUTION

Approved for public release, distribution unlimited

universal mount fixture, a three degree of freedom mathematical model was developed that simulates the man and weapon as a coupled dynamical system. A sensitivity analysis was performed on both analog and digital computers to determine which of the system parameters are critical to the design of the mount and to obtain bounds on them. The mathematical simulation was supported by an extensive test firing program, involving shooters of various sizes firing the M16 rifle and the M79 and M203 grenade launchers. In these tests the shoulder reaction force and the dynamical motions of the man-weapon system were recorded. Information provided by the tests was used to estimate some of the critical parameters of the system and to provide a means for validating the model predictions. Results of this study indicate the feasibility of designing a universal small arms mount based on a two degree of freedom concept that would be capable of testing a variety of small arm weapons.

universal mount fixture, a three degree of freedom mathematical model was developed that simulates the man and weapon as a coupled dynamical system. A sensitivity analysis was performed on both analog and digital computers to determine which of the system parameters are critical to the design of the mount and to obtain bounds on them. The mathematical simulation was supported by an extensive test firing program, involving shooters of various sizes firing the M16 rifle and the M79 and M203 grenade launchers. In these tests the shoulder reaction force and the dynamical motions of the man-weapon system were recorded. Information provided by the tests was used to estimate some of the critical parameters of the system and to provide a means for validating the model predictions. Results of this study indicate the feasibility of designing a universal small arms mount based on a two degree of freedom concept that would be capable of testing a variety of small arm weapons.

universal mount fixture, a three degree of freedom mathematical model was developed that simulates the man and weapon as a coupled dynamical system. A sensitivity analysis was performed on both analog and digital computers to determine which of the system parameters are critical to the design of the mount and to obtain bounds on them. The mathematical simulation was supported by an extensive test firing program, involving shooters of various sizes firing the M16 rifle and the M79 and M203 grenade launchers. In these tests the shoulder reaction force and the dynamical motions of the man-weapon system were recorded. Information provided by the tests was used to estimate some of the critical parameters of the system and to provide a means for validating the model predictions. Results of this study indicate the feasibility of designing a universal small arms mount based on a two degree of freedom concept that would be capable of testing a variety of small arm weapons.

universal mount fixture, a three degree of freedom mathematical model was developed that simulates the man and weapon as a coupled dynamical system. A sensitivity analysis was performed on both analog and digital computers to determine which of the system parameters are critical to the design of the mount and to obtain bounds on them. The mathematical simulation was supported by an extensive test firing program, involving shooters of various sizes firing the M16 rifle and the M79 and M203 grenade launchers. In these tests the shoulder reaction force and the dynamical motions of the man-weapon system were recorded. Information provided by the tests was used to estimate some of the critical parameters of the system and to provide a means for validating the model predictions. Results of this study indicate the feasibility of designing a universal small arms mount based on a two degree of freedom concept that would be capable of testing a variety of small arm weapons.